A UNITED STATES DEPARTMENT OF COMMERCE PUBLICATION

# EASTROPAC ATLAS

U.S. DEPARTMENT OF COMMERCE
National Oceanic and Atmospheric Administration
National Marine Fisheries Service

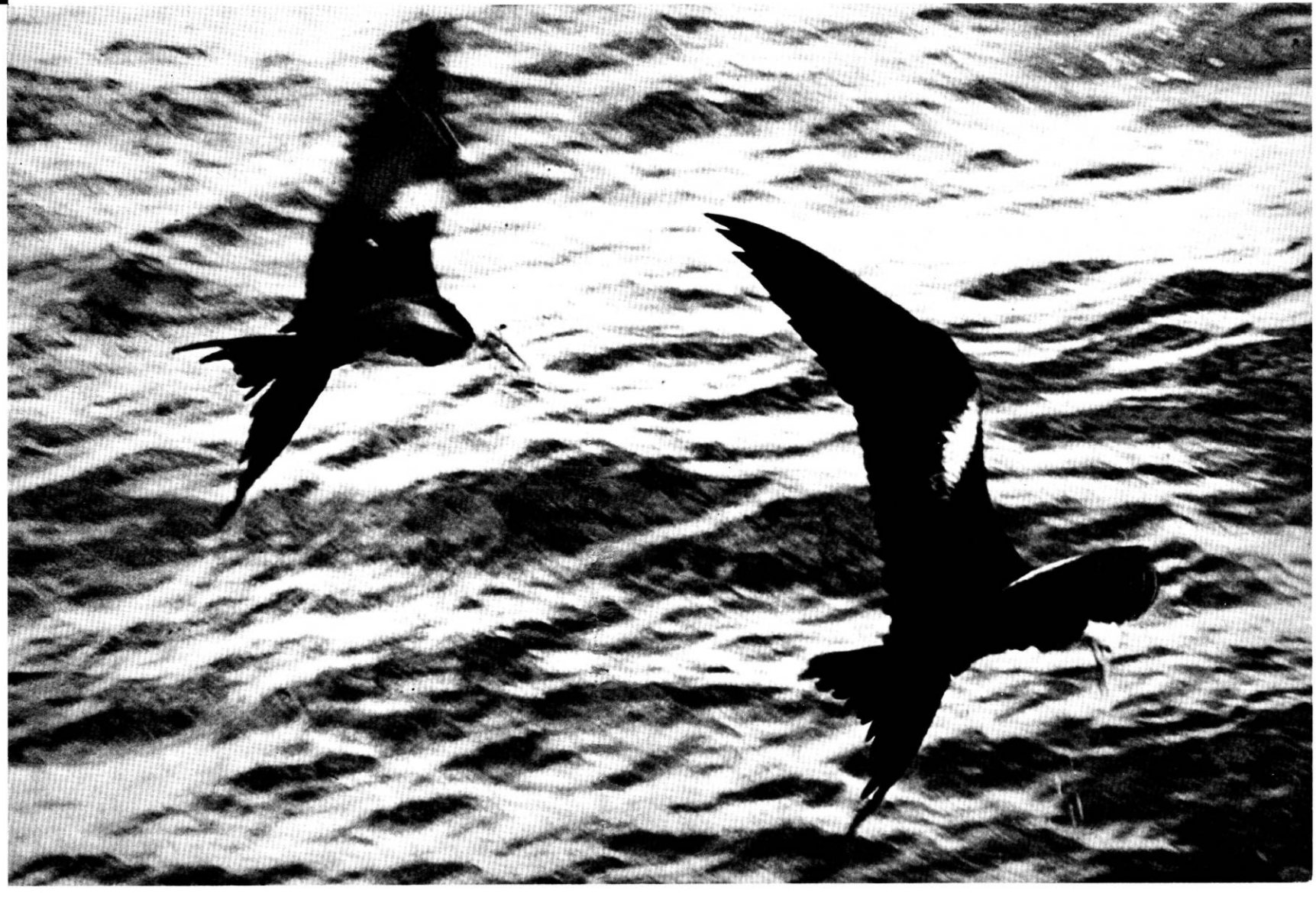

CIRCULAR
330
VOLUME 9
FEBRUARY
1975

## EASTROPAC *Atlas*

| | | |
|---|---|---|
| Volume 1 | Physical oceanographic and meteorological data from principal participating ships, first survey cruise, February-March 1967. | Published June 1972 |
| Volume 2 | Biological and nutrient chemistry data from principal participating ships, first survey cruise, February-March 1967. | Published April 1971 |
| Volume 3 | Physical oceanographic and meteorological data from principal participating ships, first and second monitor cruises, April-July 1967. | Published September 1971 |
| Volume 4 | Biological and nutrient chemistry data from principal participating ships, first and second monitor cruises, April-July 1967. | Published November 1970 |
| Volume 5 | Physical oceanographic and meteorological data from principal participating ships, second survey cruise, August-September 1967. | Published September 1972 |
| Volume 6 | Biological and nutrient chemistry data from principal participating ships, second survey cruise, August-September 1967. | Published December 1972 |
| Volume 7 | Physical oceanographic and meteorological data from principal participating ships and *Oceanographer*, third and fourth monitor cruises, October 1967-January 1968. | Published July 1973 |
| Volume 8 | Biological and nutrient chemistry data from principal participating ships and *Oceanographer*, third and fourth monitor cruises, October 1967-January 1968. | Published March 1974 |
| Volume 9 | Physical oceanographic and meteorological data from principal participating ships, third survey cruise, February-March 1968. | Published February 1975 |
| Volume 10 | Biological and nutrient chemistry data from principal participating ships, third survey cruise, February-March 1968. | In preparation |
| Volume 11 | Data from Latin American cooperating ships and ships of opportunity, all cruises, February 1967-March 1968. | In preparation |

Cover. Immature magnificent frigatebirds near Cocos Island.
Photo by John H. Taylor, Scripps Institution of Oceanography.

## ABSTRACT

This atlas contains charts depicting the distribution of physical, chemical, and biological oceanographic properties and associated meteorological properties observed during EASTROPAC. EASTROPAC was an international cooperative investigation of the eastern tropical Pacific Ocean (20° N. to 20° S., and from the west coasts of the American continents to 119° W.) which was intended to provide data necessary for a more effective use of the marine resources of the area, especially tropical tunas, and also to increase knowledge of the ocean circulation, air-sea interaction, and ecology. The Bureau of Commercial Fisheries (now National Marine Fisheries Service) was the coordinating agency. The field work, from February 1967 through March 1968, was divided into seven 2-month cruise periods. During each cruise period one or more ships were operating in the study area.

On completion of the field work the data seemed too numerous for a classical data report. Instead, it was decided to produce an 11-volume atlas of the results, with 5 volumes containing physical oceanographic and meteorological data from the principal participating ships, 5 volumes containing biological and nutrient chemistry data from the same ships, and 1 volume containing all data from Latin American cooperating ships and ships of opportunity. Extensive use was made of a computer and automatic plotter in preparation of the atlas charts. Methods used to collect and process the data upon which the atlas is based are described in detail by the contributors of the following categories of charts: temperature, salinity, and derived quantities; thickness of the upper mixed layer; dissolved oxygen; meteorology; nutrient chemistry; phytoplankton standing stocks and production; zooplankton and fish larvae; micronekton; birds, fish schools, and marine mammals.

UNITED STATES DEPARTMENT OF COMMERCE
Frederick B. Dent, *Secretary*

NATIONAL OCEANIC AND ATMOSPHERIC ADMINISTRATION
Robert M. White, *Administrator*

NATIONAL MARINE FISHERIES SERVICE
Robert W. Schoning, *Director*

# EASTROPAC ATLAS

## VOLUME 9

PHYSICAL OCEANOGRAPHIC AND METEOROLOGICAL DATA FROM
PRINCIPAL PARTICIPATING SHIPS
THIRD SURVEY CRUISE, FEBRUARY-MARCH 1968

CUTHBERT M. LOVE, *Editor*

CIRCULAR 330
WASHINGTON, D.C.
FEBRUARY 1975

For sale by the Superintendent of Documents, U.S. Government Printing Office, Washington, D.C. 20402—Price $4.75 per volume

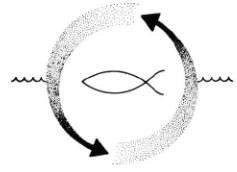

## COORDINATOR, EASTROPAC PROJECT

WARREN S. WOOSTER, Scripps Institution of Oceanography, June 27, 1966-May 15, 1967
ALAN R. LONGHURST, National Marine Fisheries Service, May 15, 1967-June 30, 1970

## ATLAS CONTRIBUTORS

ELBERT H. AHLSTROM—National Marine Fisheries Service, Fish Larvae
MAURICE BLACKBURN—Scripps Institution of Oceanography, Micronekton
WITOLD L. KLAWE—Inter-American Tropical Tuna Commission, Scombroid Larvae
R. MICHAEL LAURS—National Marine Fisheries Service, Zooplankton, Micronekton, Bird and Mammal Observations
FORREST R. MILLER—Inter-American Tropical Tuna Commission, Meteorology
ROBERT W. OWEN, Jr.—National Marine Fisheries Service, Phytoplankton, Oxygen, Mixed Layer Depth
BRUCE A. TAFT—Scripps Institution of Oceanography, Physical Oceanography
WILLIAM H. THOMAS—Scripps Institution of Oceanography, Nutrient Chemistry
MIZUKI TSUCHIYA—Scripps Institution of Oceanography, Physical Oceanography
BERNT ZEITZSCHEL—Scripps Institution of Oceanography, Phytoplankton

## EDITORIAL COMMITTEE

CUTHBERT M. LOVE, National Marine Fisheries Service
BRUCE A. TAFT, Scripps Institution of Oceanography
R. MICHAEL LAURS, National Marine Fisheries Service

National Marine Fisheries Service
Southwest Fisheries Center
La Jolla, California 92037

Scripps Institution of Oceanography
University of California, San Diego
La Jolla, California 92037

Inter-American Tropical Tuna Commission
% Scripps Institution of Oceanography
La Jolla, California 92037

# INTRODUCTION

EASTROPAC was an international cooperative investigation of the eastern tropical Pacific Ocean which was intended to provide data necessary for a more effective use of the marine resources of the area, especially tropical tunas, and also to increase knowledge of the ocean circulation, air-sea interaction, and ecology. The National Marine Fisheries Service (NMFS), formerly Bureau of Commercial Fisheries (BCF), was the coordinating agency. The field work, from February 1967 through March 1968, was divided into seven 2-month cruise periods.

At a meeting of the EASTROPAC Coordinating Committee held at La Jolla in April 1968, it was decided that the data derived from the cruises were so numerous as to render classical data reports impractical and that a comprehensive atlas of the physical and biological results of the project should be produced instead. The atlas has been divided into 11 volumes, with five volumes containing physical oceanographic and meteorological data from the principal participating ships, five volumes containing biological and nutrient chemistry data from the same ships, and one volume containing all data from Latin-American cooperating ships and ships of opportunity.

Volume 9 contains physical oceanographic and meteorological data collected mainly by the principal participating ships during the third survey cruise period (70-series cruises), February-March 1968. (Because of various delays both *Washington* cruise 75 and *Rockaway* cruise 77 actually extended well into the month of April). The companion volume presenting the corresponding biological and nutrient chemistry data is volume 10. The locations of stations occupied by the principal participating ships and ships of opportunity are shown in figure 70-TC-a; those occupied by Latin-American cooperating ships during the same period are shown in figure 70-TC-b.

Information concerning the history and organization of the EASTROPAC Project, a description of the cruises undertaken, the program of observations, the methods used for preparation of the charts, and remarks on the organization of the atlas is contained in volumes 1 and 4 with descriptions by the contributing scientists of the methods used to collect and process the data upon which the atlas charts are based.

CUTHBERT M. LOVE
Editor

## Abbreviations used in figure designation system

| Cruise or cruise period | Property represented | Mnemonic to explain choice of letters | Indicator for vertical sections or type of horizontal surface |
|---|---|---|---|
| Numbers 11, 12, 13, etc., indicate principal cruises. See figure 1. | T Temperature | | v1, v2, etc., indicate vertical sections. |
| | S Salinity | | |
| | $\delta$ Thermosteric anomaly ($\delta_T$) | | Vertical sections are assigned consecutive numbers within each cruise which follow the chronological order in which the ship ran the sections. |
| | G Geostrophic velocity | | |
| | $O_2$ Oxygen concentration | | |
| | $O_2Sa$ Oxygen saturation | | Number 10 or 100 following $O_2Sa$ or horizontal P, Si, $NO_3$, $NO_2$, or $NH_3$ charts indicates distribution at that depth (m.). |
| | ML Thickness of the mixed layer | | |
| | $\delta$300 300 cl./t. thermosteric anomaly surface | | s Distribution at the sea surface |
| | AP Acceleration Potential | | $\delta$300 Distribution on the surface where $\delta_T$=300 cl./t. |
| | P Phosphate-phosphorus | | ei Distribution integrated over the euphotic layer |
| | Si Silicate-silicon | | 150i Distribution integrated to 150 m. depth |
| | $NO_3$ Nitrate-nitrogen | | z Depth of a surface |
| | $NO_2$ Nitrite-nitrogen | | |
| | $NH_3$ Ammonia-nitrogen | | Number 1 or 2 following SP or SW charts indicates one of two 6-month periods into which those observations were divided. |
| | Ch Chlorophyll-a | | |
| | Ph Phaeophytin | | |
| | PP Primary production | | |
| | EL Thickness of the euphotic layer | | |
| | FCp Fish and cephalopod standing stock | | |
| | Cr Crustacean standing stock | | |
| | Nk Total micronekton standing stock | | |
| | ZhN Zooplankton standing stock from 50-cm. net hauls, night | Zooplankton, half-meter, Night | |
| | Z1N Zooplankton standing stock from 1-m. net hauls, night | Zooplankton, 1-meter, Night | |
| | ZhD Zooplankton standing stock from 50-cm. net hauls, day | Zooplankton, half-meter, Day | |
| | Z1D Zooplankton standing stock from 1-m. net hauls, day | Zooplankton, 1-meter, Day | |
| | FLN Total fish larvae, night hauls | Fish Larvae, Night | |
| | FLD Total fish larvae, day hauls | Fish Larvae, Day | |
| | FE Total fish eggs | | |
| | FS Total skipjack tuna larvae | Fish, Skipjack | |
| | FA Total *Auxis* larvae | Fish, *Auxis* | |
| | FC Total *Coryphaena* larvae | Fish, *Coryphaena* | |
| | FMN Total myctophid larvae, night hauls | Fish, Myctophid, Night | |
| | FMD Total myctophid larvae, day hauls | Fish, Myctophid, Day | |
| | FGN Total gonostomatid and sternoptychid larvae, night hauls | Fish, Gonostomatid, Night | |
| | FGD Total gonostomatid and sternoptychid larvae, day hauls | Fish, Gonostomatid, Day | |
| | BP Relative abundance of plankton-feeding birds | Birds, Plankton-feeding | |
| | BF Relative abundance of fish and cephalopod-feeding birds | Birds, Fish-feeding | |
| | SP Porpoise sightings | Sightings, Porpoise | |
| | SW Whale sightings | Sightings, Whales | |
| | ST Tuna school sightings, all cruises | Sightings, Tuna | |
| | UA Upper atmosphere meteorology | | |
| | MW Surface meteorological analysis, winds and pressure | Meteorology, Winds | |
| | MC Surface meteorological analysis, clouds, dewpoint, temperature | Meteorology, Clouds | |
| | MT Surface meteorological analysis, sea temperature, sea-air temperature difference, sea temperature anomaly | Meteorology, Temperature | Numbers 1 to 4 or 1 to 6 following MT or MW charts indicate one of the approximate 2-week periods into which those observations were divided. For all cruise periods except 40, the MT and MW charts were drawn for four 2-week periods. For the 40 cruise period these charts were drawn for six periods ranging from 12 to 16 days in length, but with several days overlap between some periods. Number 1 or 2 following MC charts indicates one of the monthly periods for which those charts were drawn. |
| | RM Reference map | | |
| | TC Track chart | | |
| MZ-4 *Yolanda*, MZ-4 | | | |
| MZ-5 *Yolanda*, MZ-5 | | | |
| MZ-6 *Yolanda*, MZ-6 | | | |
| MZ-7 *Defiance*, MZ-7 | | | |
| MZ-8 *Turpan*, MZ-8 | | | |
| H1 *Huayaipe*-1 | | | |
| H2 *Huayaipe*-2 | | | |
| H3 *Huayaipe*-3 | | | |
| U1 *Unanue* 6702 | | | |
| U2 *Unanue* 6708 | | | |
| U3 *Unanue* 6802 | | | |
| Y5 *Yelcho* MARCHILE V | | | |
| Y6 *Yelcho* MARCHILE VI | | | |
| Y7 *Yelcho* MARCHILE VII | | | |
| E6 *Esmeralda* BE VI | | | |
| OP *Oceanographer* | | | |
| CD *Charles H. Davis* | | | |
| T3 *Te Vega* 13 | | | |
| T4 *Te Vega* 14 | | | |
| T5 *Te Vega* 15 | | | |
| T6 *Te Vega* 16 | | | |
| T7 *Te Vega* 17 | | | |
| Numbers 10, 20, 30, 40, 50, 60, 70, indicate 2-month cruise periods. | | | |

Letters or letter-number combinations indicate cruises of Latin American cooperating ships or ships of opportunity, as follows:

### Thermosteric anomaly and geostrophic velocity—Yellow pages

FIGURE 76-$\delta$-v4.—Vertical distribution of thermosteric anomaly, $\delta_T$, (cl./t.) along a section from 12° N., 112° W. to Manzanillo, March 26-30, 1968.

FIGURE 76-$\delta$-v1.—Vertical distribution of thermosteric anomaly $\delta_T$, (cl./t.) along a section from Acapulco to 12° N., 105° W., February 26-28, 1968.

FIGURE 76-$\delta$-v2.—Vertical distribution of thermosteric anomaly, $\delta_T$, (cl./t.) along 105° W., February 28-March 14, 1968.

FIGURE 76-G-v4.—Vertical distribution of the component of geostrophic velocity (cm./sec.), relative to 500 db., normal to a section from 12° N., 112° W. to Manzanillo, March 26-30, 1968. Dark shading indicates flow toward the southeast with a velocity greater than 5 cm./sec.; light shading indicates flow toward the northwest with a velocity greater than 5 cm./sec.

FIGURE 76-G-v1.—Vertical distribution of the component of geostrophic velocity (cm./sec.), relative to 500 db., normal to a section from Acapulco to 12° N., 105° W., February 26-28, 1968. The dark shading indicates flow toward the southeast with a velocity greater than 5 cm./sec.

FIGURE 76-G-v2.—Vertical distribution of the zonal component of geostrophic velocity (cm./sec.), relative to 500 db., along 105° W., February 28-March 14, 1968. Dark shading indicates eastward flow with a velocity greater than 5 cm./sec.; light shading indicates westward flow with a velocity greater than 5 cm./sec.

### Oxygen—Green pages

FIGURE 76-$O_2$-v4.—Vertical distribution of oxygen (ml./l.) along a section from 12° N., 112° W. to Manzanillo, March 26-30, 1968.

FIGURE 76-$O_2$-v1.—Vertical distribution of oxygen (ml./l.) along a section from Acapulco to 12° N., 105° W., February 26-28, 1968.

FIGURE 76-$O_2$-v2.—Vertical distribution of oxygen (ml./l.) along 105° W., February 28-March 14, 1968.

### Temperature and salinity—White pages

FIGURE 77-T-v1.—Vertical distribution of temperature (°C.) along a section in the Panama Bight near the coasts of Panama and Colombia from 7°25′ N. to 6°10′ N., January 30-31, 1968.

FIGURE 77-T-v2.—Vertical distribution of temperature (°C.) across the northern portion of the Panama Bight from the coast of Colombia to Cabo Mala, Panama, January 31-February 1, 1968.

FIGURE 77-T-v3.—Vertical distribution of temperature (°C.) along the coast of Panama from 79°57′ W. to 80°53′ W., February 1, 1968.

FIGURE 77-T-v5.—Vertical distribution of temperature (°C.) along a northeast-southwest section from the coast of Colombia to 0°54′ N., 82°00′ W., February 4-9, 1968.

FIGURE 77-T-v4.—Vertical distribution of temperature (°C.) along a northwest-southeast section across the Panama Bight from Peninsula de Azuero, Panama, to the coast of Colombia, February 1-3, 1968.

FIGURE 77-T-v6.—Vertical distribution of temperature (°C.) along 82° W., February 4-9, 1968.

FIGURE 77-T-v8.—Vertical distribution of temperature (°C.) along the coast of Peru from 10°40′ S. to 12°17′ S., February 12-13, 1968.

FIGURE 77-T-v7.—Vertical distribution of temperature (°C.) along a southwest-northeast section from 9°57′ S., 81°49′ W. to the coast of Peru, February 9, 1968.

FIGURE 77-T-v9.—Vertical distribution of temperature (°C.) along a northeast-southwest section from the coast of Peru to 14°59′ S., 84°56′ W., February 13-15, 1968.

FIGURE 77-T-v12.—Vertical distribution of temperature (°C.) along 15° S., April 8-9, 1968.

FIGURE 77-T-v10.—Vertical distribution of temperature (°C.) along 85° W., February 15-25, 1968.

FIGURE 77-T-v11.—Vertical distribution of temperature (°C.) along 88° W., March 30-April 8, 1968.

FIGURE 77-T-v13.—Vertical distribution of temperature (°C.) along 95° W., March-April 1968. Stations 302-313 were occupied on March 3-4, Stations 457-571 on April 9-18. The interruption in the contours indicates the 44½-day interval between Stations 313 and 571.

FIGURE 77-S-v1.—Vertical distribution of salinity (‰) along a section in the Panama Bight near the coasts of Panama and Colombia from 7°25′ N. to 6°10′ N., January 30-31, 1968. Some contours in the range 31.0 to 34.5 ‰ have been omitted in order to avoid excessive crowding near the top of the chart.

FIGURE 77-S-v2.—Vertical distribution of salinity (‰) across the northern portion of the Panama Bight from the coast of Colombia to Cabo Mala, Panama, January 31-February 1, 1968.

FIGURE 77-S-v3.—Vertical distribution of salinity (‰) along the coast of Panama from 79°57′ W. to 80°53′ W., February 1, 1968. Some contours in the range 31.4 to 34.4 ‰ have been omitted in order to avoid excessive crowding near the top of the chart.

FIGURE 77-S-v5.—Vertical distribution of salinity (‰) along a northeast-southwest section from the coast of Colombia to 0°54′ N., 82°00′ W., February 3-4, 1968. Some contours in the range 32.4 to 34.6 ‰ have been omitted in order to avoid excessive crowding near the top of the chart.

FIGURE 77-S-v4.—Vertical distribution of salinity (‰) along a northwest-southeast section across the Panama Bight from Peninsula de Azuero, Panama, to the coast of Colombia, February 1-3, 1968. Some contours in the range 31.4 to 34.4 ‰ have been omitted in order to avoid excessive crowding near the top of the chart.

FIGURE 77-S-v6.—Vertical distribution of salinity (‰) along 82° W., February 4-9, 1968.

FIGURE 77-S-v8.—Vertical distribution of salinity (‰) along the coast of Peru from 10°40′ S. to 12°17′ S. February 12-13, 1968.

FIGURE 77-S-v7.—Vertical distribution of salinity (‰) along a southwest-northeast section from 9°57′ S., 81°49′ W. to the coast of Peru, February 9, 1968.

FIGURE 77-S-v9.—Vertical distribution of salinity (‰) along a northeast-southwest section from the coast of Peru to 14°59′ S., 84°56′ W., February 13-15, 1968.

FIGURE 77-S-v12.—Vertical distribution of salinity (‰) along 15° S., April 8-9, 1968.

FIGURE 77-S-v10.—Vertical distribution of salinity (‰) along 85° W., February 15-25 ,1968.

FIGURE 77-S-v11.—Vertical distribution of salinity (‰) along 88° W., March 30-April 8, 1968.

FIGURE 77-S-v13.—Vertical distribution of salinity (‰) along 95° W., March-April 1968. Stations 302-313 were occupied on March 3-4, Stations 457-571 on April 9-18. The interruption in the contours indicates the 44½-day interval between Stations 313 and 571.

### Thermosteric anomaly and geostrophic velocity—Yellow pages

FIGURE 77-$\delta$-v1.—Vertical distribution of thermosteric anomaly, $\delta_T$, (cl./t.) along a section of the Panama Bight near the coasts of Panama and Colombia from 7°25′ N. to 6°10′ N., January 30-31, 1968.

FIGURE 77-$\delta$v2.— Vertical distribution of thermosteric anomaly, $\delta_T$, (cl./t.) across the northern portion of the Panama Bight from the coast of Colombia to Cabo Mala, Panama, January 31-February 1, 1968.

FIGURE 77-$\delta$-v3.—Vertical distribution of thermosteric anomaly, $\delta_T$, (cl./t.) along the coast of Panama from 79°57′ W. to 80°53′ W., February 1, 1968.

FIGURE 77-$\delta$-v5.—Vertical distribution of thermosteric anomaly, $\delta_T$, (cl./t.) along a northeast-southwest section from the coast of Colombia to 0°54′ N., 82°00′ W., February 4-9, 1968.

FIGURE 77-$\delta$-v4.—Vertical distribution of thermosteric anomaly, $\delta_T$, (cl./t.) along a northwest-southeast section across the Panama Bight from Peninsula de Azuero, Panama, to the coast of Colombia, February 1-3, 1968.

FIGURE 77-$\delta$-v6.—Vertical distribution of thermosteric anomaly, $\delta_T$, (cl./t.) along 82° W., February 4-9, 1968.

FIGURE 77-$\delta$-v8.—Vertical distribution of thermosteric anomaly, $\delta_T$, (cl./t.) along the coast of Peru from 10°40′ S. to 12°17′ S., February 12-13, 1968.

FIGURE 77-$\delta$-v7.—Vertical distribution of thermosteric anomaly, $\delta_T$, (cl./t.) along a southwest-northeast section from 9°57′ S., 81°49′ W. to the coast of Peru, February 9, 1968.

FIGURE 70-MT-3.—Analysis of sea surface temperatures based on averages for 2-degree (latitude-longitude) squares from all available ship observations for the period March 1-16, 1968. Solid lines are sea surface isotherms (°C.); the isotherms are dashed where data are sparse. Dark hatching outlines areas with positive temperature anomalies (computed from mean sea surface temperatures averaged over 22 years) greater than 1° C.; light hatching shows areas with negative anomalies greater than 1° C. Sea surface temperature (°C. x 10) averaged for 5-degree squares is plotted above the mean position of the square; sea temperature minus air temperature difference (°C. x 10) is plotted below the symbol.

FIGURE 70-MT-4.—Analysis of sea surface temperatures based on averages for 2-degree (latitude-longitude) squares from all available ship observations for the period March 17-31, 1968. Solid lines are sea surface isotherms (°C.); the isotherms are dashed where data are sparse. Dark hatching outlines areas with positive temperature anomalies (computed from mean sea surface temperatures averaged over 22 years) greater than 1° C.; light hatching shows areas with negative anomalies greater than 1° C. Sea surface temperature (°C. x 10) averaged for 5-degree squares is plotted above the mean position of the square; sea temperature minus air temperature difference (°C. x 10) is plotted below the symbol.

FIGURE 70-MC-1.—Analyses of the surface dew-point temperature of the air and total cloud cover based on 2-degree (latitude-longitude) averages from all available ship observations for the month of February 1968. Solid lines depict the monthly mean total cloud cover in oktas; the lines are dashed where data are sparse. Dash-dot lines are isotherms of the mean monthly dew-point temperature at 2-degree (°C.) intervals. Areas where 15 percent or more of the ships reported rain of any type at or within sight of the ship are shaded. Dew-point temperature (°C. x 10) averaged for 5-degree squares is plotted above the mean position of the square, with total cloud cover (oktas) below and rainfall frequency (%) to the right of the symbol.

FIGURE 70-MC-2.—Analyses of the surface dew-point temperature of the air and total cloud cover based on 2-degree (latitude-longitude) averages from all available ship observations for the month of March 1968. Solid lines depict the monthly mean total cloud cover in oktas; the lines are dashed where data are sparse. Dash-dot lines are isotherms of the mean monthly dew-point temperature at 2-degree (°C.) intervals. Areas where 15 percent or more of the ships reported rain of any type at or within sight of the ship are shaded. Dew-point temperature (°C. x 10) averaged for 5-degree squares is plotted above the mean position of the square, with total cloud cover (oktas) below and rainfall frequency (%) to the right of the symbol.

### Temperature and salinity—White pages

FIGURE 75-T-v1.—Vertical distribution of temperature (°C.) along 119° W. from 21°46′ N. to 9°34′ N., February 18-22, 1968.

FIGURE 75-T-v3.—Vertical distribution of temperature (°C.) along 20° S., March 4-7, 1968.

FIGURE 75-T-v2.—Vertical distribution of temperature (°C.) along 119° W. from 15°05′ N. to 20°01′ S., February 20-March 4, 1968.

FIGURE 75-T-v4.) 76-T-v3.)—Vertical distribution of temperature (°C.) along 112° W., March 1968. Southern portion of section run by *Washington* March 7-11; northern portion by *Jordan*, March 17-26.

FIGURE 75-T-v5.—Vertical distribution of temperature (°C.) along 98° W., March 21-April 8, 1968. The interruption in the contours indicates a 9-day interval between stations 205 and 223 in the upper (0-500m.) portion of the section, or between stations 204 and 223 in the lower portion.

FIGURE 75-S-v1.—Vertical distribution of salinity (‰) along 119° W. from 21°46′ N. to 9°34′ N., February 18-22, 1968.

FIGURE 75-S-v3.—Vertical distribution of salinity (‰) along 20° S., March 4-7, 1968.

FIGURE 75-S-v2.—Vertical distribution of salinity (‰) along 119° W. from 15°05′ N. to 20°01′ S., February 20-March 4, 1968.

FIGURE 75-S-v4.) 76-S-v3.)—Vertical distribution of salinity (‰) along 112° W., March 1968. Southern portion of section run by *Washington*, March 7-11; northern portion by *Jordan*, March 17-26.

FIGURE 75-S-v5.—Vertical distribution of salinity (‰) along 98° W., March 21-April 8, 1968. The interruption in the contours indicates a 9-day interval between stations 205 and 223 in the upper (0-500m.) portion of the section, or between stations 204 and 223 in the lower portion.

### Thermosteric anomaly and geostrophic velocity—Yellow pages

FIGURE 75-$\delta$-v1.—Vertical distribution of thermosteric anomaly, $\delta_x$, (cl./t.) along 119° W. from 21°46′ N. to 9°34′ N., February 18-22, 1968.

FIGURE 75-$\delta$-v3.—Vertical distribution of thermosteric anomaly, $\delta_x$, (cl./t.) along 20° S., March 4-7, 1968.

FIGURE 75-$\delta$-v2.—Vertical distribution of thermosteric anomaly, $\delta_x$, (cl./t.) along 119° W. from 15°05′ N. to 20°01′ S., February 20-March 4, 1968.

FIGURE 75-$\delta$-v4.) 76-$\delta$-v3.)—Vertical distribution of thermosteric anomaly, $\delta_x$, (cl./t.) along 112° W., March 1968. Southern portion of section run by *Washington*, March 7-11; northern portion by *Jordan*, March 17-26.

FIGURE 75-$\delta$-v5.—Vertical distribution of thermosteric anomaly, $\delta_x$, (cl./t.) along 98° W., March 21-April 8, 1968. The interruption in the contours indicates a 9-day interval between stations 205 and 223 in the upper (0-500m.) portion of the section, or between stations 204 and 223 in the lower portion.

FIGURE 75-G-v1.—Vertical distribution of the zonal component of geostrophic velocity (cm./sec.), relative to 500 db., along 119° W. from 21°04′ N. to 10°19′ N., February 18-22, 1968. Dark shading indicates eastward flow with a velocity greater than 5 cm./sec; light shading indicates westward flow with a velocity greater than 5 cm./sec.

FIGURE 75-G-v3.—Vertical distribution of the meridonial component of geostrophic velocity (cm./sec.), relative to 500 db., along 20° S., March 4-6, 1968. The dark shading indicates northward flow with a velocity greater than 5 cm./sec.

FIGURE 75-G-v2.—Vertical distribution of the zonal component of geostrophic velocity (cm./sec.), relative to 500 db., along 119° W. from 14°28′ N. to 20°01′ S., February 21-March 4, 1968. Dark shading indicates eastward flow with a velocity greater than 5 cm./sec.; light shading indicates westward flow with a velocity greater than 5 cm./sec.

FIGURE 75-G-v4.) 76-G-v3.)—Vertical distribution of the zonal component of geostrophic velocity (cm./sec.), relative to 500 db., along 112° W., March 1968. Southern portion of section run by *Washington*, March 7-11; northern portion by *Jordan*, March 17-25. Dark shading indicates eastward flow with a velocity greater than 5 cm./sec.; light shading indicates westward flow with a velocity greater than 5 cm./sec.

FIGURE 75-G-v5.—Vertical distribution of the zonal component of geostrophic velocity (cm./sec.), relative to 500 db., along 98° W., March 21-April 8, 1968. Dark shading indicates eastward flow with a velocity greater than 5 cm./sec.; light shading indicates westward flow with a velocity greater than 5 cm./sec.

### Oxygen—Green pages

FIGURE 75-$O_2$-v1.—Vertical distribution of oxygen (ml./l.) along 119° W. from 21°46′ N. to 9°34′ N. February 18-22, 1968.

FIGURE 75-$O_2$-v2.—Vertical distribution of oxygen (ml./l.) along 119° W. from 15°05′ N. to 20°01′ S., February 20-March 4, 1968.

FIGURE 75-$O_2$-v4.) 76-$O_2$-v3.)—Vertical distribution of oxygen (ml./l) along 112° W., March 1968. Southern portion of section run by *Washington*, March 7-11; northern portion by *Jordan*, March 17-26.

FIGURE 75-$O_2$-v5.—Vertical distribution of oxygen (ml./l.) along 98° W., March 21-April 8, 1968. The interruption in the contours indicates a 9-day interval between station 205 and 223.

### Temperature and salinity—White pages

FIGURE 76-T-v4.—Vertical distribution of temperature (°C.) along a section from 12° N., 112° W. to Manzanillo, March 26-30, 1968.

FIGURE 76-T-v1.—Vertical distribution of temperature (°C.) along a section from Acapulco to 12° N., 105° W., February 26-28, 1968.

FIGURE 76-T-v2.—Vertical distribution of temperature (°C.) along 105° W., February 28-March 14, 1968.

FIGURE 76-S-v4.—Vertical distribution of salinity (‰) along a section from 12° N., 112° W. to Manzanillo, March 26-30, 1968.

FIGURE 76-S-v1.—Vertical distribution of salinity (‰) along a section from Acapulco to 12° N., 105° W., February 26-28, 1968.

FIGURE 76-S-v2.—Vertical distribution of salinity (‰) along 105° W., February 28-March 14, 1968.

### Thermosteric anomaly and geostrophic velocity—Yellow pages

FIGURE 76-δ-v4.—Vertical distribution of thermosteric anomaly, $\delta_s$, (cl./t.) along a section from 12° N., 112° W. to Manzanillo, March 26-30, 1968.

FIGURE 76-δ-v1.—Vertical distribution of thermosteric anomaly $\delta_s$, (cl./t.) along a section from Acapulco to 12° N., 105° W., February 26-28, 1968.

FIGURE 76-δ-v2.—Vertical distribution of thermosteric anomaly, $\delta_s$, (cl./t.) along 105° W., February 28-March 14, 1968.

FIGURE 76-G-v4.—Vertical distribution of the component of geostrophic velocity (cm./sec.), relative to 500 db., normal to a section from 12° N., 112° W. to Manzanillo, March 26-30, 1968. Dark shading indicates flow toward the southeast with a velocity greater than 5 cm./sec.; light shading indicates flow toward the northwest with a velocity greater than 5 cm./sec.

FIGURE 76-G-v1.—Vertical distribution of the component of geostrophic velocity (cm./sec.), relative to 500 db., normal to a section from Acapulco to 12° N., 105° W., February 26-28, 1968. The dark shading indicates flow toward the southeast with a velocity greater than 5 cm./sec.

FIGURE 76-G-v2.—Vertical distribution of the zonal component of geostrophic velocity (cm./sec.), relative to 500 db., along 105° W., February 28-March 14, 1968. Dark shading indicates eastward flow with a velocity greater than 5 cm./sec.; light shading indicates westward flow with a velocity greater than 5 cm./sec.

### Oxygen—Green pages

FIGURE 76-$O_2$-v4.—Vertical distribution of oxygen (ml./l.) along a section from 12° N., 112° W. to Manzanillo, March 26-30, 1968.

FIGURE 76-$O_2$-v1.—Vertical distribution of oxygen (ml./l.) along a section from Acapulco to 12° N., 105° W., February 26-28, 1968.

FIGURE 76-$O_2$-v2.—Vertical distribution of oxygen (ml./l.) along 105° W., February 28-March 14, 1968.

### Temperature and salinity—White pages

FIGURE 77-T-v1.—Vertical distribution of temperature (°C.) along a section in the Panama Bight near the coasts of Panama and Colombia from 7°25′ N. to 6°10′ N., January 30-31, 1968.

FIGURE 77-T-v2.—Vertical distribution of temperature (°C.) across the northern portion of the Panama Bight from the coast of Colombia to Cabo Mala, Panama, January 31-February 1, 1968.

FIGURE 77-T-v3.—Vertical distribution of temperature (°C.) along the coast of Panama from 79°57′ W. to 80°53′ W., February 1, 1968.

FIGURE 77-T-v5.—Vertical distribution of temperature (°C.) along a northeast-southwest section from the coast of Colombia to 0°54′ N., 82°00′ W., February 4-9, 1968.

FIGURE 77-T-v4.—Vertical distribution of temperature (°C.) along a northwest-southeast section across the Panama Bight from Peninsula de Azuero, Panama, to the coast of Colombia, February 1-3, 1968.

FIGURE 77-T-v6.—Vertical distribution of temperature (°C.) along 82° W., February 4-9, 1968.

FIGURE 77-T-v8.—Vertical distribution of temperature (°C.) along the coast of Peru from 10°40′ S. to 12°17′ S., February 12-13, 1968.

FIGURE 77-T-v7.—Vertical distribution of temperature (°C.) along a southwest-northeast section from 9°57′ S., 81°49′ W. to the coast of Peru, February 9, 1968.

FIGURE 77-T-v9.—Vertical distribution of temperature (°C.) along a northeast-southwest section from the coast of Peru to 14°59′ S., 84°56′ W., February 13-15, 1968.

FIGURE 77-T-v12.—Vertical distribution of temperature (°C.) along 15° S., April 8-9, 1968.

FIGURE 77-T-v10.—Vertical distribution of temperature (°C.) along 85° W., February 15-25, 1968.

FIGURE 77-T-v11.—Vertical distribution of temperature (°C.) along 88° W., March 30-April 8, 1968.

FIGURE 77-T-v13.—Vertical distribution of temperature (°C.) along 95° W., March-April 1968. Stations 302-313 were occupied on March 3-4, Stations 457-571 on April 9-18. The interruption in the contours indicates the 44½-day interval between Stations 313 and 571.

FIGURE 77-S-v1.—Vertical distribution of salinity (‰) along a section in the Panama Bight near the coasts of Panama and Colombia from 7°25′ N. to 6°10′ N., January 30-31, 1968. Some contours in the range 31.0 to 34.5 ‰ have been omitted in order to avoid excessive crowding near the top of the chart.

FIGURE 77-S-v2.—Vertical distribution of salinity (‰) across the northern portion of the Panama Bight from the coast of Colombia to Cabo Mala, Panama, January 31-February 1, 1968.

FIGURE 77-S-v3.—Vertical distribution of salinity (‰) along the coast of Panama from 79°57′ W. to 80°53′ W., February 1, 1968. Some contours in the range 31.4 to 34.4 ‰ have been omitted in order to avoid excessive crowding near the top of the chart.

FIGURE 77-S-v5.—Vertical distribution of salinity (‰) along a northeast-southwest section from the coast of Colombia to 0°54′ N., 82°00′ W., February 3-4, 1968. Some contours in the range 32.4 to 34.6 ‰ have been omitted in order to avoid excessive crowding near the top of the chart.

FIGURE 77-S-v4.—Vertical distribution of salinity (‰) along a northwest-southeast section across the Panama Bight from Peninsula de Azuero, Panama, to the coast of Colombia, February 1-3, 1968. Some contours in the range 31.4 to 34.4 ‰ have been omitted in order to avoid excessive crowding near the top of the chart.

FIGURE 77-S-v6.—Vertical distribution of salinity (‰) along 82° W., February 4-9, 1968.

FIGURE 77-S-v8.—Vertical distribution of salinity (‰) along the coast of Peru from 10°40′ S. to 12°17′ S. February 12-13, 1968.

FIGURE 77-S-v7.—Vertical distribution of salinity (‰) along a southwest-northeast section from 9°57′ S., 81°49′ W. to the coast of Peru, February 9, 1968.

FIGURE 77-S-v9.—Vertical distribution of salinity (‰) along a northeast-southwest section from the coast of Peru to 14°59′ S., 84°56′ W., February 13-15, 1968.

FIGURE 77-S-v12.—Vertical distribution of salinity (‰) along 15° S., April 8-9, 1968.

FIGURE 77-S-v10.—Vertical distribution of salinity (‰) along 85° W., February 15-25 ,1968.

FIGURE 77-S-v11.—Vertical distribution of salinity (‰) along 88° W., March 30-April 8, 1968.

FIGURE 77-S-v13.—Vertical distribution of salinity (‰) along 95° W., March-April 1968. Stations 302-313 were occupied on March 3-4, Stations 457-571 on April 9-18. The interruption in the contours indicates the 44½-day interval between Stations 313 and 571.

### Thermosteric anomaly and geostrophic velocity—Yellow pages

FIGURE 77-δ-v1.—Vertical distribution of thermosteric anomaly, $\delta_s$, (cl./t.) along a section of the Panama Bight near the coasts of Panama and Colombia from 7°25′ N. to 6°10′ N., January 30-31, 1968.

FIGURE 77-δv2.— Vertical distribution of thermosteric anomaly, $\delta_s$, (cl./t.) across the northern portion of the Panama Bight from the coast of Colombia to Cabo Mala, Panama, January 31-February 1, 1968.

FIGURE 77-δ-v3.—Vertical distribution of thermosteric anomaly, $\delta_s$, (cl./t.) along the coast of Panama from 79°57′ W. to 80°53′ W., February 1, 1968.

FIGURE 77-δ-v5.—Vertical distribution of thermosteric anomaly, $\delta_s$, (cl./t.) along a northeast-southwest section from the coast of Colombia to 0°54′ N., 82°00′ W., February 4-9, 1968.

FIGURE 77-δ-v4.—Vertical distribution of thermosteric anomaly, $\delta_s$, (cl./t.) along a northwest-southeast section across the Panama Bight from Peninsula de Azuero, Panama, to the coast of Colombia, February 1-3, 1968.

FIGURE 77-δ-v6.—Vertical distribution of thermosteric anomaly, $\delta_s$, (cl./t.) along 82° W., February 4-9, 1968.

FIGURE 77-δ-v8.—Vertical distribution of thermosteric anomaly, $\delta_s$, (cl./t.) along the coast of Peru from 10°40′ S. to 12°17′ S., February 12-13, 1968.

FIGURE 77-δ-v7.—Vertical distribution of thermosteric anomaly, $\delta_s$, (cl./t.) along a southwest-northeast section from 9°57′ S., 81°49′ W. to the coast of Peru, February 9, 1968.

FIGURE 77-δ-v9.—Vertical distribution of thermosteric anomaly, $\delta_T$, (cl./t.) along a northeast-southwest section from the coast of Peru to 14°59′ S., 84°56′ W., February 13-15, 1968.

FIGURE 77-δ-v12.—Vertical distribution of thermosteric anomaly, $\delta_T$, (cl./t.) along 15° S., April 8-9, 1968.

FIGURE 77-δ-v10.—Vertical distribution of thermosteric anomaly, $\delta_T$, (cl./t.) along 85° W., February 15-25, 1968.

FIGURE 77-δ-v11.—Vertical distribution of thermosteric anomaly, $\delta_T$, (cl./t.) along 88° W., March 30-April 8, 1968.

FIGURE 77-δ-v13.—Vertical distribution of thermosteric anomaly, $\delta_T$, (cl./t.) along 95° W., March-April 1968. Stations 302-313 were occupied on March 3-4, stations 457-571 on April 9-18. The interruption in the contours indicates the 44½-day interval between stations 313-571.

FIGURE 77-G-v4.—Vertical distribution of the component of geostrophic velocity (cm./sec.), relative to 500 db., normal to a northwest-southeast section across the Panama Bight from Peninsula de Azuero, Panama, to the coast of Colombia, February 1-3, 1968. Dark shading indicates flow toward the northeast with a velocity greater than 5 cm./sec.; light shading indicates flow toward the southwest with a velocity greater than 5 cm./sec.

FIGURE 77-G-v9.—Vertical distribution of the component of geostrophic velocity (cm./sec.), relative to 500 db., normal to a northeast-southwest section from the coast of Peru to 14°46′ S., 84°20′ W., February 13-15, 1968. Dark shading indicates flow toward the southeast with a velocity greater than 5 cm./sec.; light shading indicates flow toward the northwest with a velocity greater than 5 cm./sec.

FIGURE 77-G-v6.—Vertical distribution of the zonal component of geostrophic velocity (cm./sec.), relative to 500 db., along 82° W., February 6-9, 1968. Dark shading indicates eastward flow with a velocity greater than 5 cm./sec.; light shading indicates westward flow with a velocity greater than 5 cm./sec.

FIGURE 77-G-v10.—Vertical distribution of the zonal component of geostrophic velocity (cm./sec.), relative to 500 db., along 85° W., February 15-24, 1968. Dark shading indicates eastward flow with a velocity greater than 5 cm./sec.; light shading indicates westward flow with a velocity greater than 5 cm./sec.

FIGURE 77-G-v11.—Vertical distribution of the zonal component of geostrophic velocity (cm./sec.), relative to 500 db., along 88° W., March 30-April 8, 1968. Dark shading indicates eastward flow with a velocity greater than 5 cm./sec.; light shading indicates westward flow with a velocity greater than 5 cm./sec.

FIGURE 77-G-v13.—Vertical distribution of the zonal component of geostrophic velocity (cm./sec.), relative to 500 db., along 95° W., March-April 1968. Dark shading indicates eastward flow with a velocity greater than 5 cm./sec.; light shading indicates westward flow with a velocity greater than 5 cm./sec. Stations 303-313 were occupied on March 3-4, Stations 459-568 on April 10-18. The interruption in the contours and shading in the vicinity of 12° N. indicates the 44½-day interval between Stations 313 and 568.

## Oxygen—Green pages

FIGURE 77-$O_2$-v2.—Vertical distribution of oxygen (ml./l.) across the northern portion of the Panama Bight from the coast of Colombia to Cabo Mala, Panama, January 31-February 1, 1968.

FIGURE 77-$O_2$-v4.—Vertical distribution of oxygen (ml./l.) along a northwest-southeast section across the Panama Bight from Peninsula de Azuero, Panama, to the coast of Colombia, February 1-3, 1968.

FIGURE 77-$O_2$-v6.—Vertical distribution of oxygen (ml./l.) along 82° W., February 4-9, 1968.

FIGURE 77-$O_2$-v7.—Vertical distribution of oxygen (ml./l.) along a southwest-northeast section from 9°57′ S., 81°49′ W. to the coast of Peru, February 9, 1968.

FIGURE 77-$O_2$-v9.—Vertical distribution of oxygen (ml./l.) along a northeast-southwest section from the coast of Peru to 14°59′ S., 84°56′ W., February 13-15, 1968.

FIGURE 77-$O_2$-v10.—Vertical distribution of oxygen (ml./l.) along 85° W., February 15-25, 1968.

FIGURE 77-$O_2$-v11.—Vertical distribution of oxygen (ml./l.) along 88° W., March 30-April 8, 1968.

FIGURE 77-$O_2$-v13.—Vertical distribution of oxygen (ml./l.) along 95° W., March-April 1968. Stations 302-313 were occupied on March 3-4, Stations 457-571 on April 9-18. The interruption in the contours indicates the 44½-day interval between Stations 313 and 571.

## Meteorology—Blue pages

FIGURE 77-UA-v6.—Vertical section of the atmosphere along 82° W., February 1-15, 1968. Solid lines are isotherms of air temperature (°C.). Dashed lines are isopleths of mixing ratio of the air (g./kg.). Surface air temperature is plotted above surface mixing ratio and below a base line representing the surface pressure (mb.). The computed height (m.) of each standard pressure surface is plotted for the northernmost radiosonde station of the section. At other stations the difference of computed height minus the corresponding height at the northern station is shown at each standard level.

FIGURE 77-UA-v10.—Vertical section of the atmosphere along 85° W., February 16-23, 1968. Solid lines are isotherms of air temperature (°C.). Dashed lines are isopleths of mixing ratio of the air (g./kg.). Surface air temperature is plotted above surface mixing ratio and below a base line representing the surface pressure (mb.). The computed height (m.) of each standard pressure surface is plotted for the northernmost radiosonde station of the section. At other stations the difference of computed height minus the correspodning height at the northern station is shown at each standard level.

FIGURE 77-UA-v11.—Vertical section of the atmosphere along 88° W., February 24-March 9, 1968. Solid lines are isotherms of air temperature (°C.). Dashed lines are isopleths of mixing ratio of the air (g./kg.). Surface air temperature is plotted above surface mixing ratio and below a base line representing the surface pressure (mb.). The computed height (m.) of each standard pressure surface is plotted for the northernmost radiosonde station of the section. At other stations the difference of computed height minus the corresponding height at the northern station is shown at each standard level.

FIGURE 77-UA-v13.—Vertical section of the atmosphere along 95° W., March 10-18, 1968. Solid lines are isotherms of air temperature (°C.). Dashed lines are isopleths of mixing ratio of the air (g./kg.). Surface air temperature is plotted above surface mixing ratio and below a base line representing the surface pressure (mb.). The computed height (m.) of each standard pressure surface is plotted for the northernmost radiosonde station of the section. At other stations the difference of computed height minus the corresponding height at the northern station is shown at each standard level.

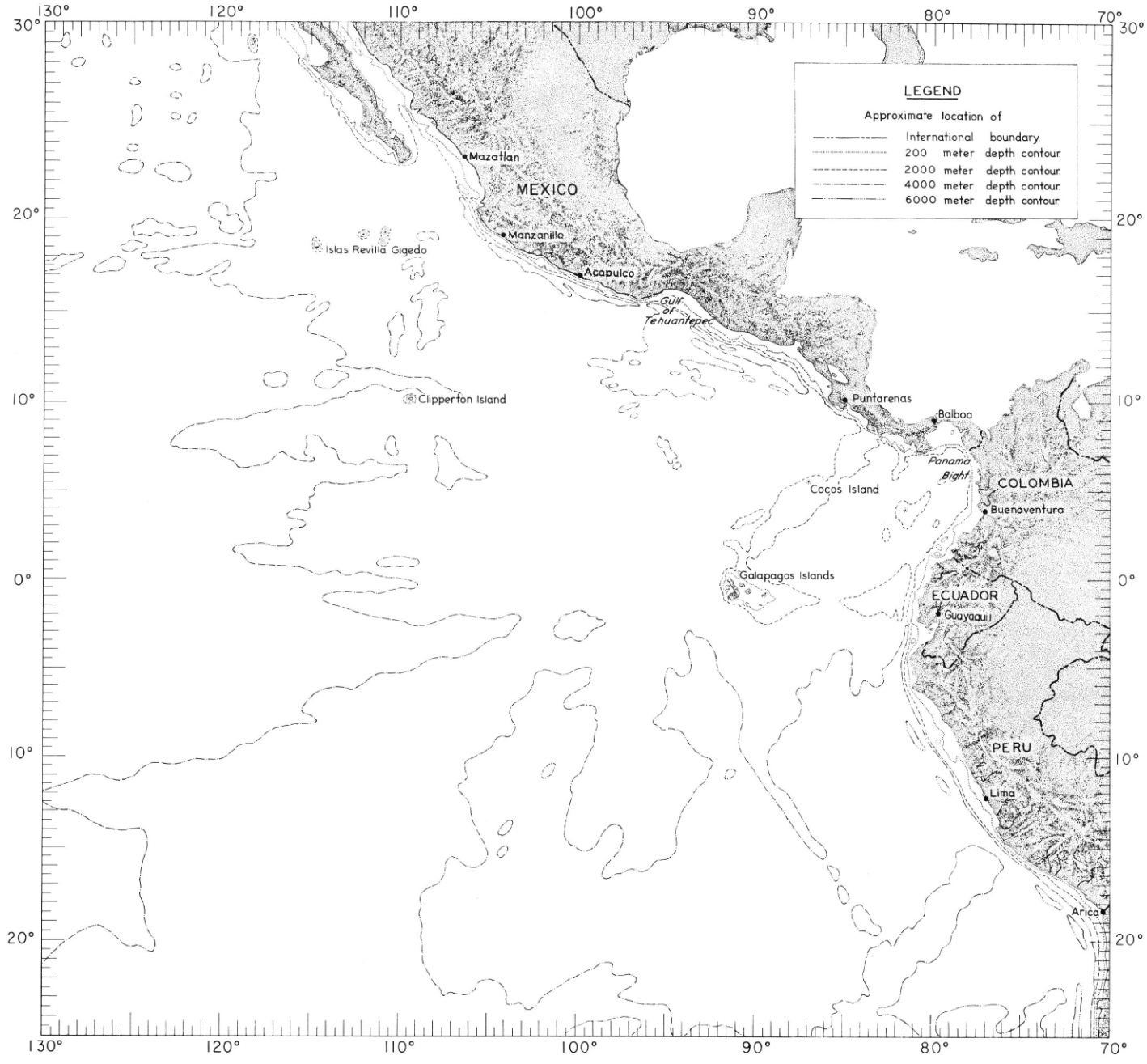


RM-a.

FIGURE RM-a. — Reference map of the main portion of the EASTROPAC area. The topographic shading and bathymetric contours are approximate only and should not be considered as portraying the latest available information.

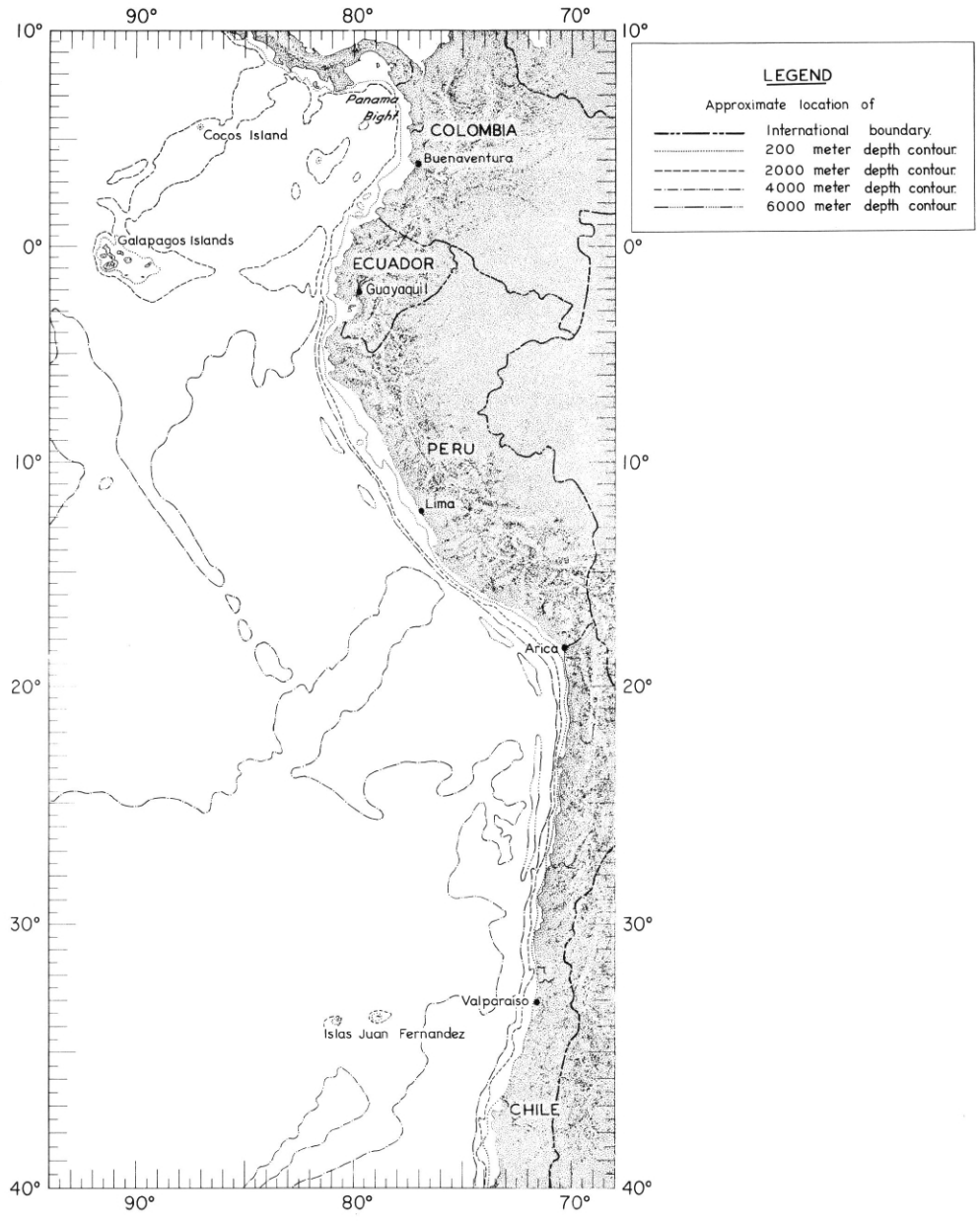


FIGURE RM-b — Reference map of the southern coastal portion of the EASTROPAC area. The topographic shading and bathymetric contours are approximate only and should not be considered as portraying the latest available information.

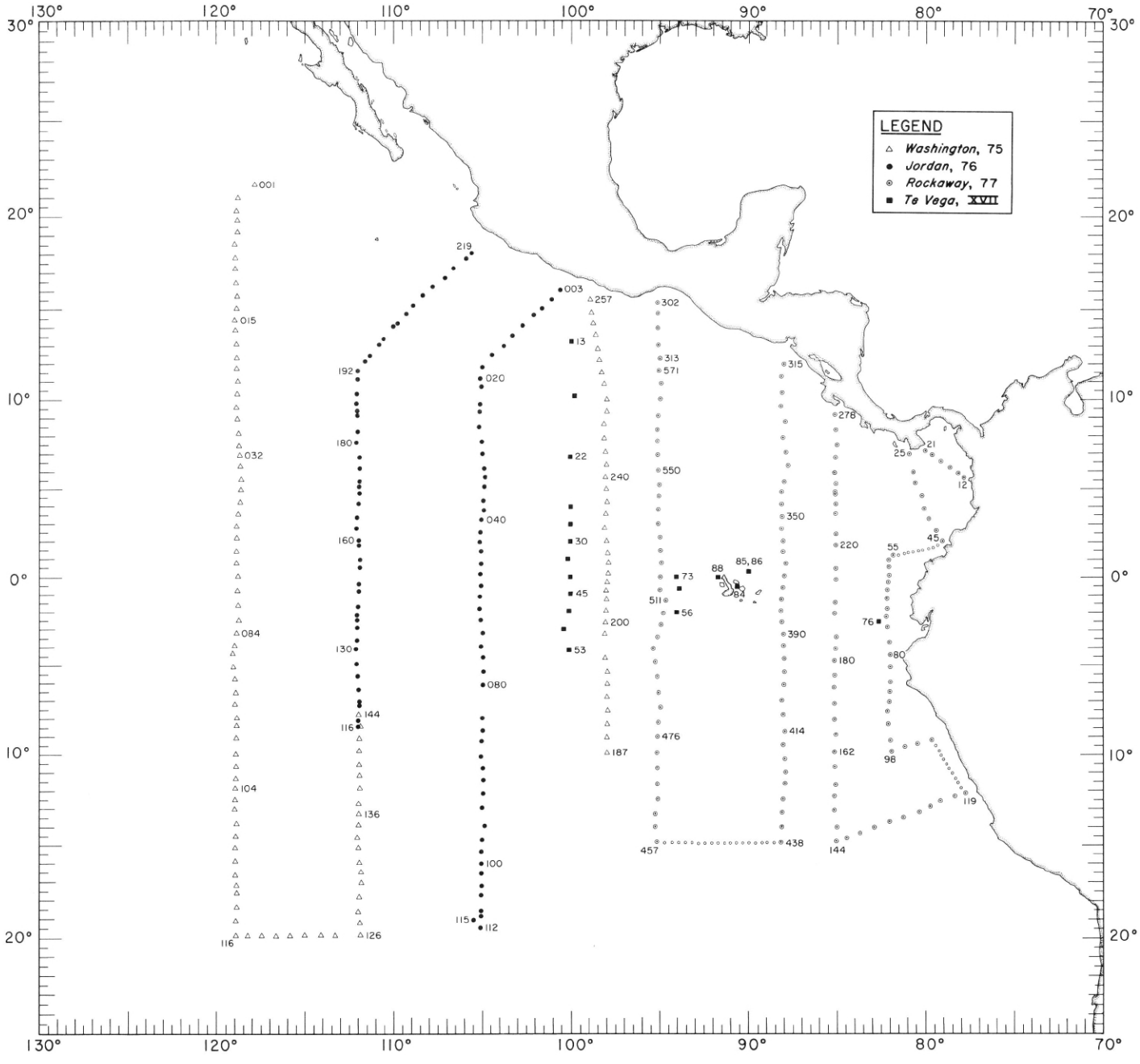


70-TC-a.

FIGURE 70-TC-a. — Locations of stations occupied by participating ships in the main portion of the EASTROPAC area during the third survey period, February-March 1968.

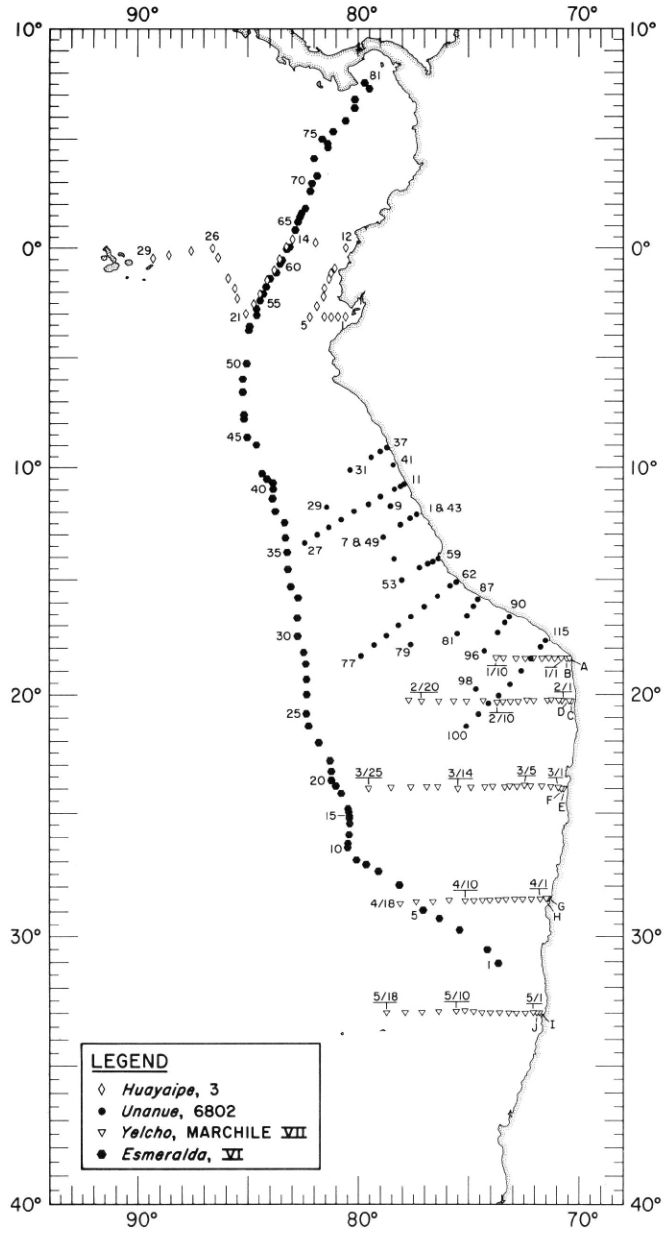


70-TC-b.

FIGURE 70-TC-b. — Locations of stations occupied by participating ships in the southern coastal portion of the EASTROPAC area during the third survey period, February-March 1968.

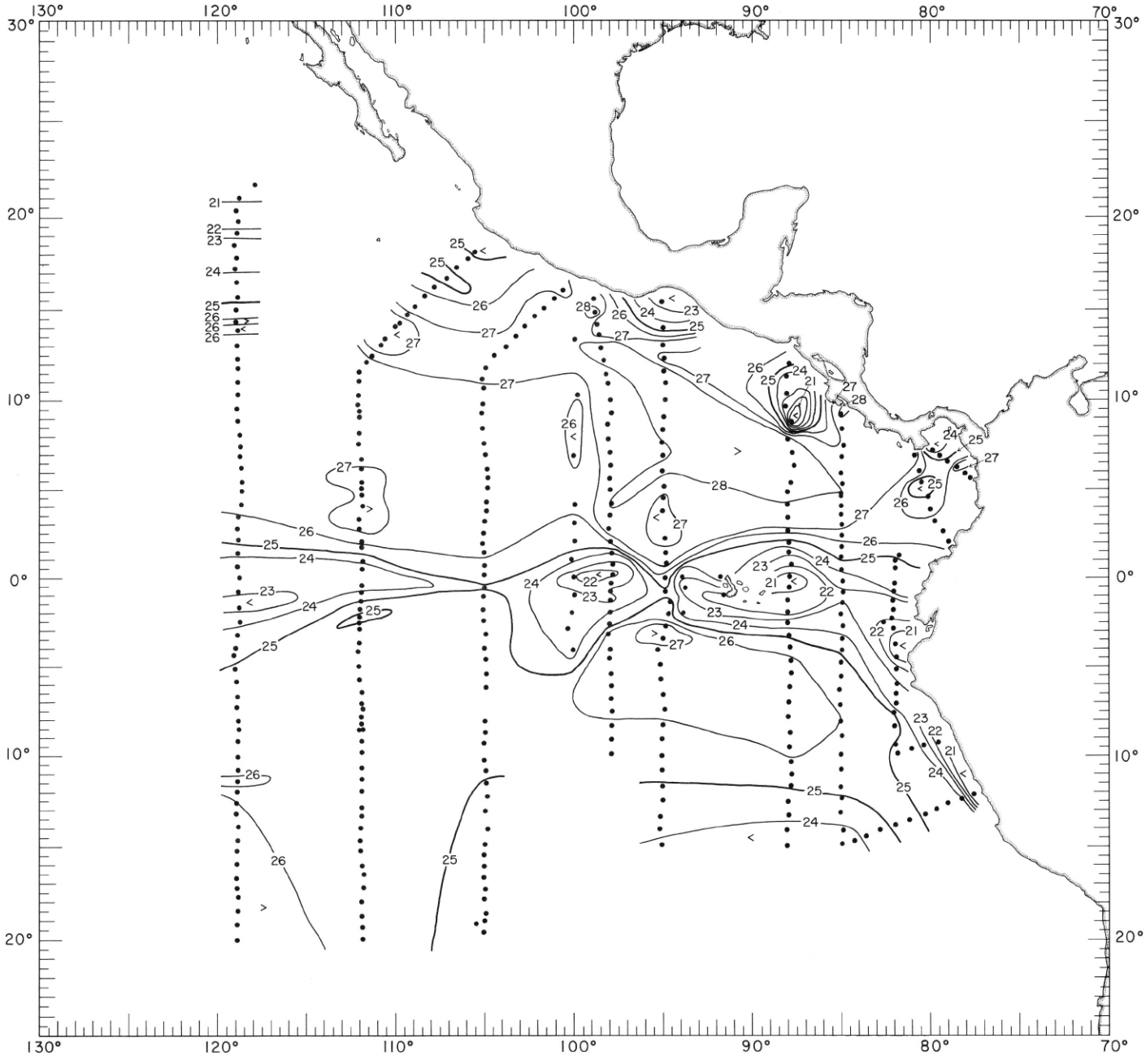


70-T-s(a).

FIGURE 70-T-s(a).—Temperature (°C.) at the sea surface in the main portion of the EASTROPAC area, February-March 1968. These contours are based on Nansen cast data.

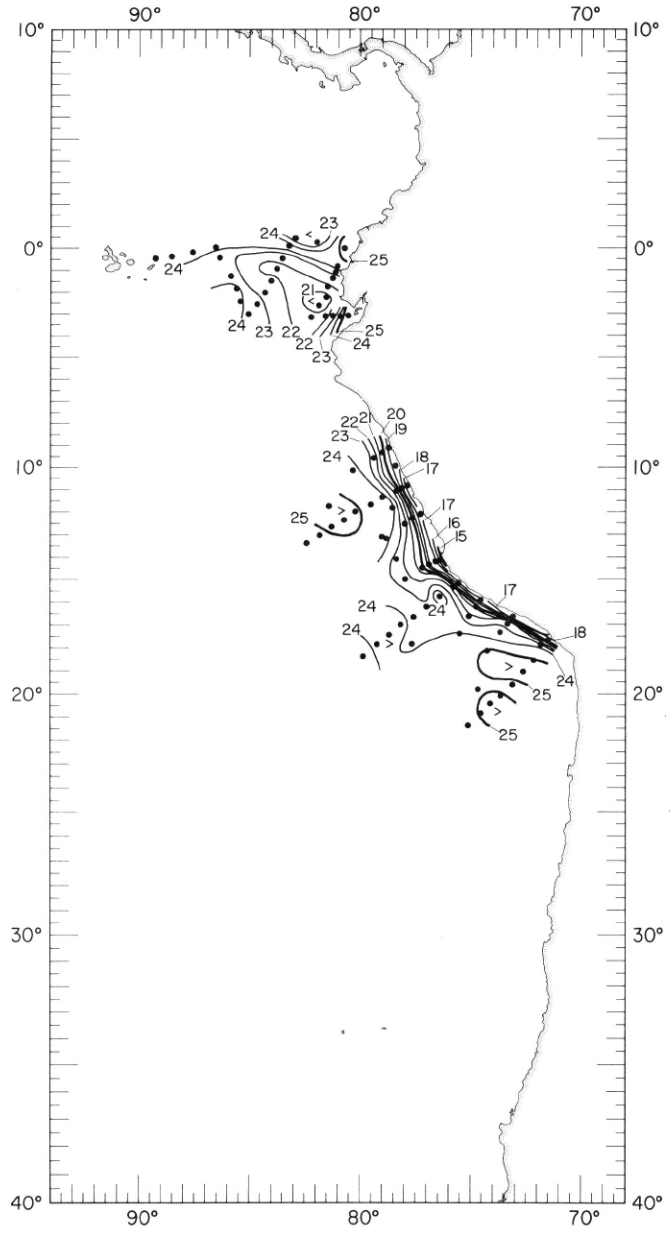


FIGURE 70-T-s(b).—Temperature (°C.) at the sea surface in the southern coastal portion of the EASTROPAC area, February-March 1968. These contours are based on Nansen cast data.

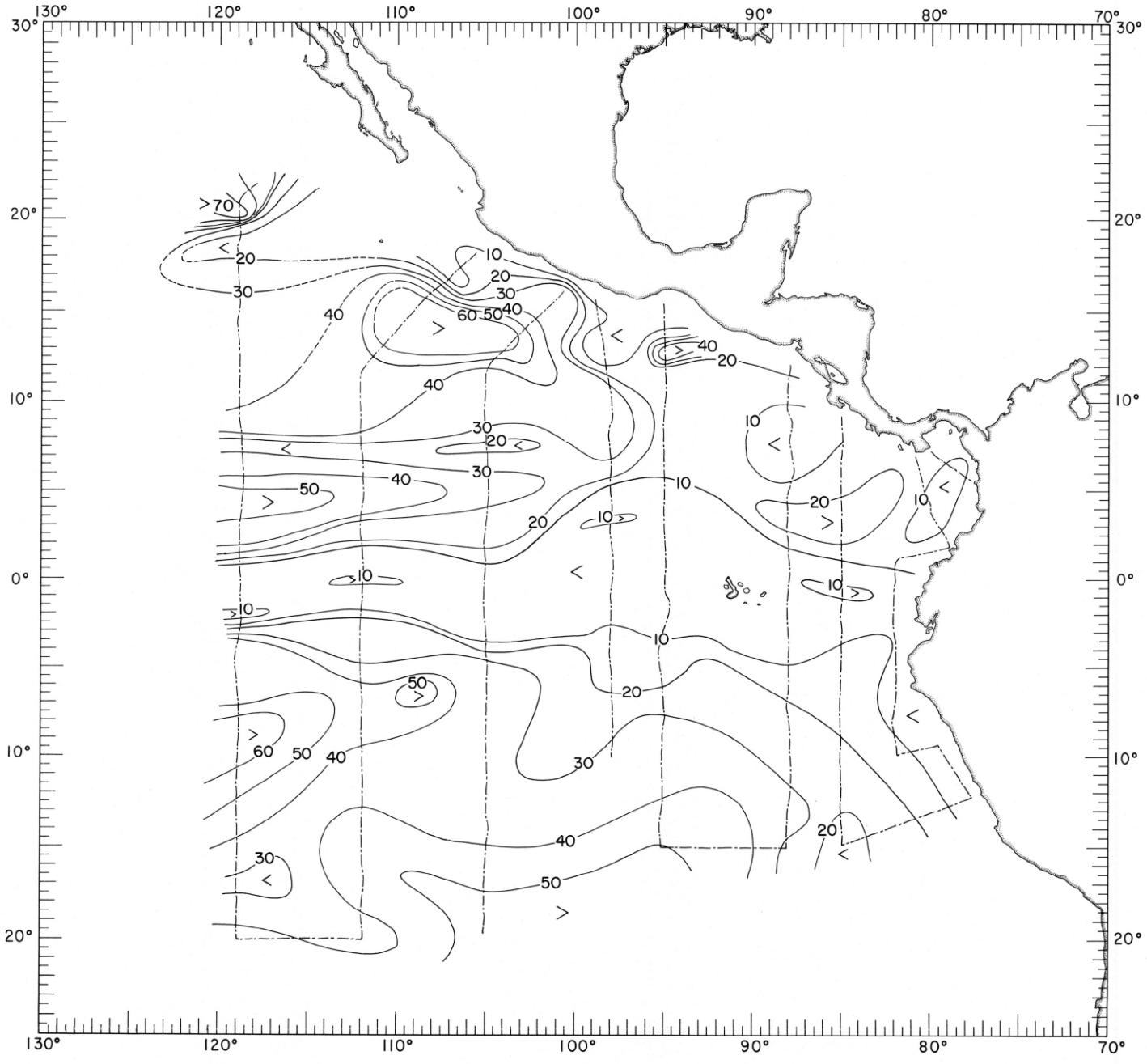


70-ML.

FIGURE 70-ML.—Thickness of the mixed layer in meters, February-March 1968. Dashed lines indicate portions of the cruise tracks where such data were collected.

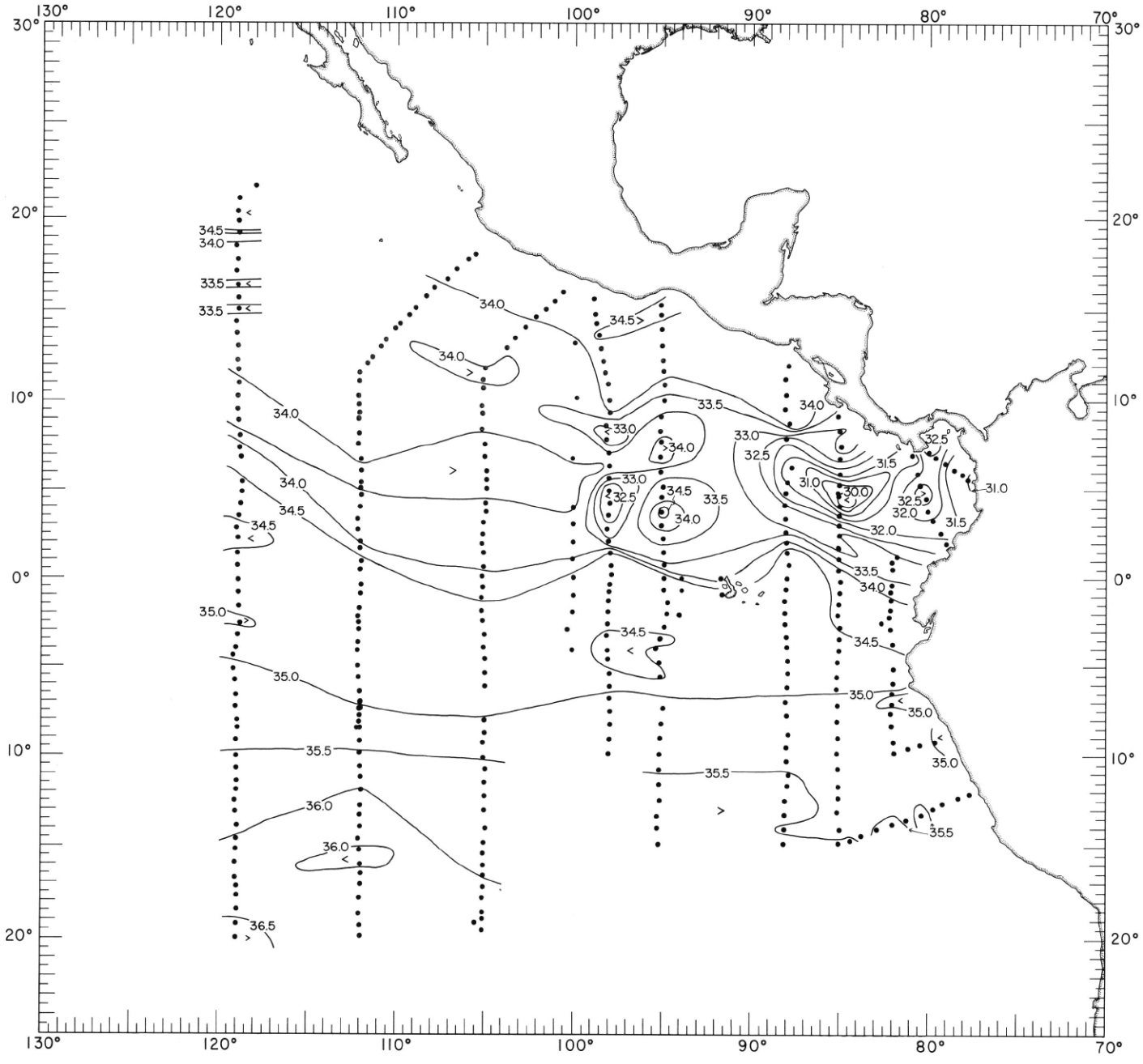


70-S-s(a).

FIGURE 70-S-s(a).—Salinity (‰) at the sea surface in the main portion of the EASTROPAC area, February-March 1968. These contours are based on Nansen cast data.

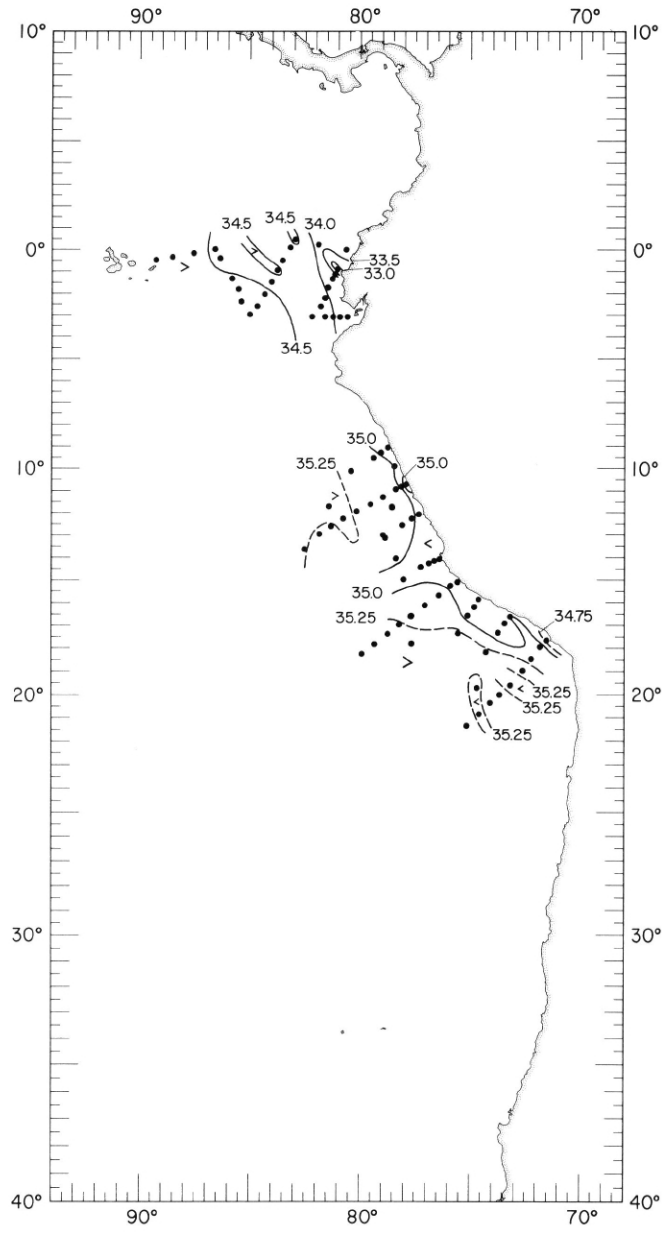


FIGURE 70-S-s(b).—Salinity (‰) at the sea surface in the southern coastal portion of the EASTROPAC area, February-March 1968. These contours are based on Nansen cast data.

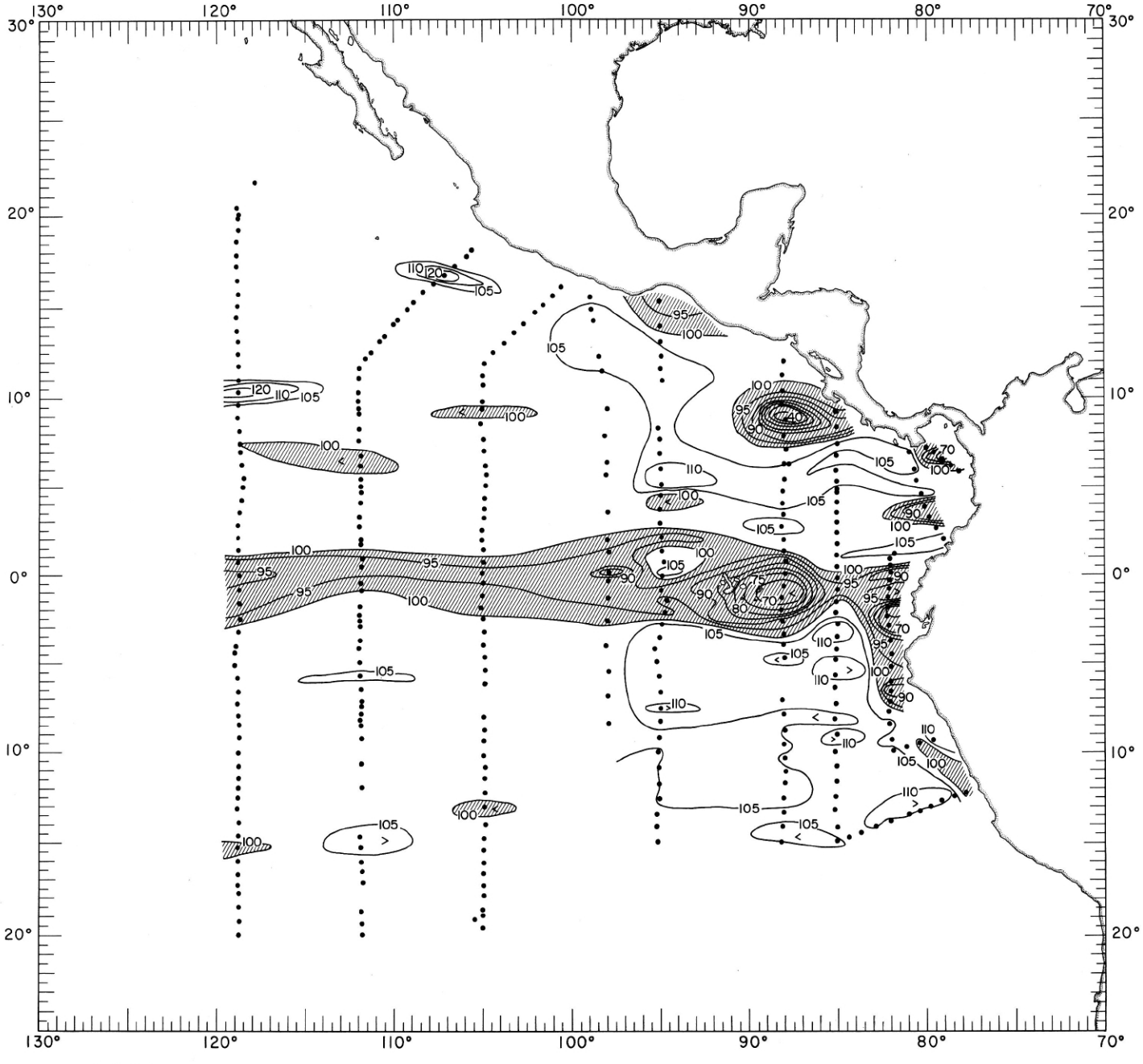


70-O₂Sa-10.

FIGURE 70-O₂Sa-10.—Oxygen saturation (%) at 10 meters, February-March 1968. Areas with less than 100% saturation are shaded.

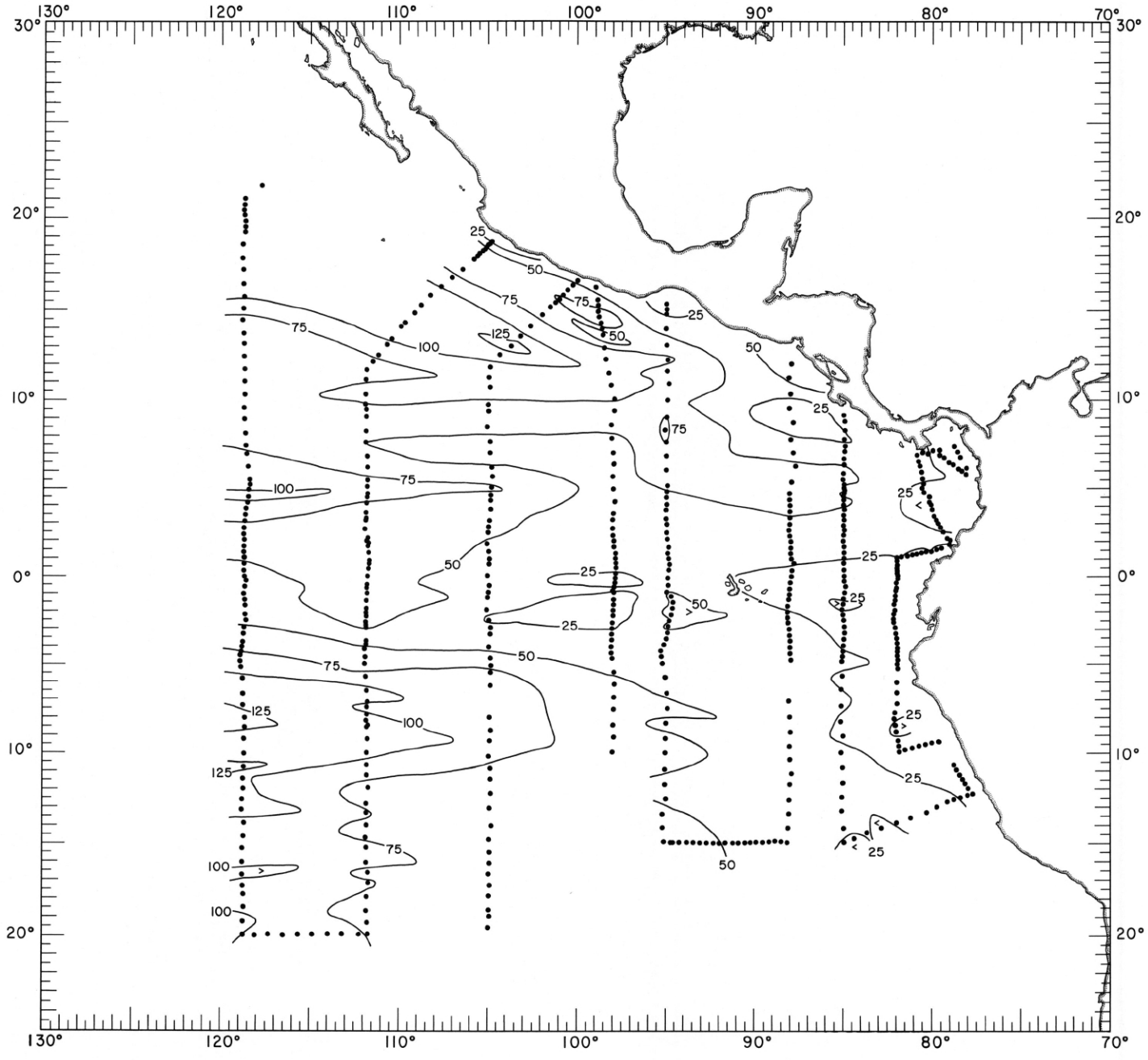


70-δ300-z.

FIGURE 70-δ300-z.—Depth (m.) of the surface where $\delta_T = 300$ cl./t., February-March 1968.

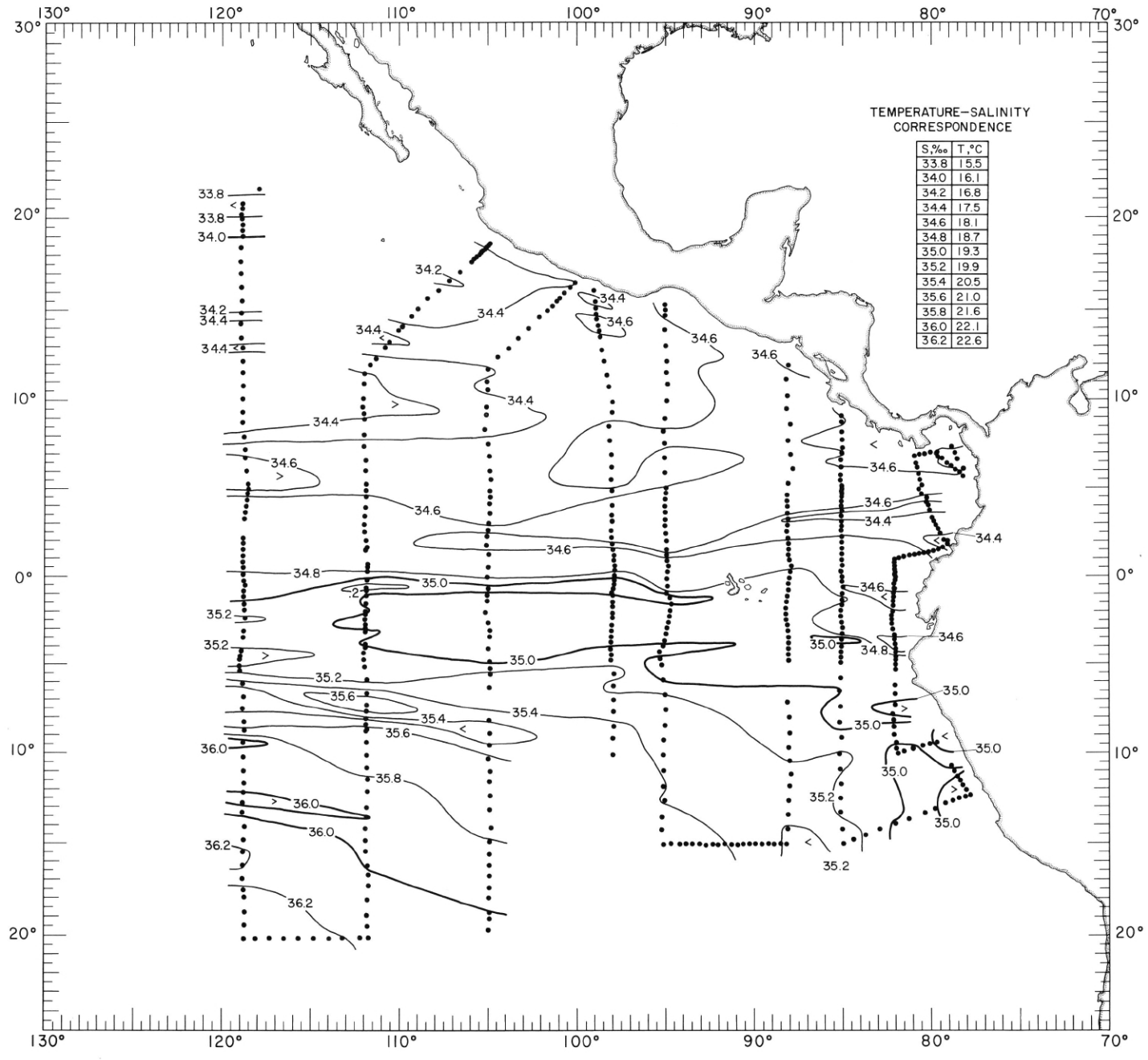


70-S-δ300.

FIGURE 70-S-δ300.—Salinity (‰) on the surface where $\delta_\tau = 300$ cl./t., February-March 1968. The table shows the temperature corresponding to each isohaline on the chart.

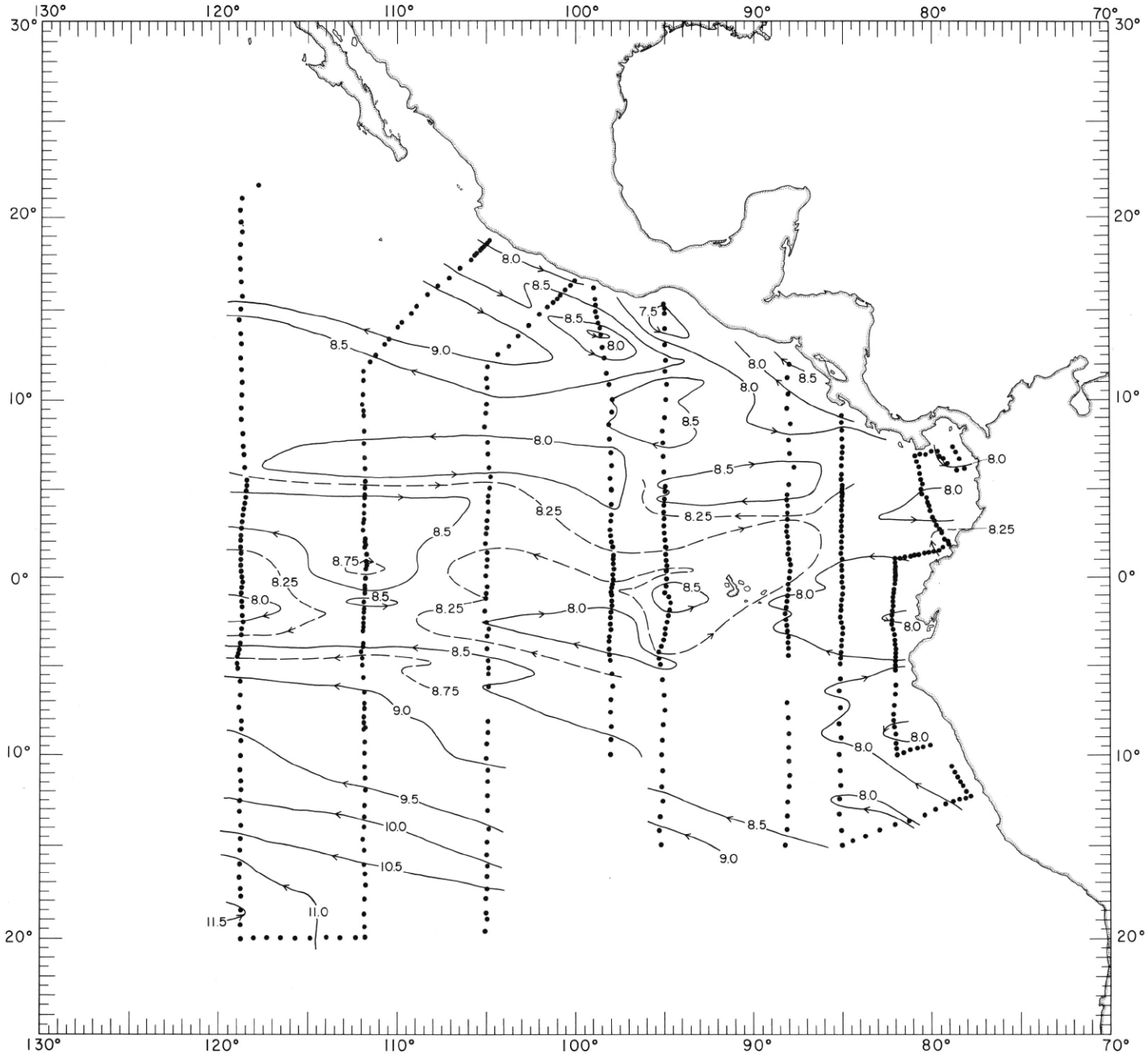


70-AP-δ300.

FIGURE 70-AP-δ300.—Acceleration potential (j./kg.), relative to 500 db., on the surface where $\delta_T = 300$ cl./t., February-March 1968. For computing acceleration potential, thermosteric anomaly, $\delta_T$, was used instead of specific volume anomaly, $\delta$.

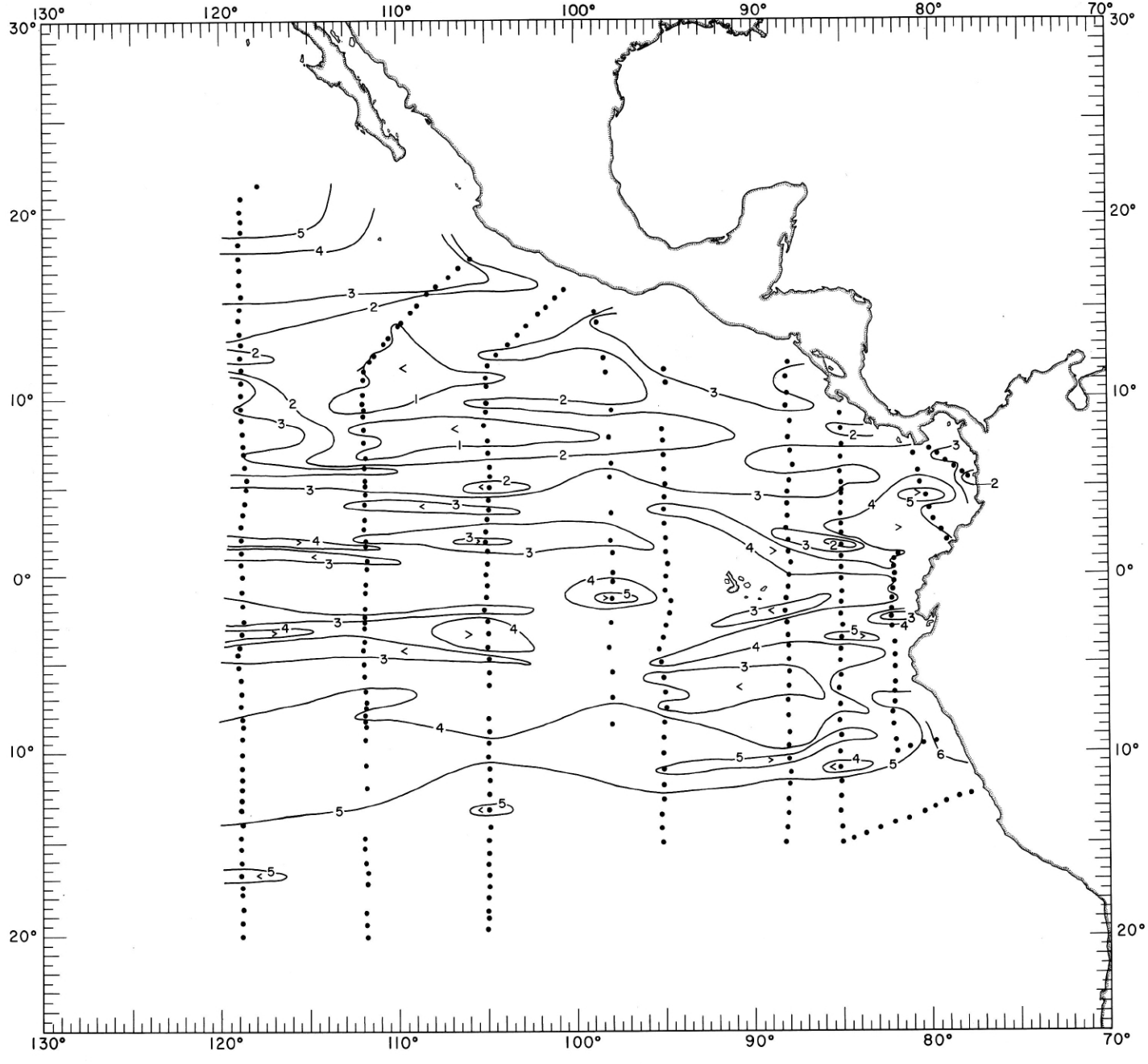


FIGURE 70-$O_2$-$\delta$300.—Oxygen (ml./l.) on the surface where $\delta_\tau = 300$ cl./t., February-March 1968.

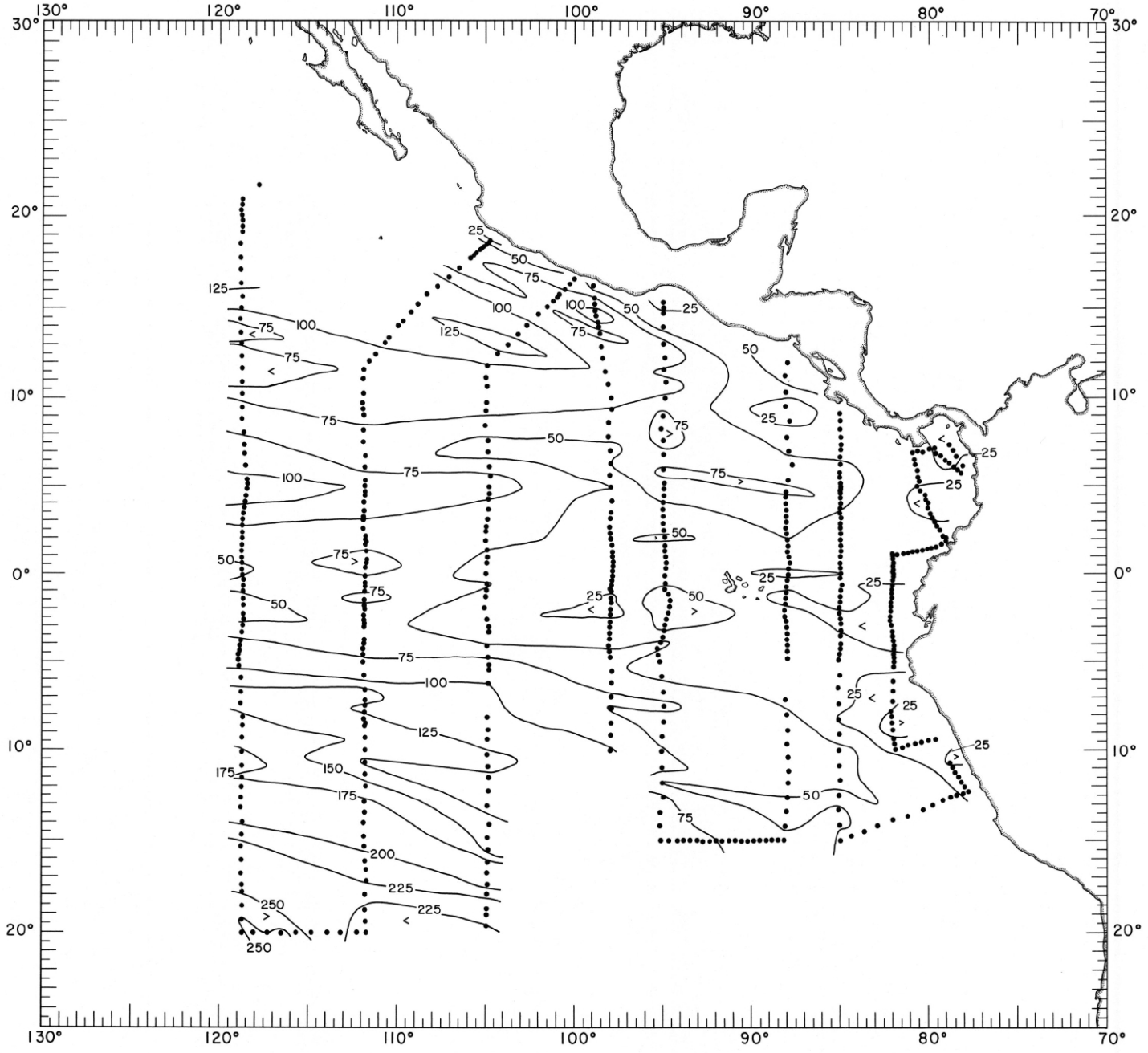


FIGURE 70-δ250-z.—Depth (m.) of the surface where $\delta_\tau = 250$ cl./t., February-March 1968.

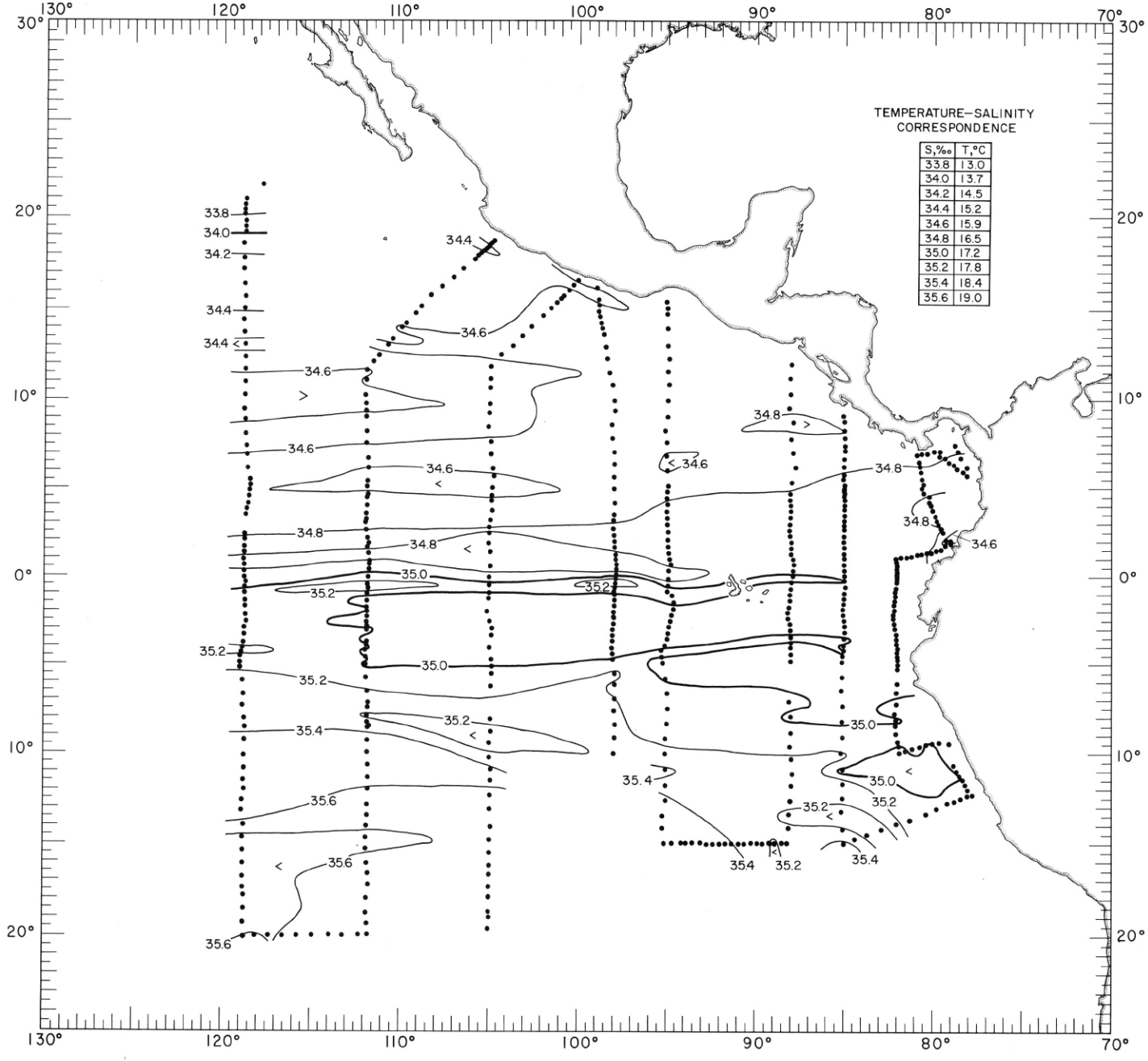


70-S-δ250.

FIGURE 70-S-δ250.—Salinity (‰) on the surface where $\delta_{\pi} = 250$ cl./t., February-March 1968. The table shows the temperature corresponding to each isohaline on the chart.

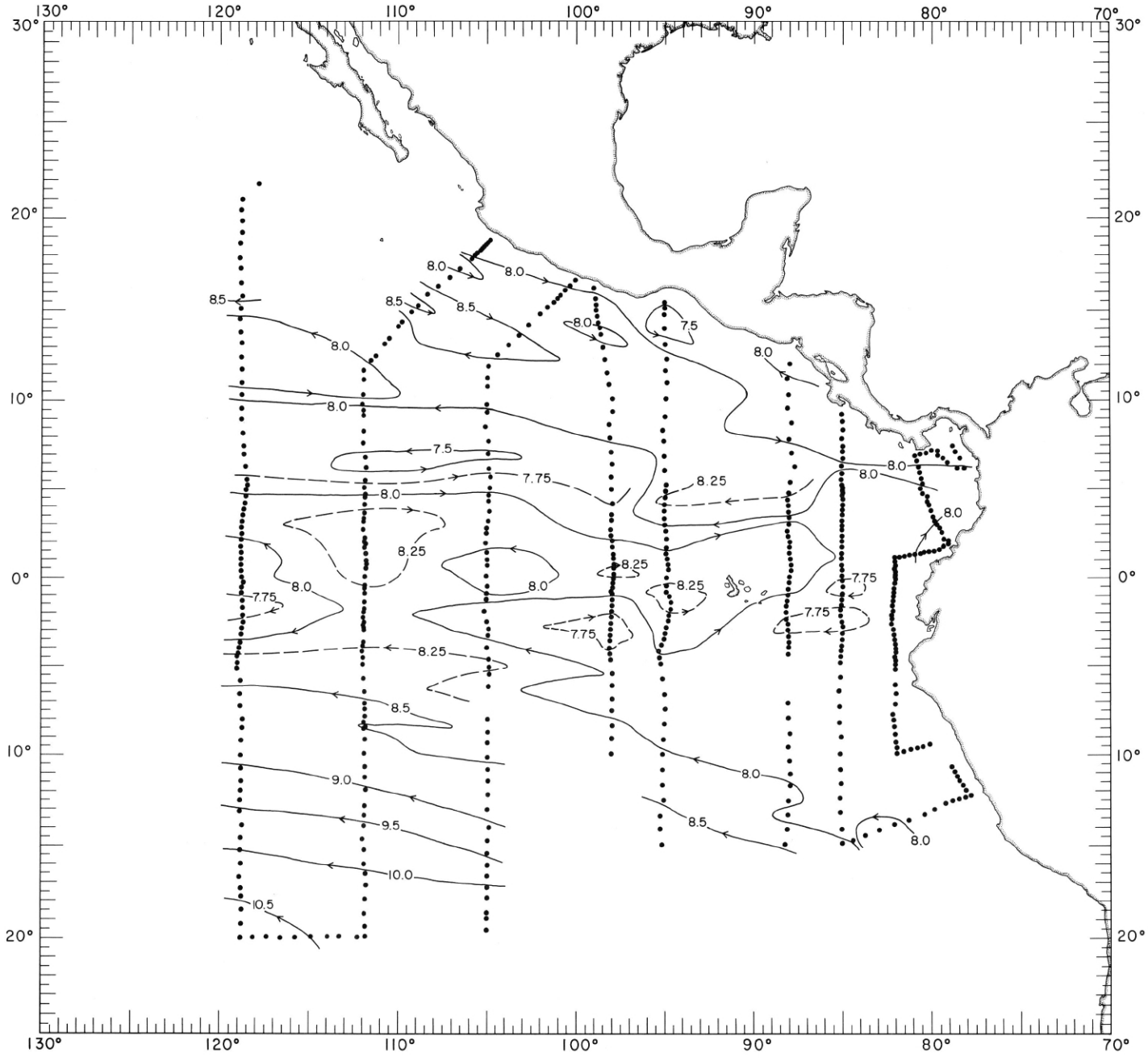


70-AP-δ250.

FIGURE 70-AP-δ250.—Acceleration potential (j./kg.), relative to 500 db., on the surface where $\delta_\tau = 250$ cl./t., February-March 1968. For computing acceleration potential, thermosteric anomaly, $\delta_\tau$, was used instead of specific volume anomaly, $\delta$.

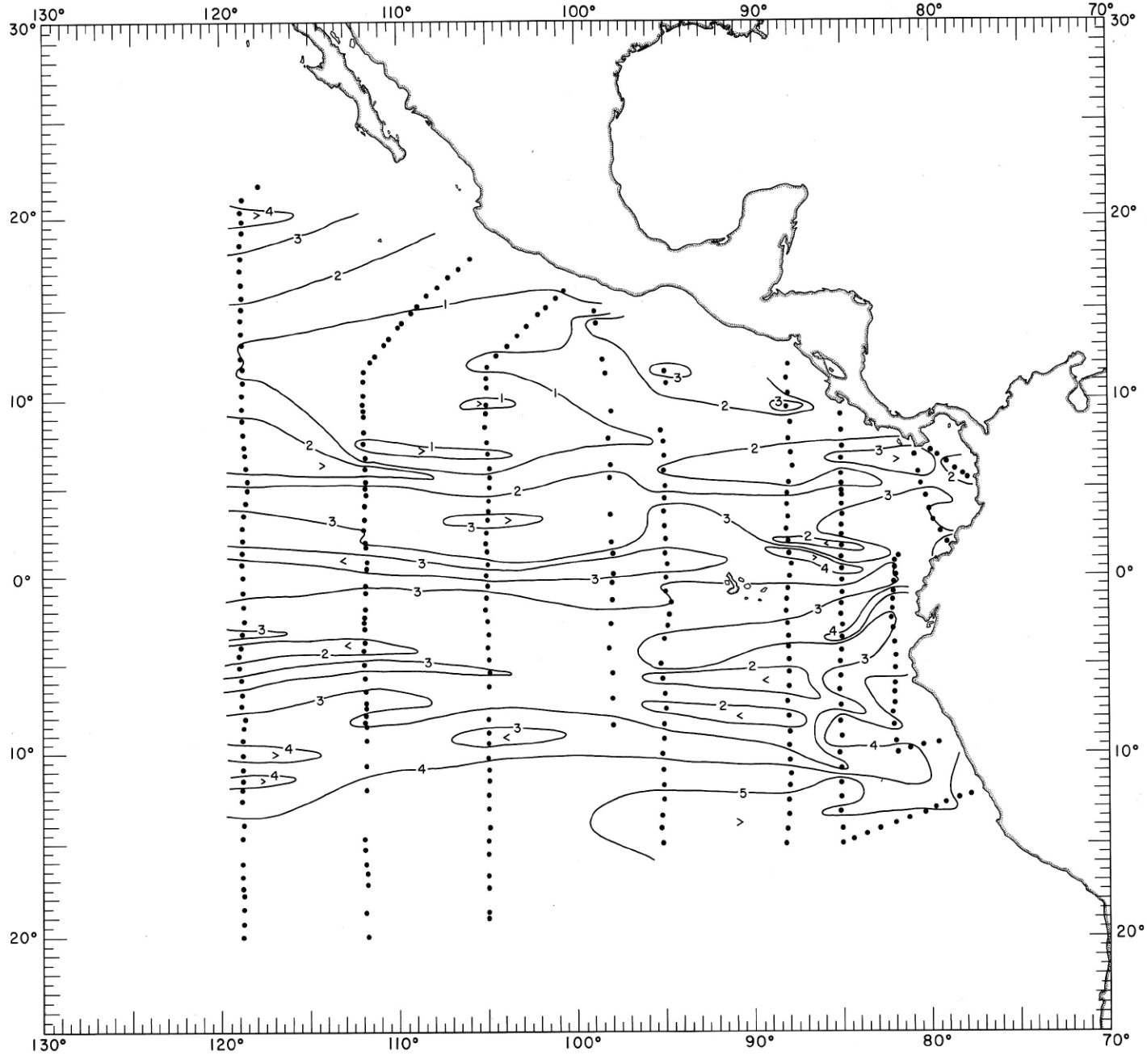


FIGURE 70-$O_2$-$\delta$250.—Oxygen (ml./l.) on the surface where $\delta_x = 250$ cl./t., February-March 1968.

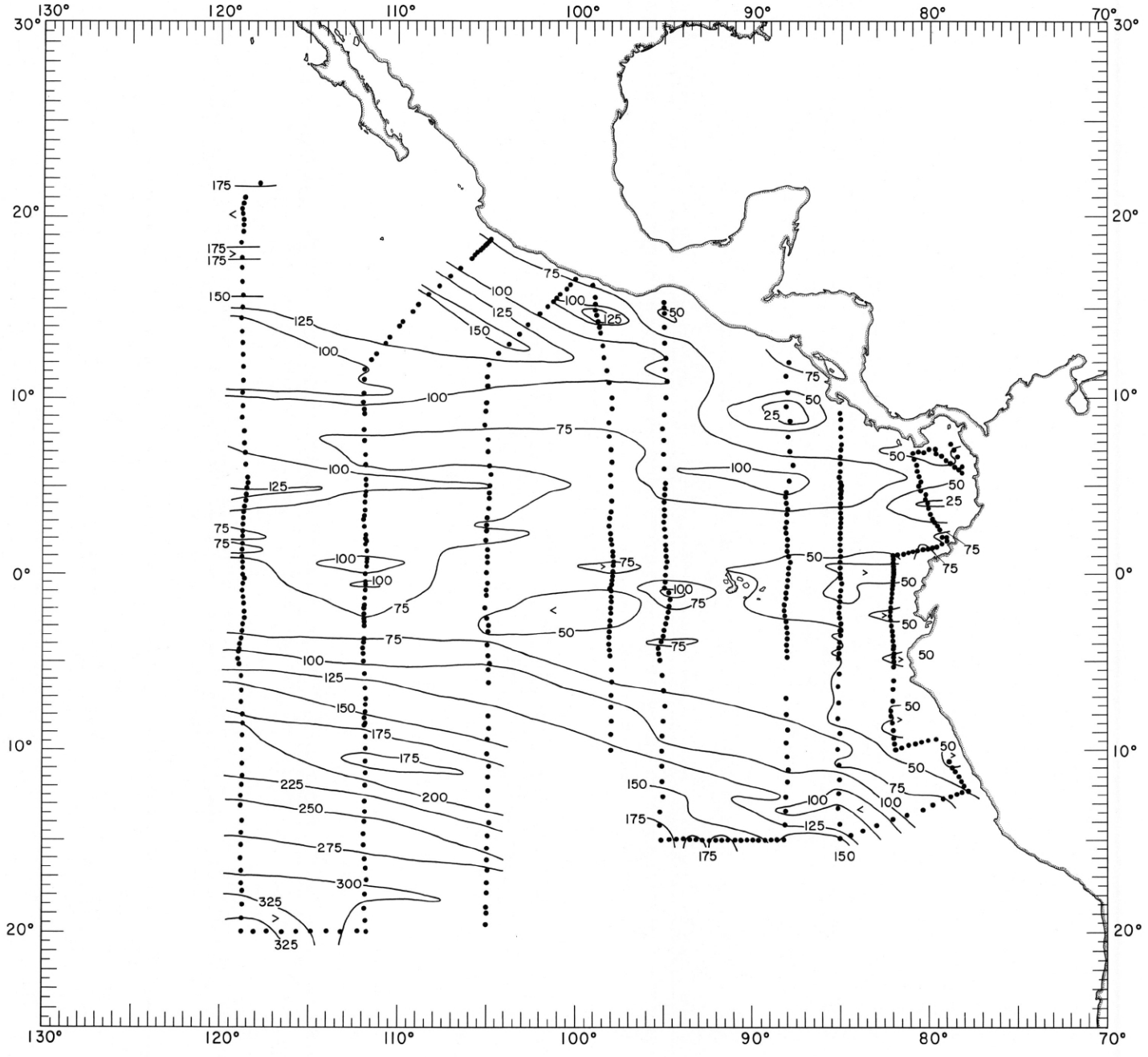


FIGURE 70-δ200-z.—Depth (m.) of the surface where $\delta_\tau = 200$ cl./t., February-March 1968.

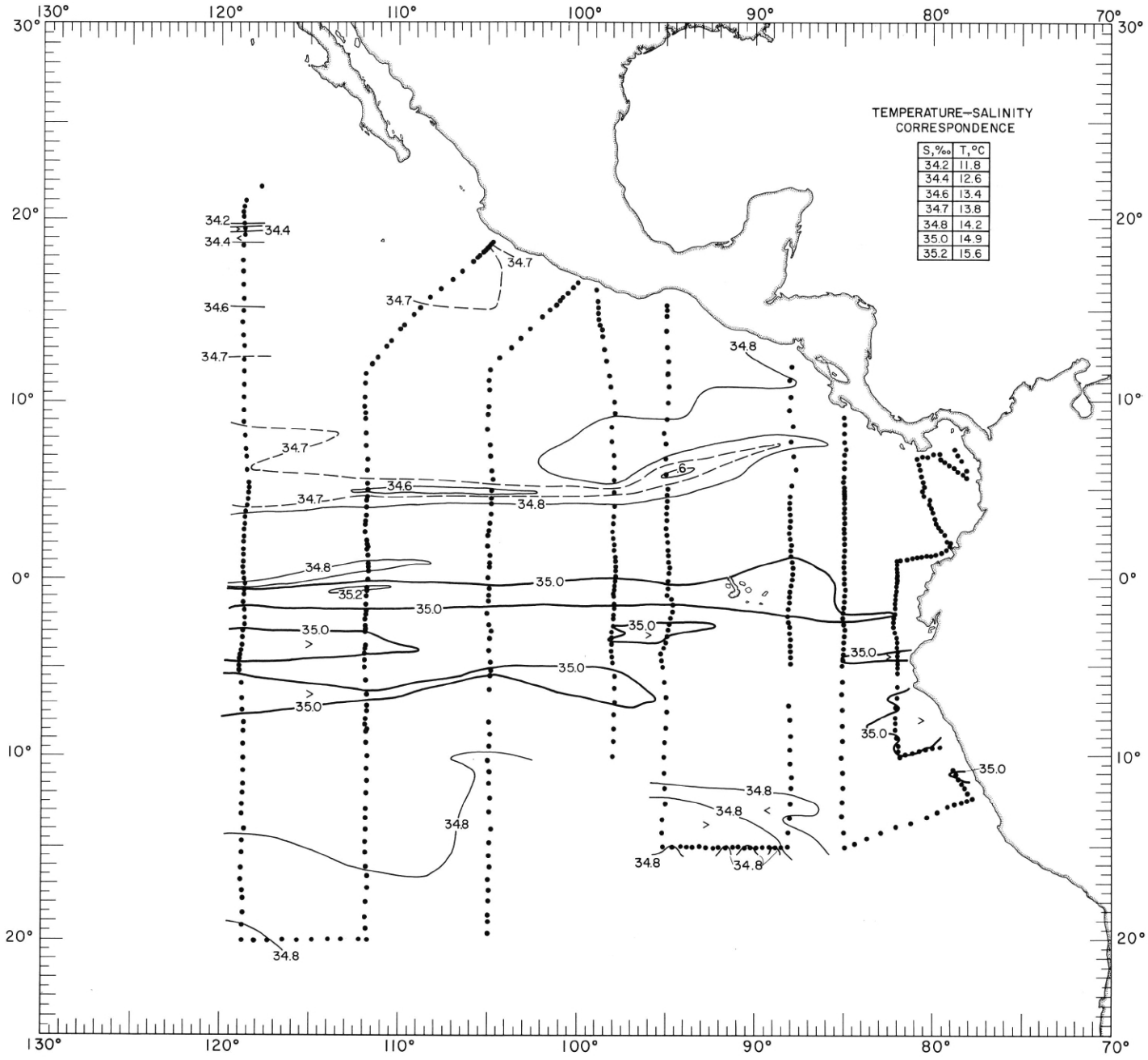


70-S-δ200.

FIGURE 70-S-δ200.—Salinity (‰) on the surface where $\delta_T = 200$ cl./t., February-March 1968. The table shows the temperature corresponding to each isohaline on the chart.

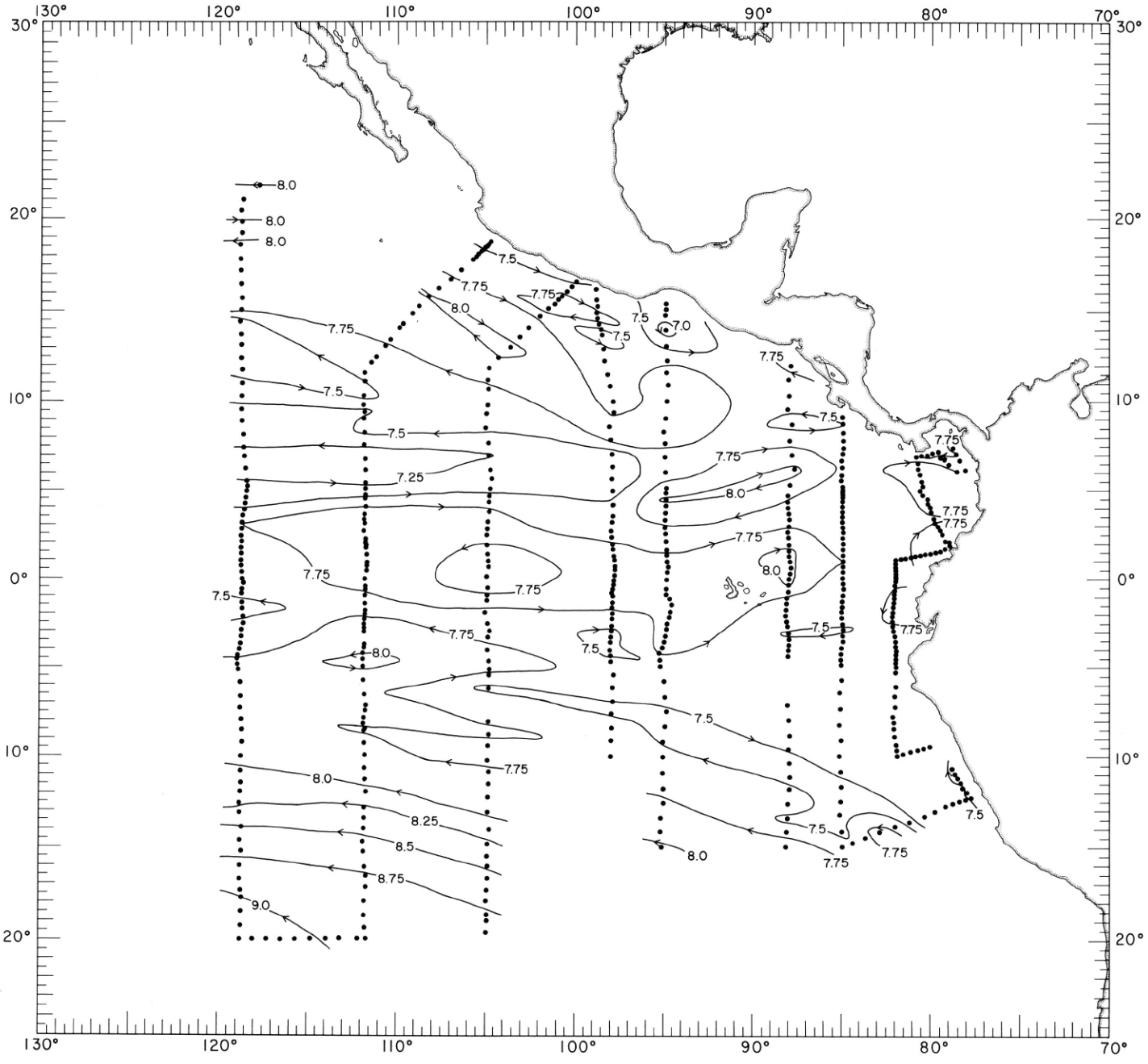


70-AP-δ200.

FIGURE 70-AP-δ200.—Acceleration potential (j./kg.), relative to 500 db., on the surface where $\delta_\tau = 200$ cl./t., February-March 1968. For computing acceleration potential, thermosteric anomaly, $\delta_\tau$, was used instead of specific volume anomaly, $\delta$.

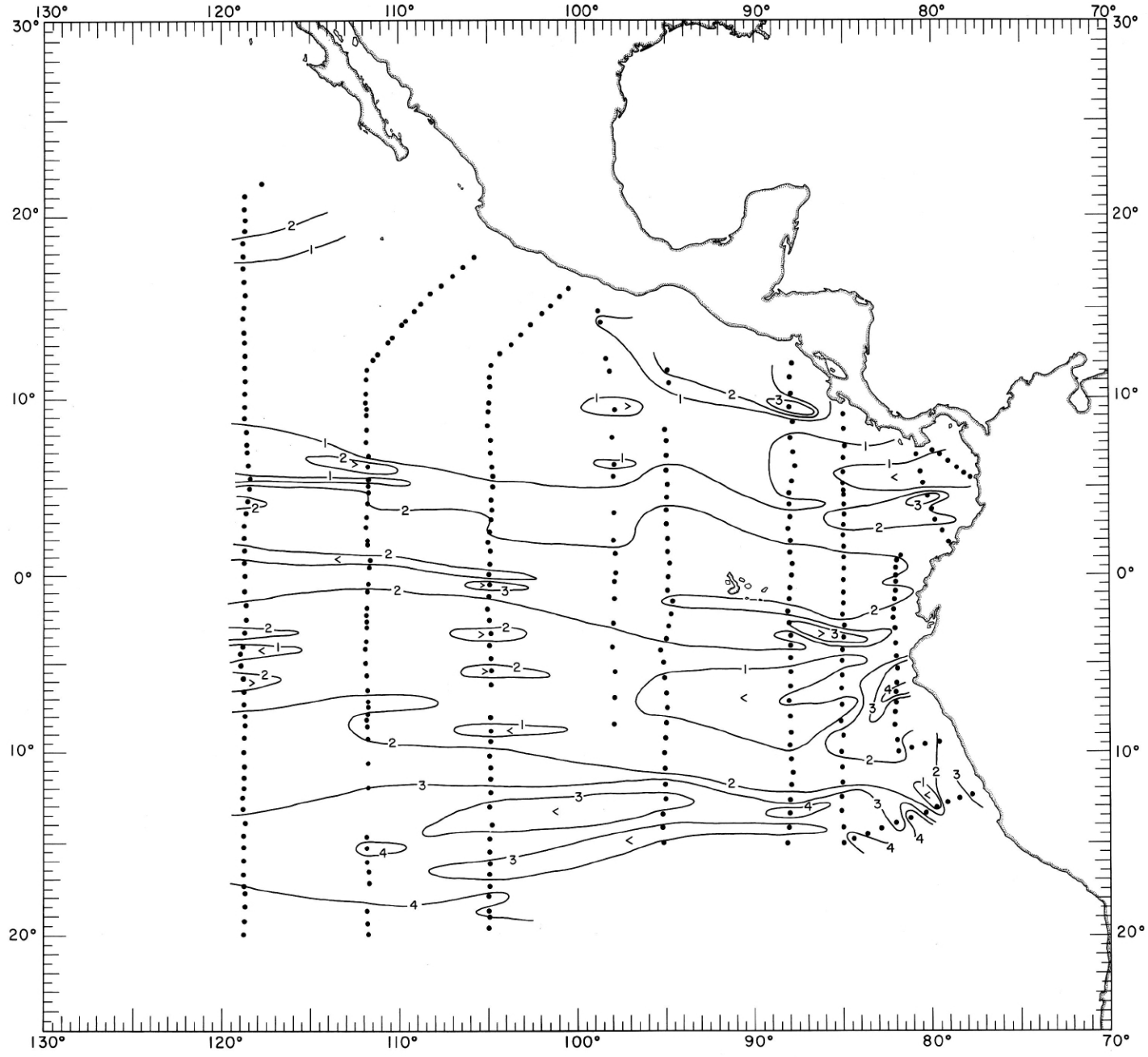


70-$O_2$-$\delta$200.

FIGURE 70-$O_2$-$\delta$200.—Oxygen (ml./l.) on the surface where $\delta_T = 200$ cl./t., February-March 1968.

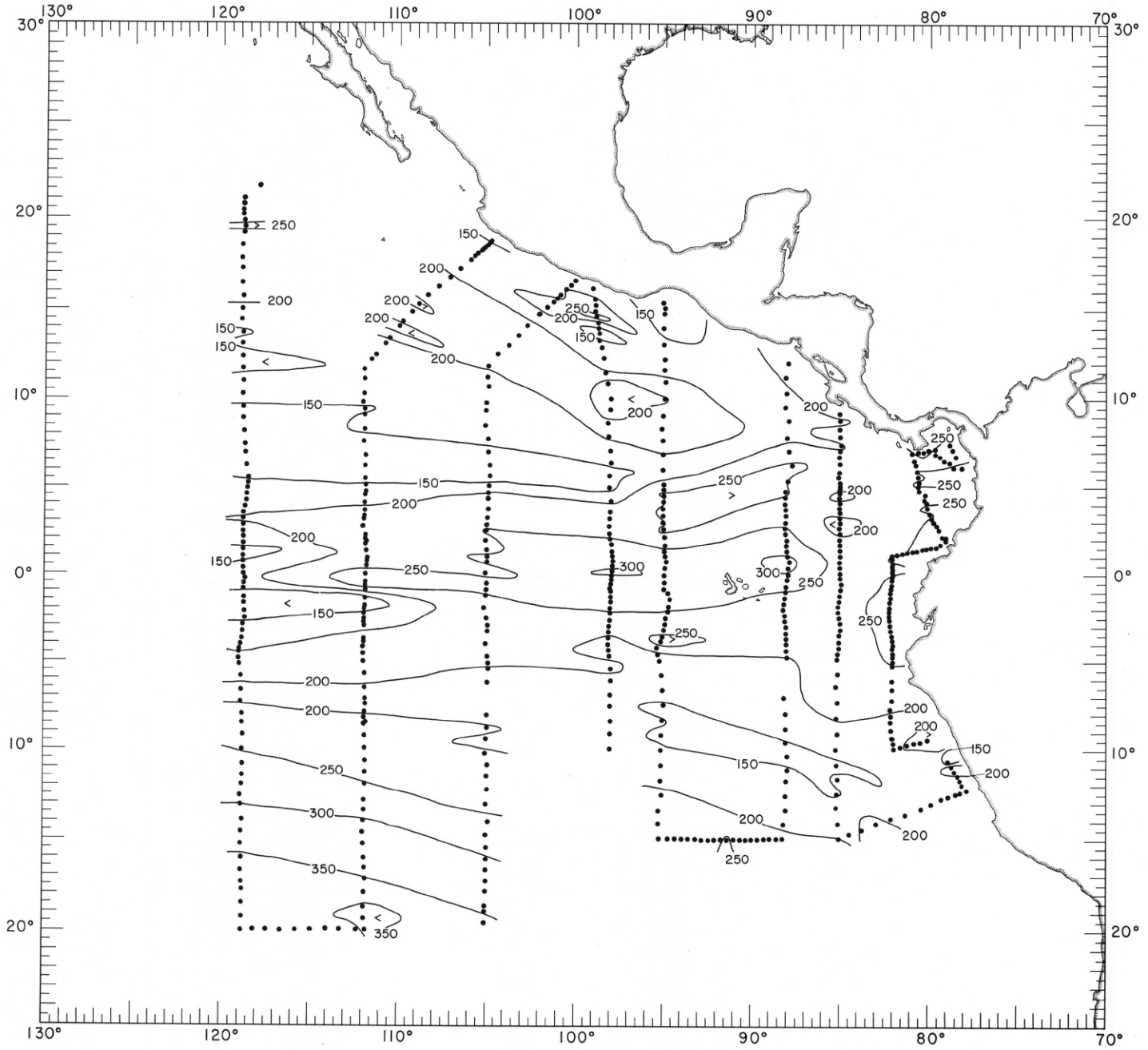


FIGURE 70-δ160-z.—Depth (m.) of the surface where $\delta_\tau = 160$ cl./t., February-March 1968.

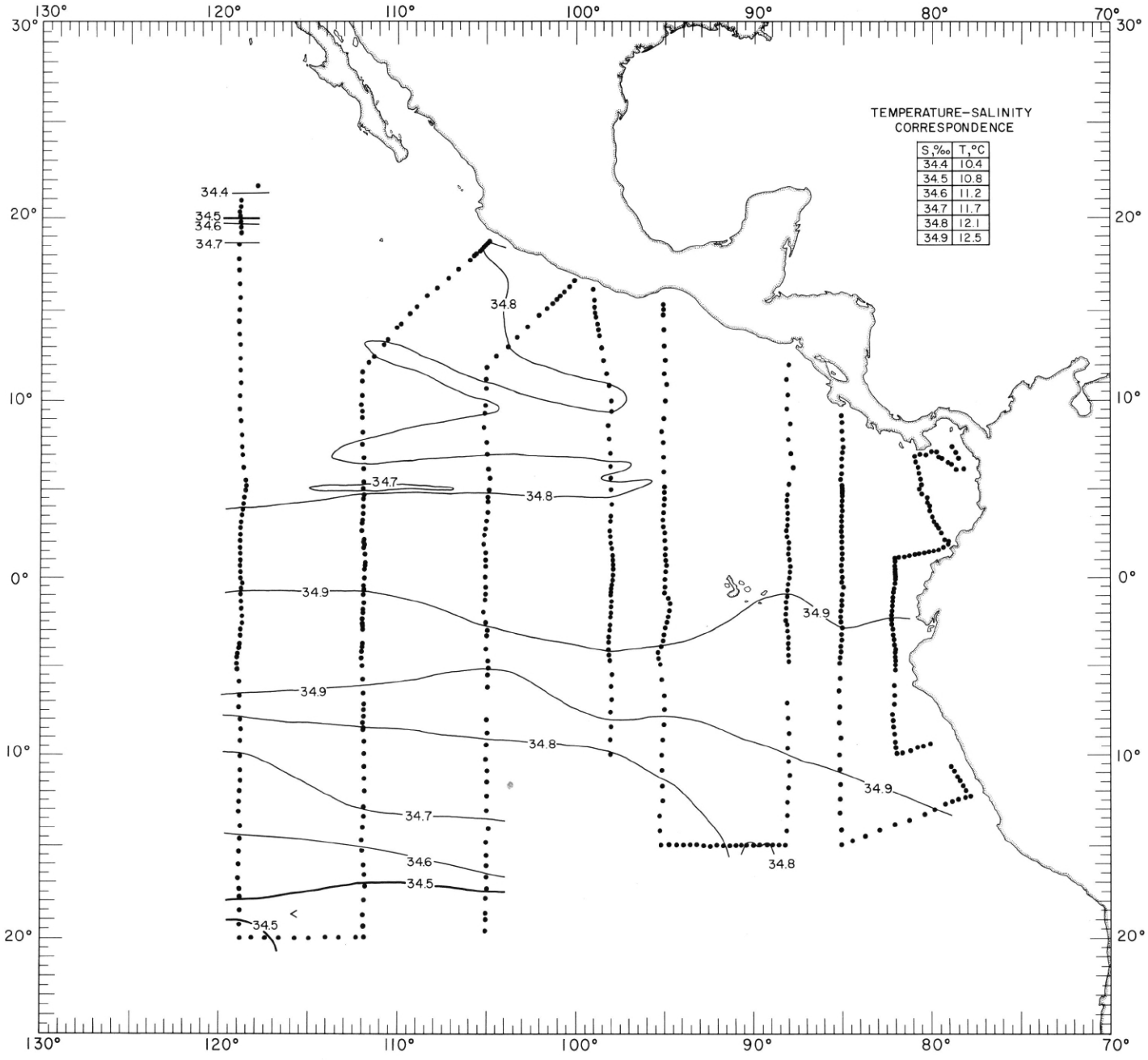


70-S-δ160.

FIGURE 70-S-δ160.—Salinity (‰) on the surface where $\delta_\tau = 160$ cl./t., February-March 1968. The table shows the temperature corresponding to each isohaline on the chart.

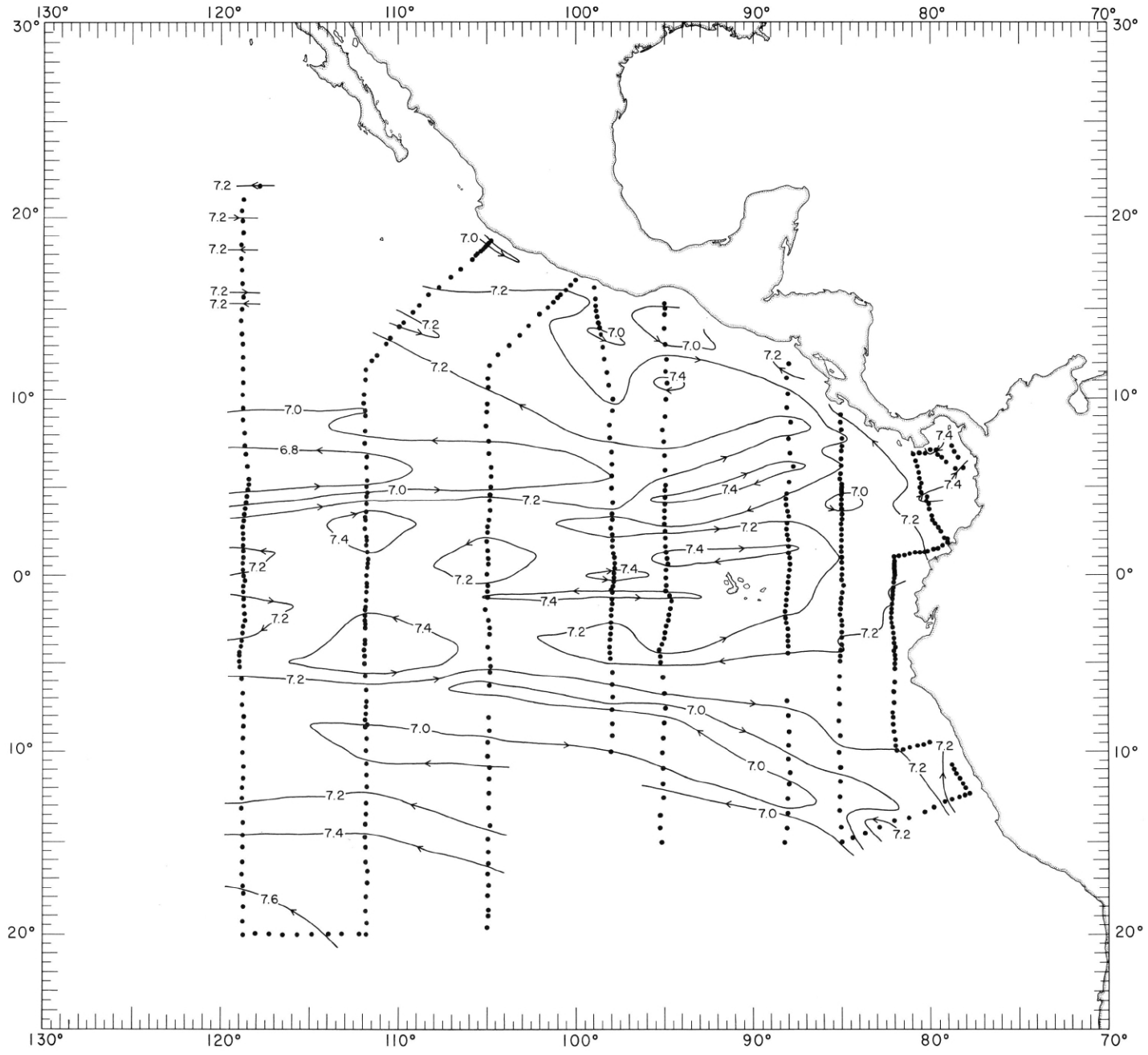


70-AP-δ160.

FIGURE 70-AP-δ160.—Acceleration potential (j./kg.), relative to 500 db., on the surface where $\delta_\tau = 160$ cl./t., February-March 1968. For computing acceleration potential, thermosteric anomaly, $\delta_\tau$, was used instead of specific volume anomaly, $\delta$.

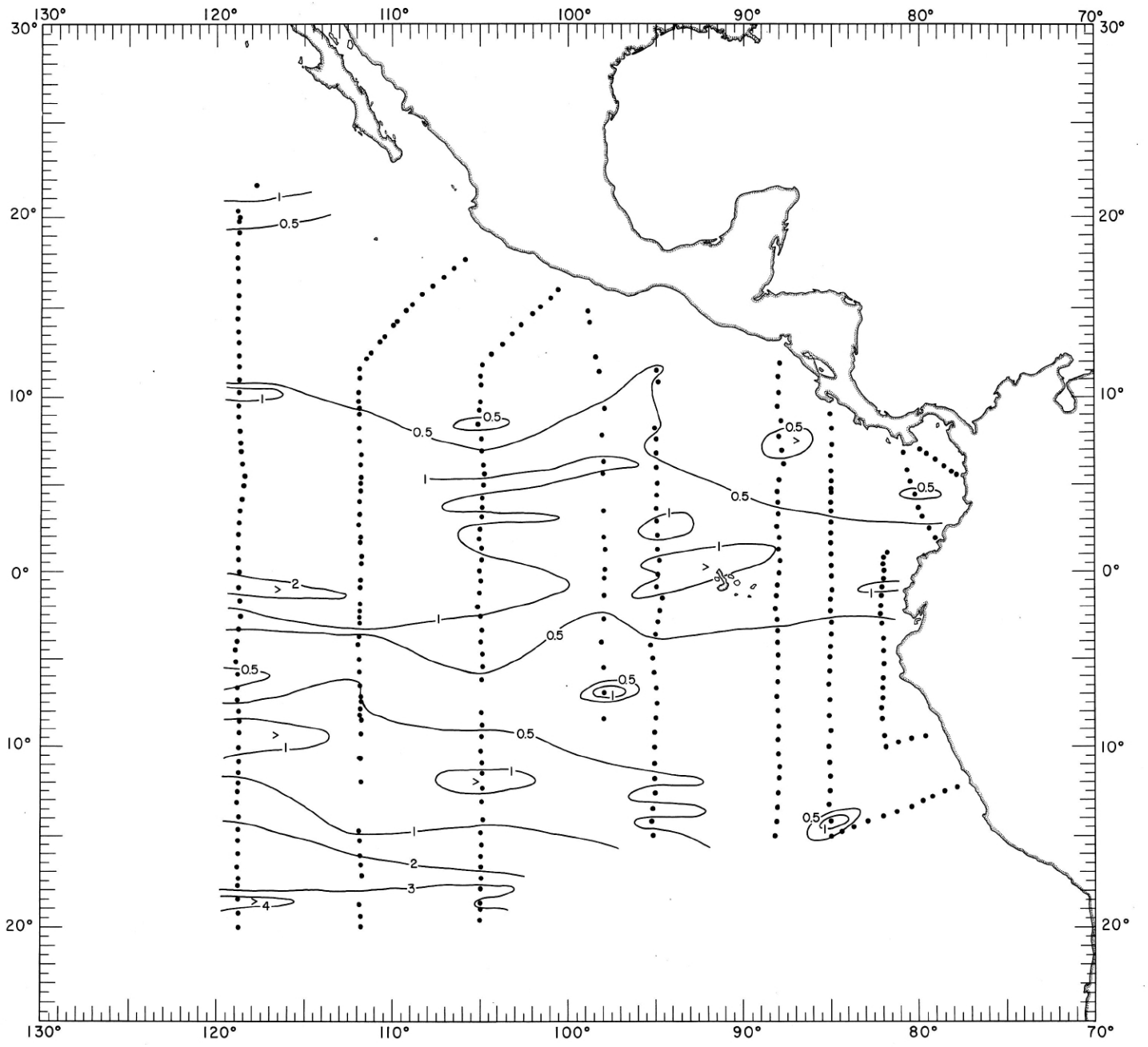


FIGURE 70-$O_2$-$\delta$160.—Oxygen (ml./l.) on the surface where $\delta_T = 160$ cl./t., February-March 1968.

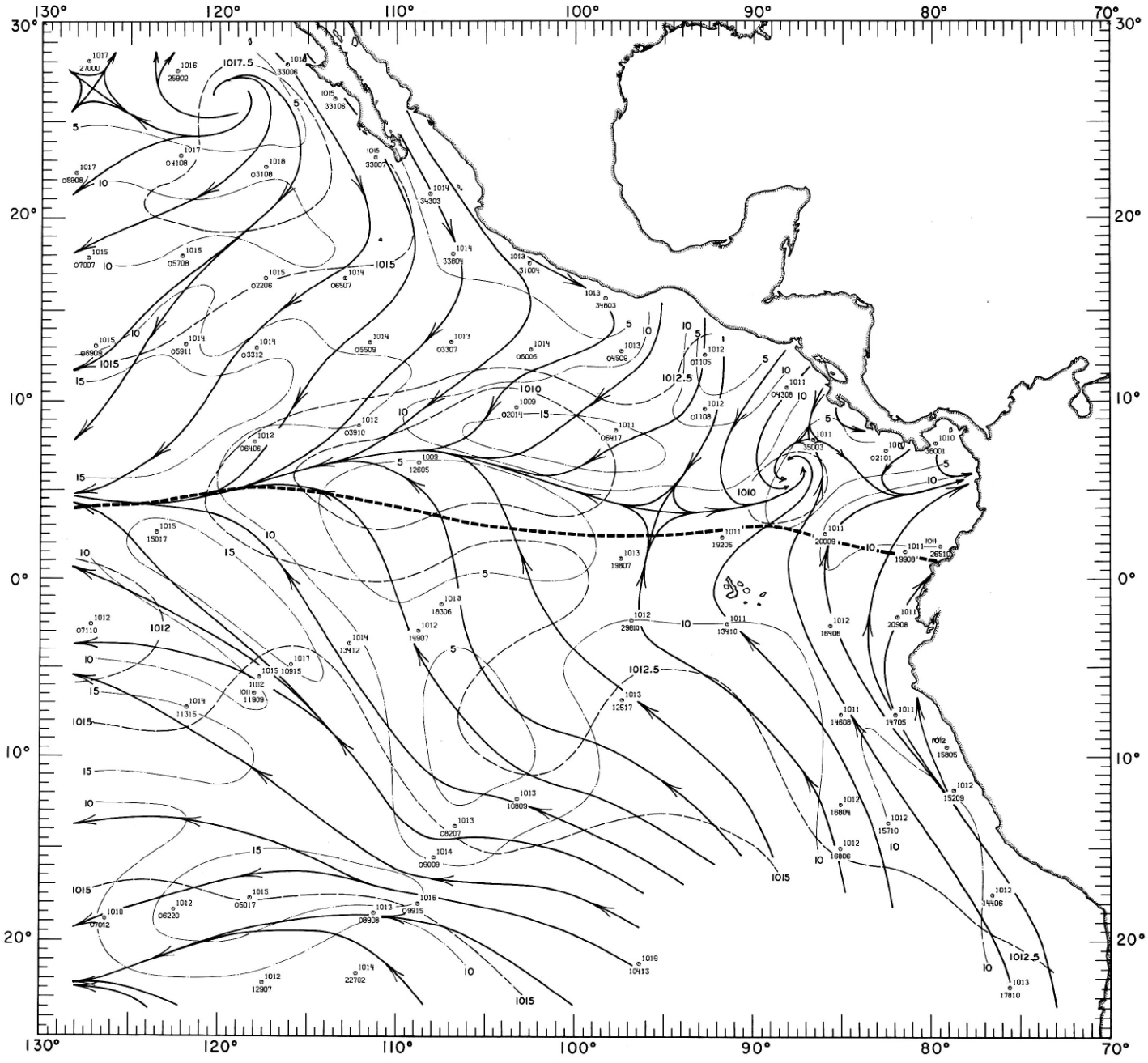


70-MW-1.

FIGURE 70-MW-1.—Analyses of the surface air pressure and surface winds from all available ship observations, averaged over 2-degree (latitude-longitude) squares for the period February 1-15, 1968. Heavy dashed lines are isobars. Solid lines are streamlines showing the mean resultant direction of wind flow. Light dash-dot lines are isotachs indicating mean resultant wind speed (kn.). Pressure (mb.) averaged for 5-degree squares is plotted above the mean position of the square, and resultant wind direction followed by speed (kn.) is plotted below. The monthly climatological position of the intertropical convergence zone is shown by a wide dashed band.

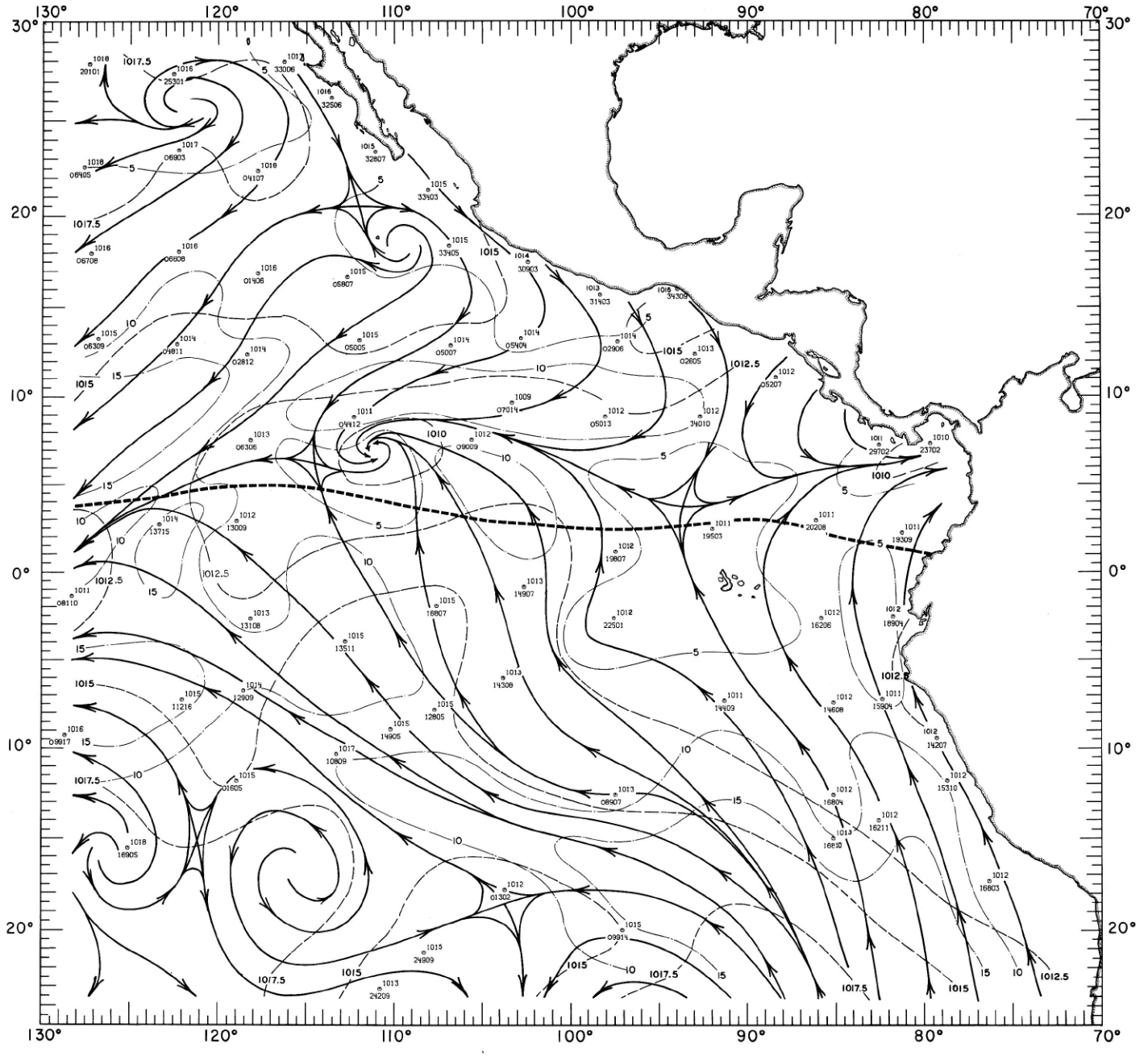


70-MW-2.

FIGURE 70-MW-2.—Analyses of the surface air pressure and surface winds from all available ship observations, averaged over 2-degree (latitude-longitude) squares for the period February 16-29, 1968. Heavy dashed lines are isobars. Solid lines are streamlines showing the mean resultant direction of wind flow. Light dash-dot lines are isotachs indicating mean resultant wind speed (kn.). Pressure (mb.) averaged for 5-degree squares is plotted above the mean position of the square, and resultant wind direction followed by speed (kn.) is plotted below. The monthly climatological position of the intertropical convergence zone is shown by a wide dashed band.

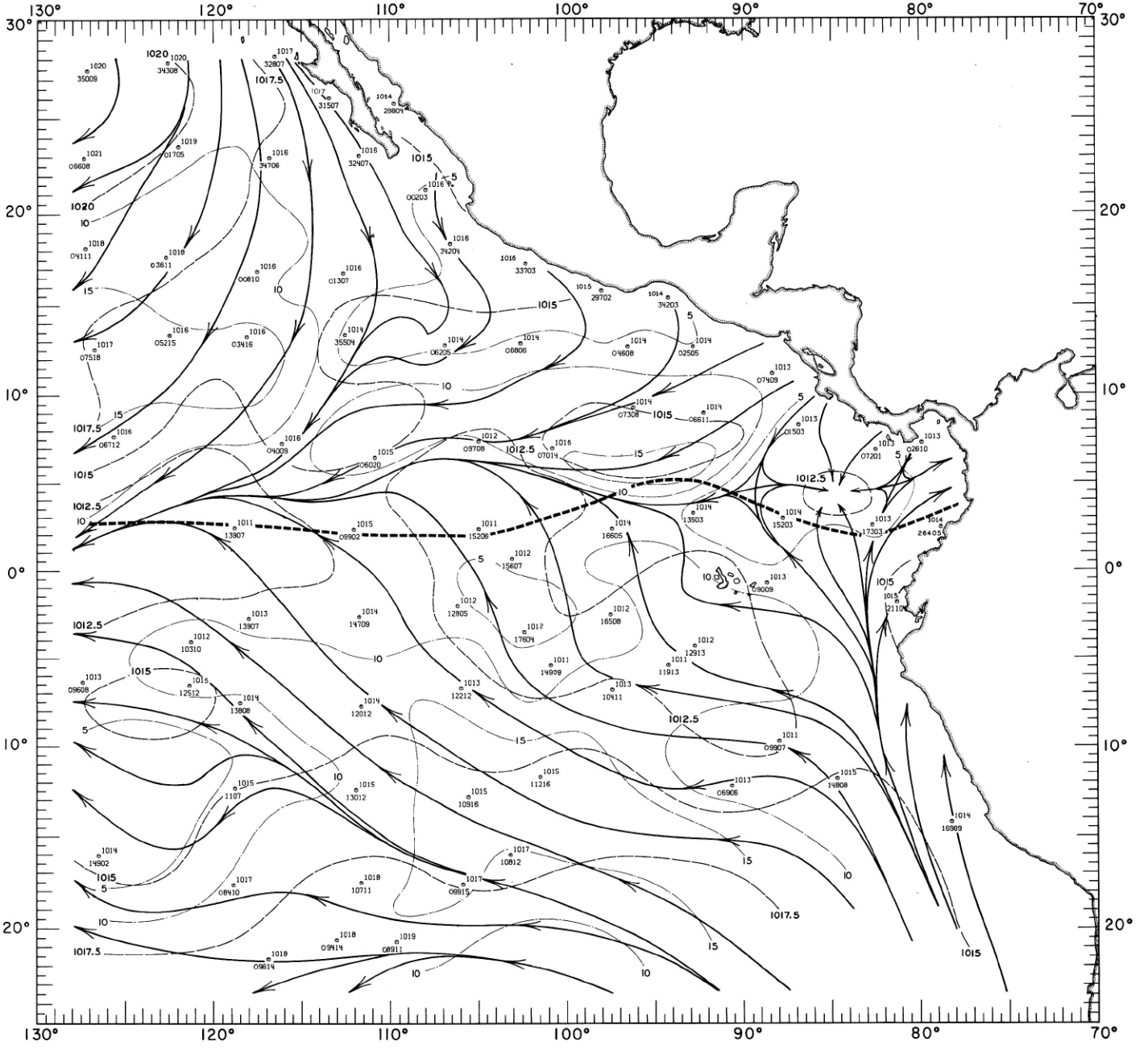


70-MW-3.

FIGURE 70-MW-3.—Analyses of the surface air pressure and surface winds from all available ship observations, averaged over 2-degree (latitude-longitude) squares for the period March 1-16, 1968. Heavy dashed lines are isobars. Solid lines are streamlines showing the mean resultant direction of wind flow. Light dash-dot lines are isotachs indicating mean resultant wind speed (kn.). Pressure (mb.) averaged for 5-degree squares is plotted above the mean position of the square, and resultant wind direction followed by speed (kn.) is plotted below. The monthly climatological position of the intertropical convergence zone is shown by a wide dashed band.

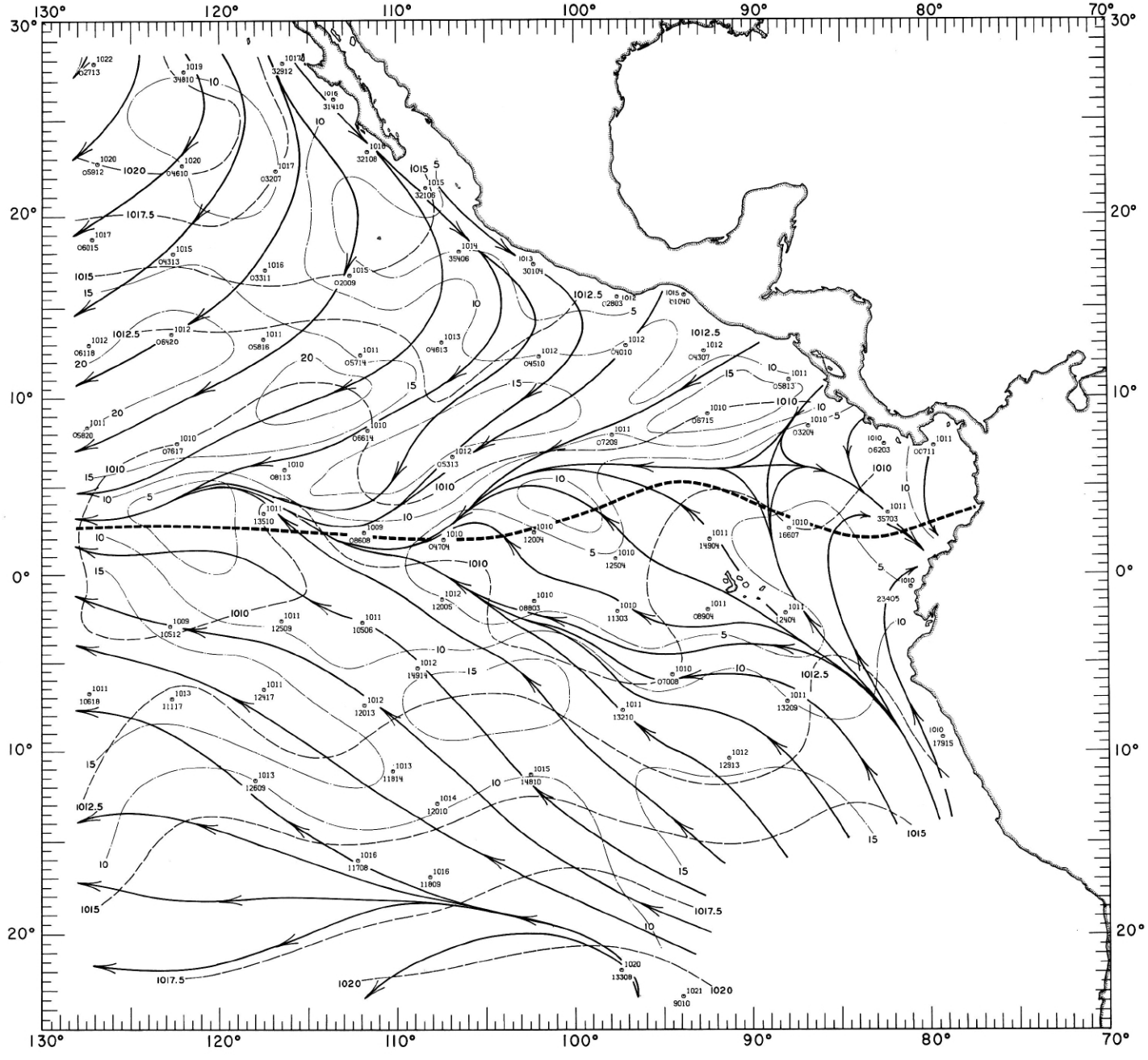


70-MW-4.

FIGURE 70-MW-4.—Analyses of the surface air pressure and surface winds from all available ship observations, averaged over 2-degree (latitude-longitude) squares for the period March 17-31, 1968. Heavy dashed lines are isobars. Solid lines are streamlines showing the mean resultant direction of wind flow. Light dash-dot lines are isotachs indicating mean resultant wind speed (kn.). Pressure (mb.) averaged for 5-degree squares is plotted above the mean position of the square, and resultant wind direction followed by speed (kn.) is plotted below. The monthly climatological position of the intertropical convergence zone is shown by a wide dashed band.

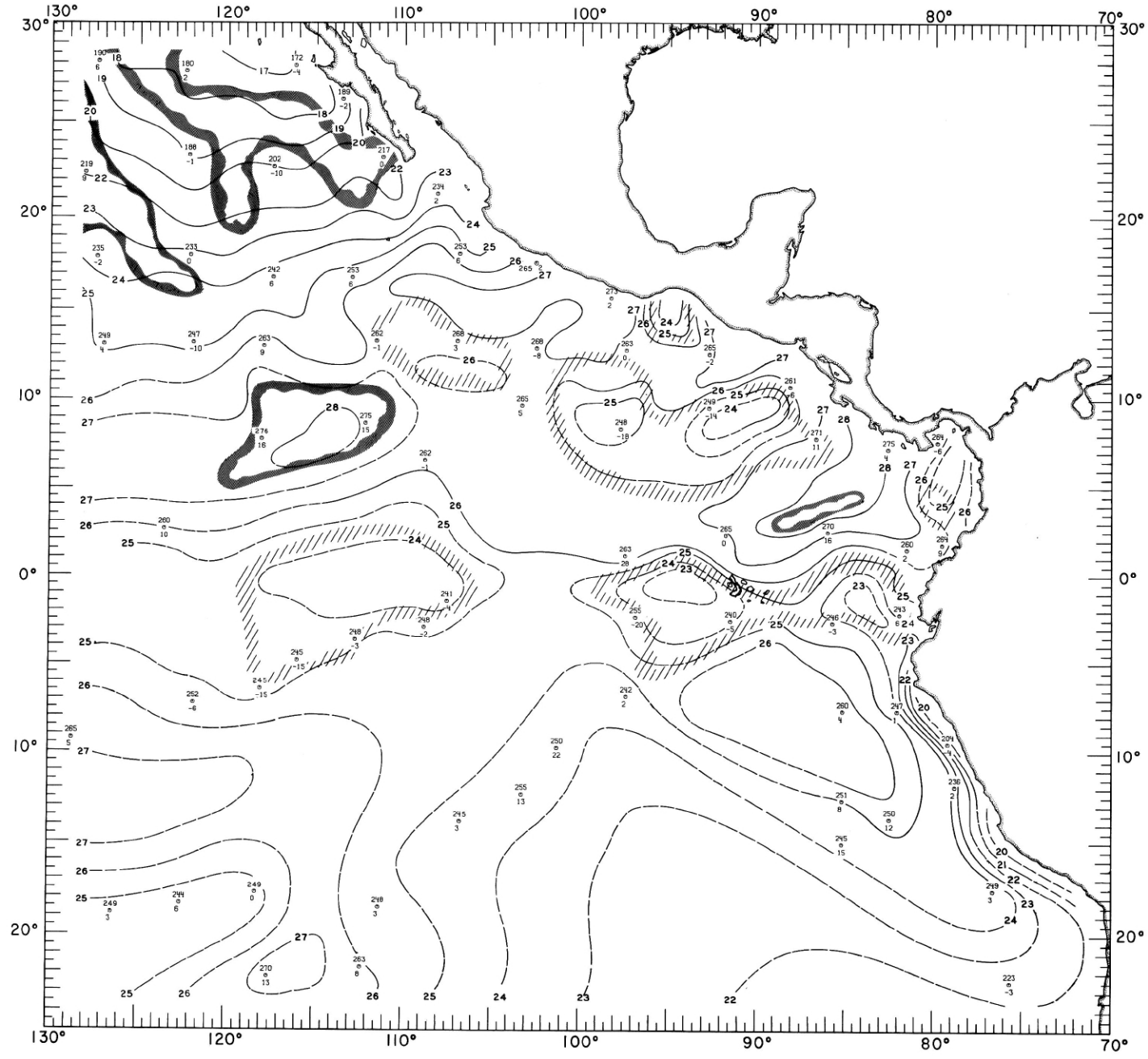


70-MT-1.

FIGURE 70-MT-1.—Analysis of sea surface temperatures based on averages for 2-degree (latitude-longitude) squares from all available ship observations for the period February 1-15, 1968. Solid lines are sea surface isotherms (°C.); the isotherms are dashed where data are sparse. Dark hatching outlines areas with positive temperature anomalies (computed from mean sea surface temperatures averaged over 22 years) greater than 1° C.; light hatching shows areas with negative anomalies greater than 1° C. Sea surface temperature (°C. x 10) averaged for 5-degree squares is plotted above the mean position of the square; sea temperature minus air temperature difference (°C. x 10) is plotted below the symbol.

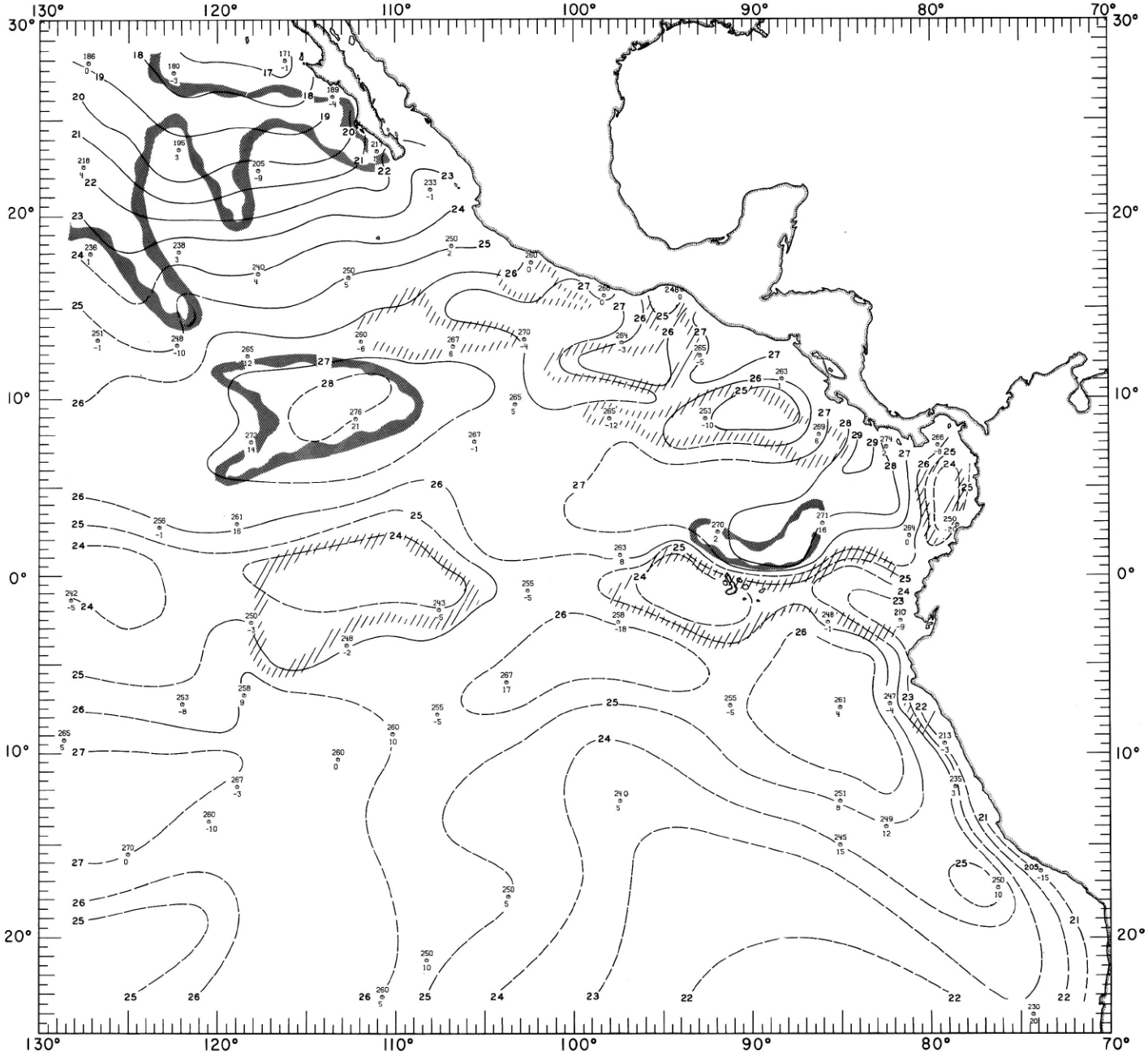


70-MT-2.

FIGURE 70-MT-2.—Analysis of sea surface temperatures based on averages for 2-degree (latitude-longitude) squares from all available ship observations for the period February 16-29, 1968. Solid lines are sea surface isotherms (°C.); the isotherms are dashed where data are sparse. Dark hatching outlines areas with positive temperature anomalies (computed from mean sea surface temperatures averaged over 22 years) greater than 1° C.; light hatching shows areas with negative anomalies greater than 1° C. Sea surface temperature (°C. x 10) averaged for 5-degree squares is plotted above the mean position of the square; sea temperature minus air temperature difference (°C. x 10) is plotted below the symbol.

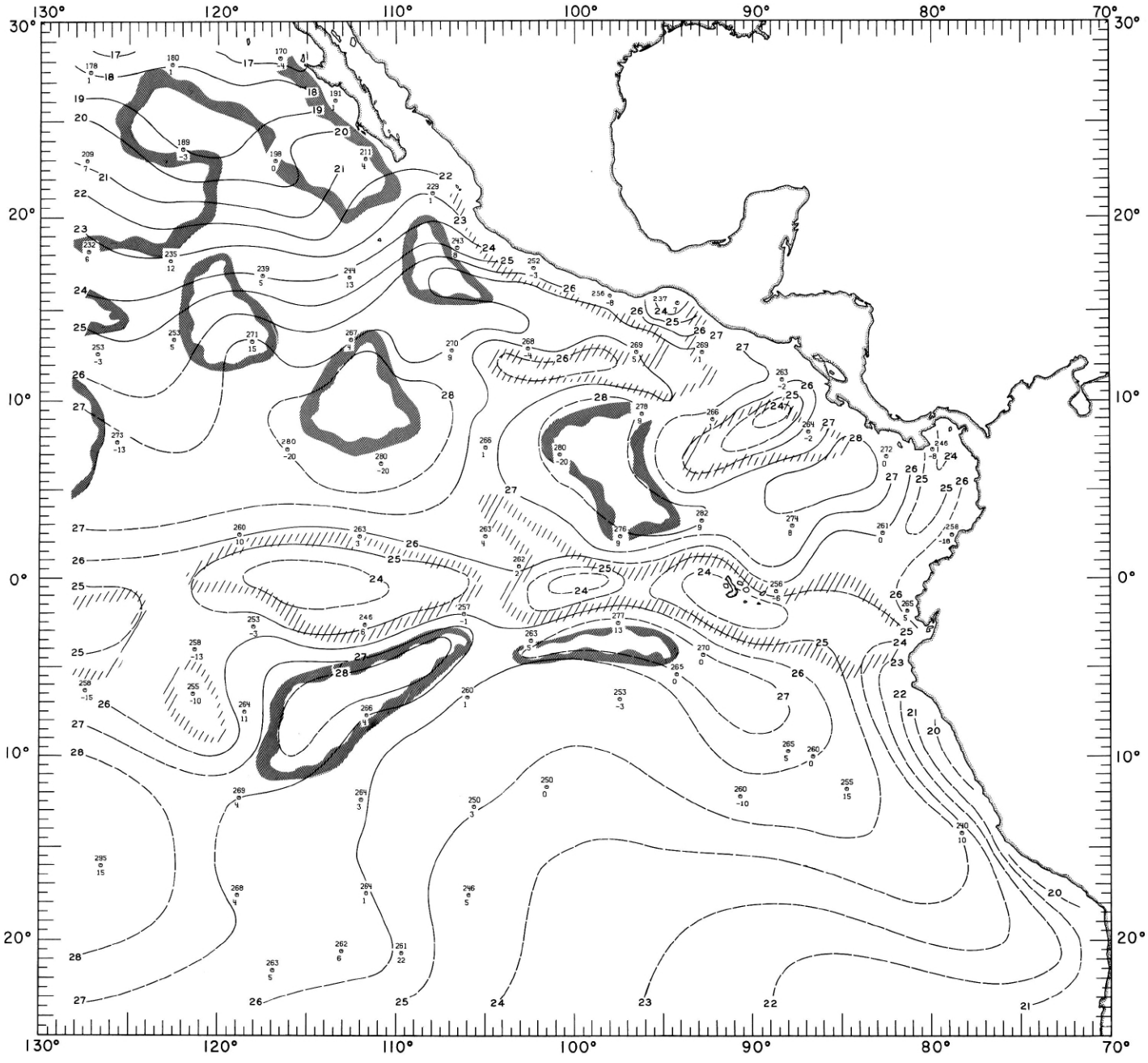


FIGURE 70-MT-3.—Analysis of sea surface temperatures based on averages for 2-degree (latitude-longitude) squares from all available ship observations for the period March 1-16, 1968. Solid lines are sea surface isotherms (°C.); the isotherms are dashed where data are sparse. Dark hatching outlines areas with positive temperature anomalies (computed from mean sea surface temperatures averaged over 22 years) greater than 1° C.; light hatching shows areas with negative anomalies greater than 1° C. Sea surface temperature (°C. x 10) averaged for 5-degree squares is plotted above the mean position of the square; sea temperature minus air temperature difference (°C. x 10) is plotted below the symbol.

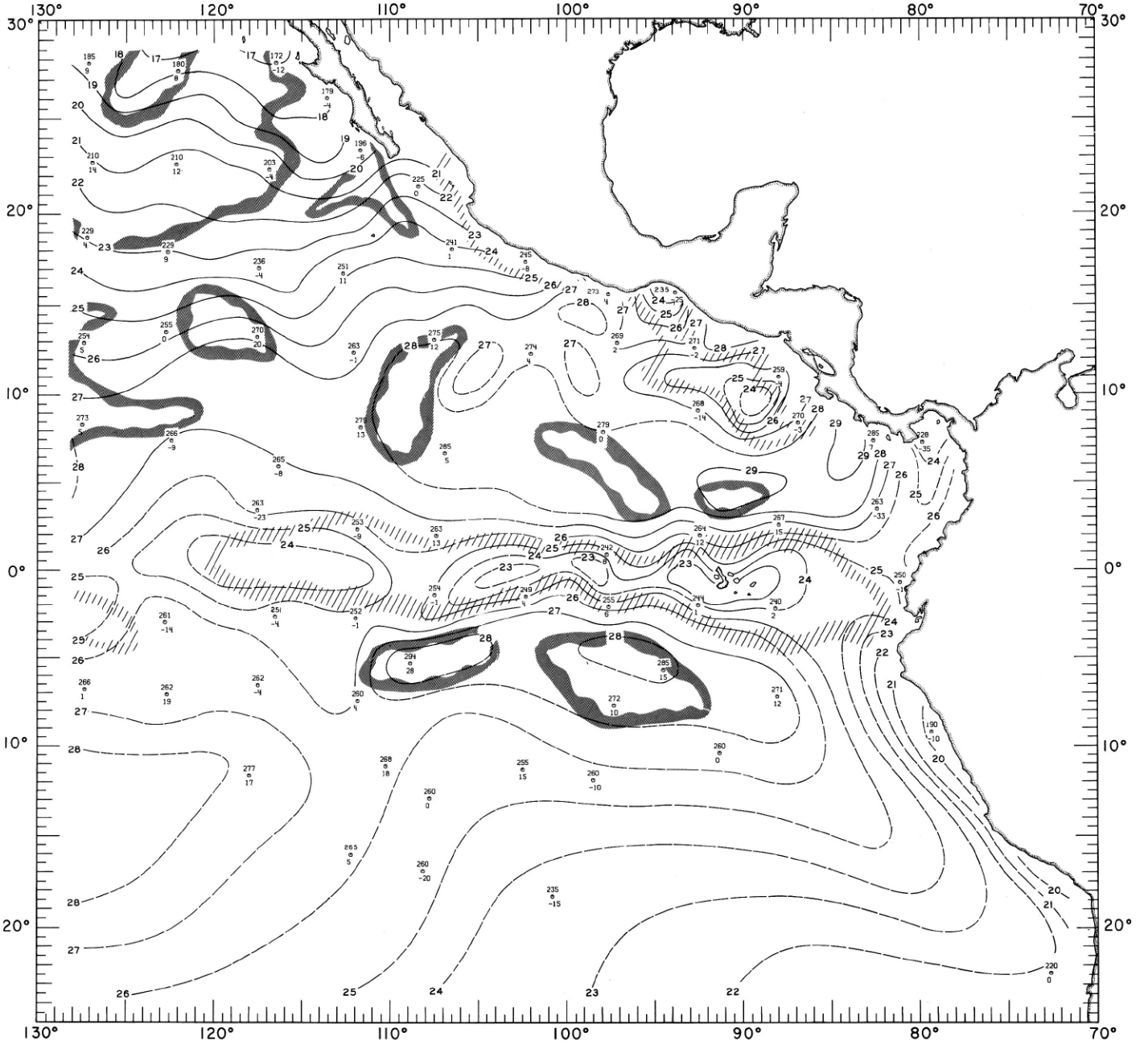


70-MT-4

FIGURE 70-MT-4.—Analysis of sea surface temperatures based on averages for 2-degree (latitude-longitude) squares from all available ship observations for the period March 17-31, 1968. Solid lines are sea surface isotherms (°C.); the isotherms are dashed where data are sparse. Dark hatching outlines areas with positive temperature anomalies (computed from mean sea surface temperatures averaged over 22 years) greater than 1° C.; light hatching shows areas with negative anomalies greater than 1° C. Sea surface temperature (°C. x 10) averaged for 5-degree squares is plotted above the mean position of the square; sea temperature minus air temperature difference (°C. x 10) is plotted below the symbol.

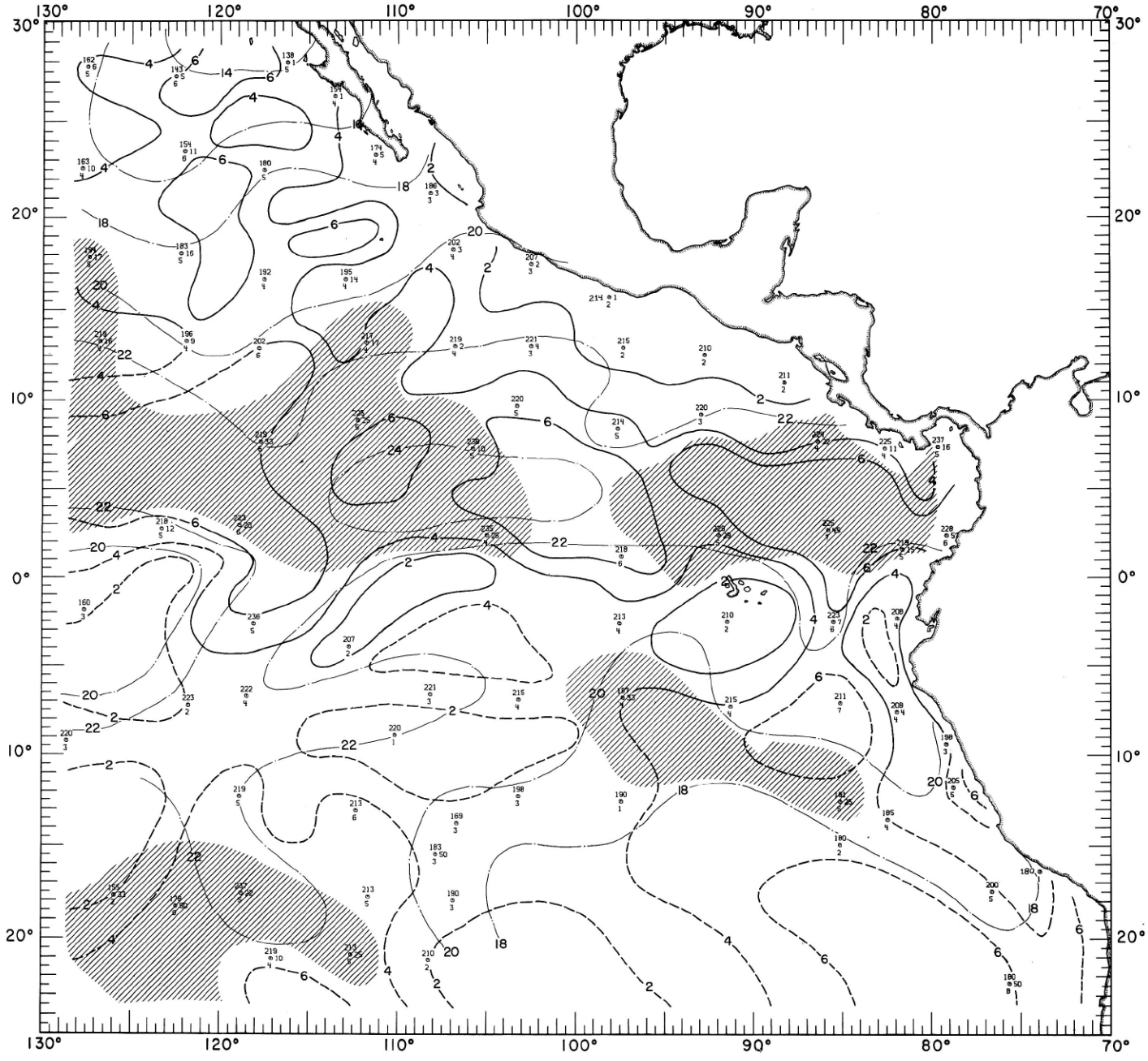


70-MC-1.

FIGURE 70-MC-1.—Analyses of the surface dew-point temperature of the air and total cloud cover based on 2-degree (latitude-longitude) averages from all available ship observations for the month of February 1968. Solid lines depict the monthly mean total cloud cover in oktas; the lines are dashed where data are sparse. Dash-dot lines are isotherms of the mean monthly dew-point temperature at 2-degree (°C.) intervals. Areas where 15 percent or more of the ships reported rain of any type at or within sight of the ship are shaded. Dew-point temperature (°C. x 10) averaged for 5-degree squares is plotted above the mean position of the square, with total cloud cover (oktas) below and rainfall frequency (%) to the right of the symbol.

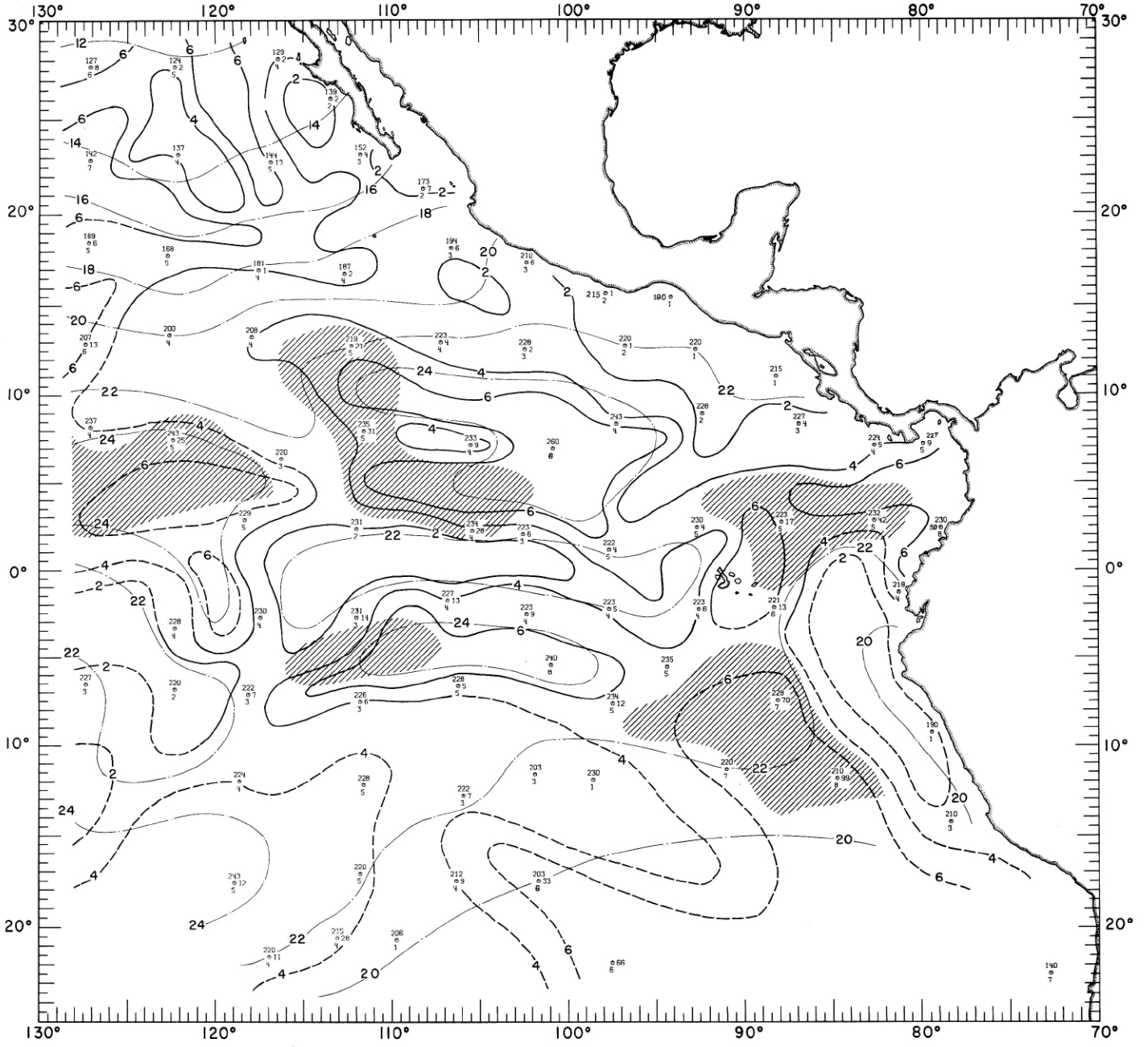


70-MC-2.

FIGURE 70-MC-2.—Analyses of the surface dew-point temperature of the air and total cloud cover based on 2-degree (latitude-longitude) averages from all available ship observations for the month of March 1968. Solid lines depict the monthly mean total cloud cover in oktas; the lines are dashed where data are sparse. Dash-dot lines are isotherms of the mean monthly dew-point temperature at 2-degree (°C.) intervals. Areas where 15 percent or more of the ships reported rain of any type at or within sight of the ship are shaded. Dew-point temperature (°C. x 10) averaged for 5-degree squares is plotted above the mean position of the square, with total cloud cover (oktas) below and rainfall frequency (%) to the right of the symbol.

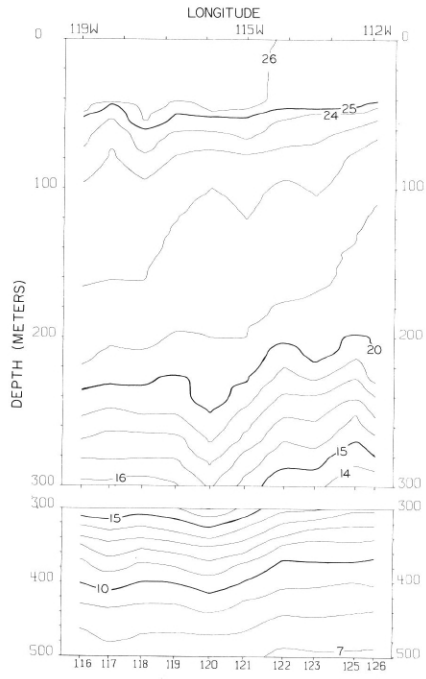


FIGURE 75-T-v3.—Vertical distribution of temperature (°C.) along 20° S., March 4-7, 1968.

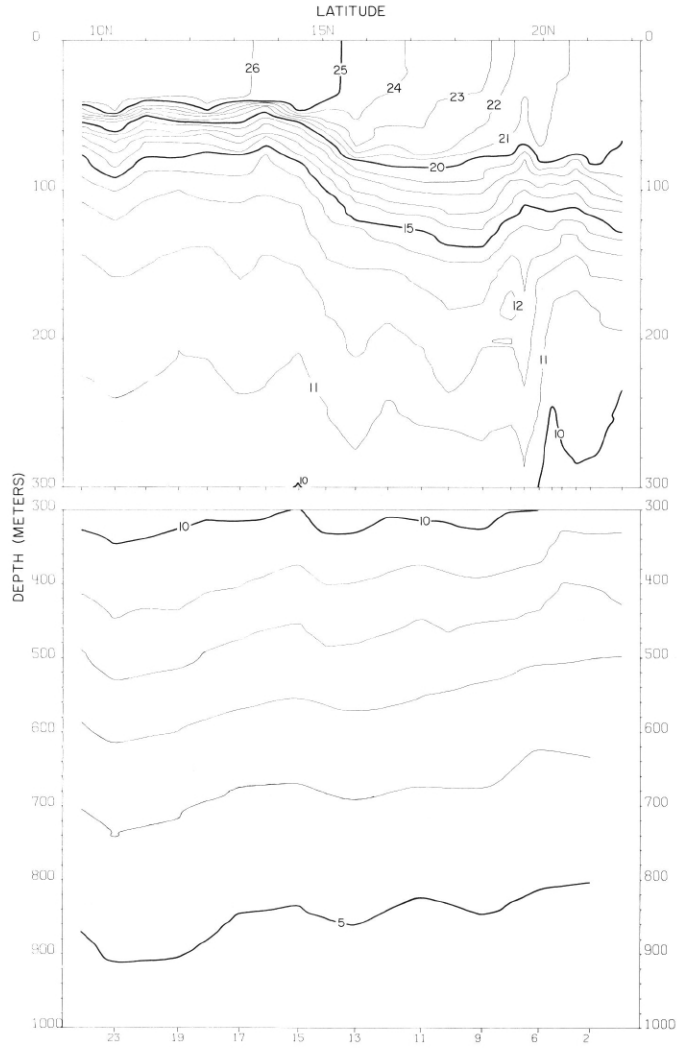


FIGURE 75-T-v1.—Vertical distribution of temperature (°C.) along 119° W. from 21°46′ N. to 9°34′ N., February 18-22, 1968.

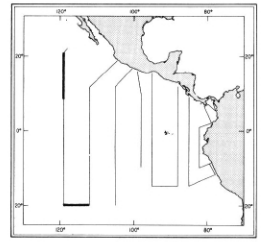

75-T-v1.

75-T-v3.

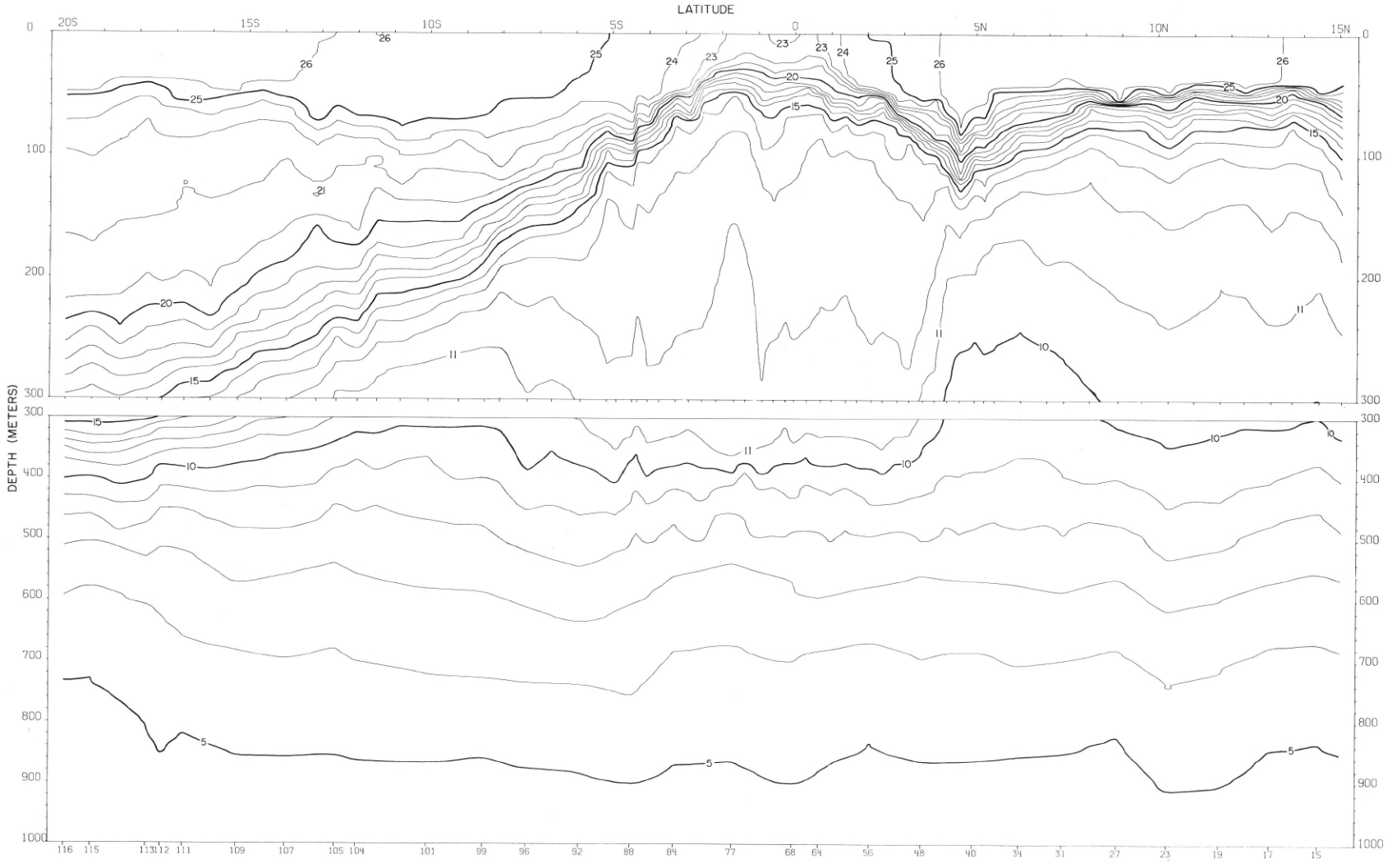


FIGURE 75-T-v2.—Vertical distribution of temperature (°C.) along 119° W. from 15°05′ N. to 20°01′ S., February 20-March 4, 1968.

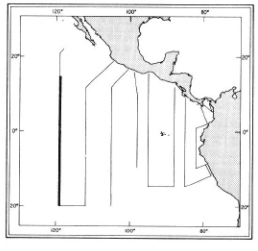

75-T-v2.

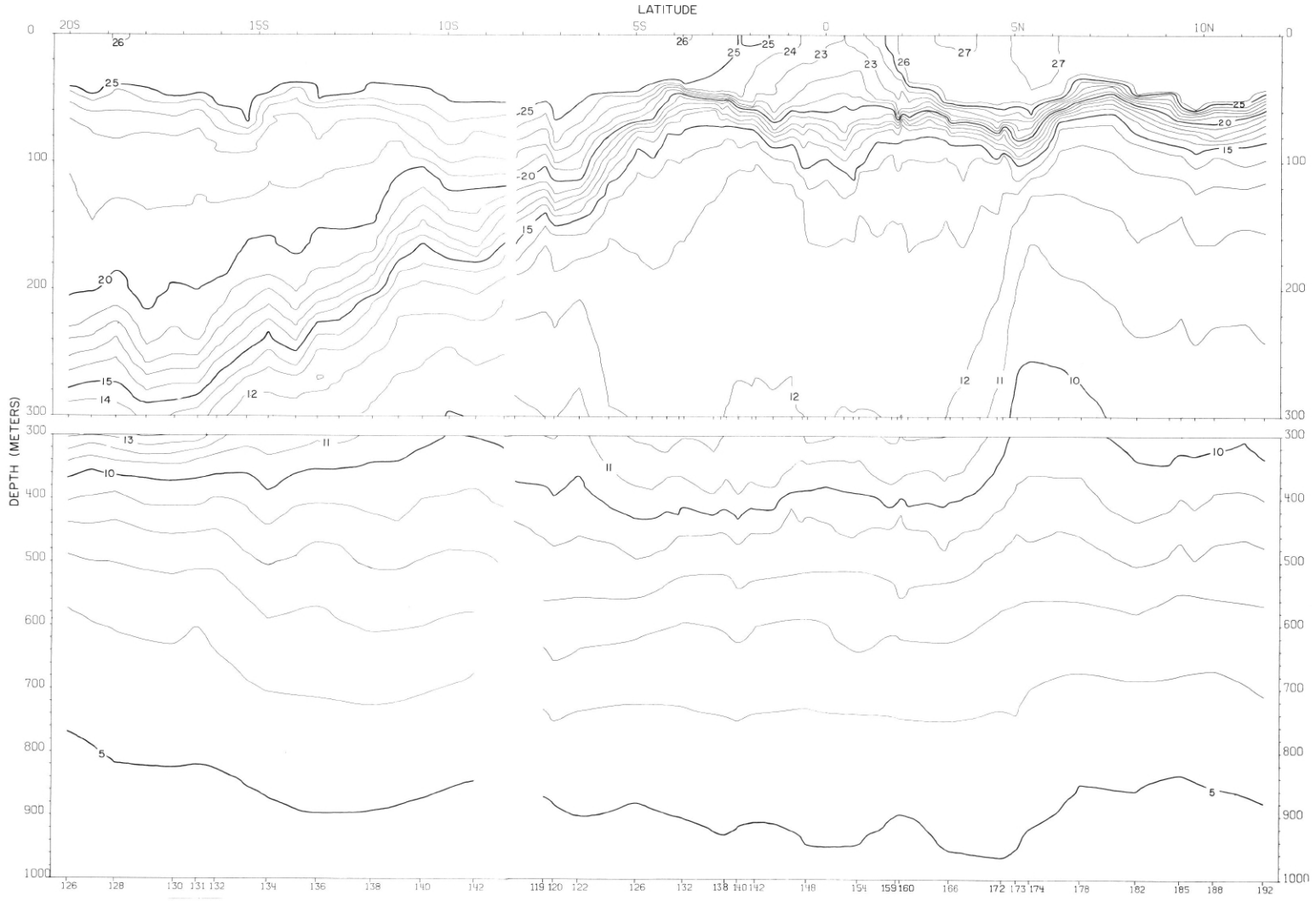


FIGURE 75-T-v4.) 76-T-v3.)—Vertical distribution of temperature (°C.) along 112° W., March 1968. Southern portion of section run by *Washington* March 7-11; northern portion by *Jordan*, March 17-26.

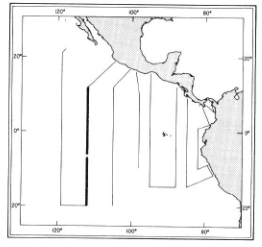

75-T-v4.
76-T-v3.

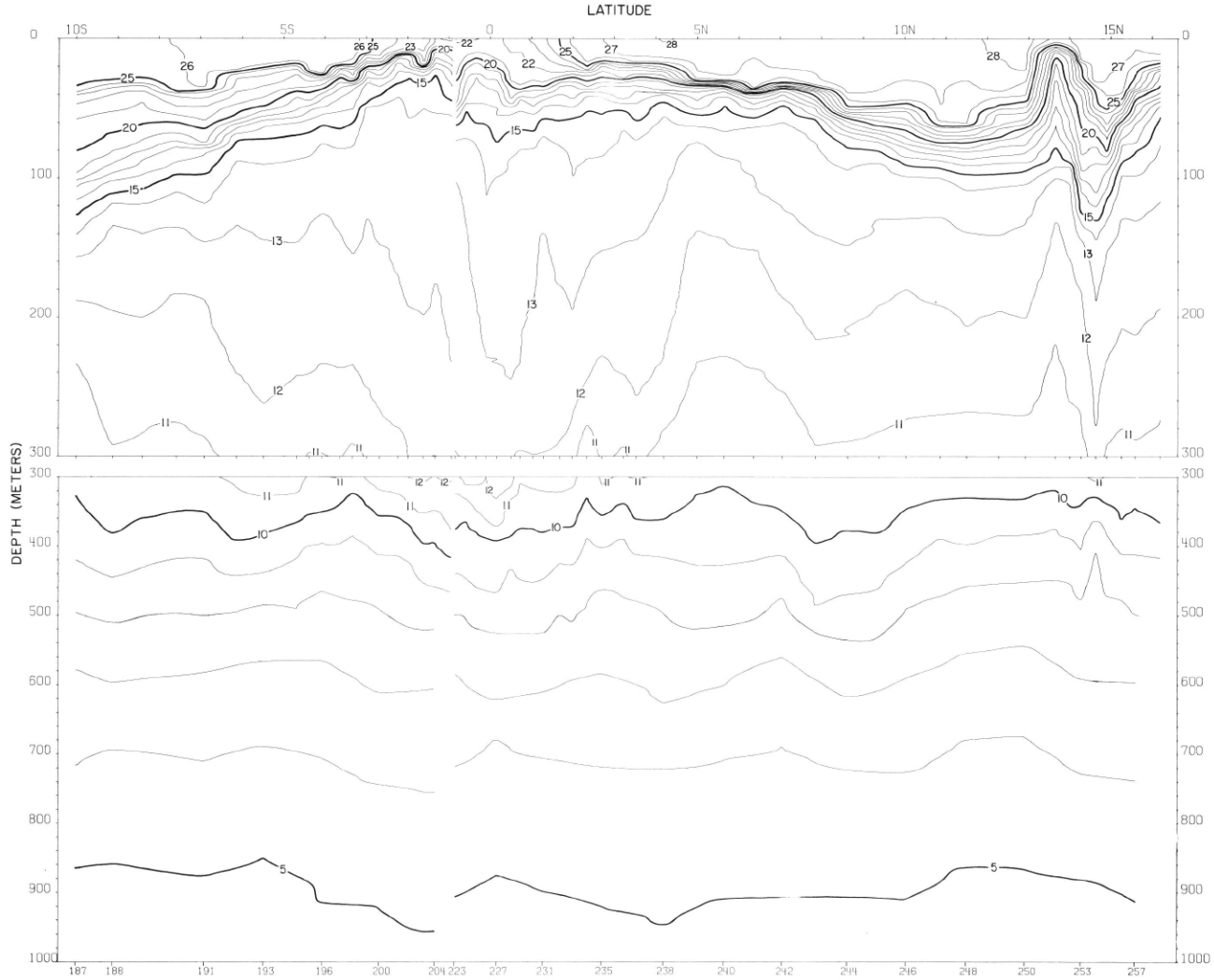


FIGURE 75-T-v5.—Vertical distribution of temperature (°C.) along 98° W., March 21-April 8, 1968. The interruption in the contours indicates a 9-day interval between stations 205 and 223 in the upper (0-500m.) portion of the section, or between stations 204 and 223 in the lower portion.

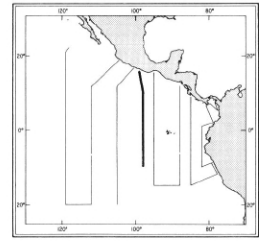

75-T-v5.

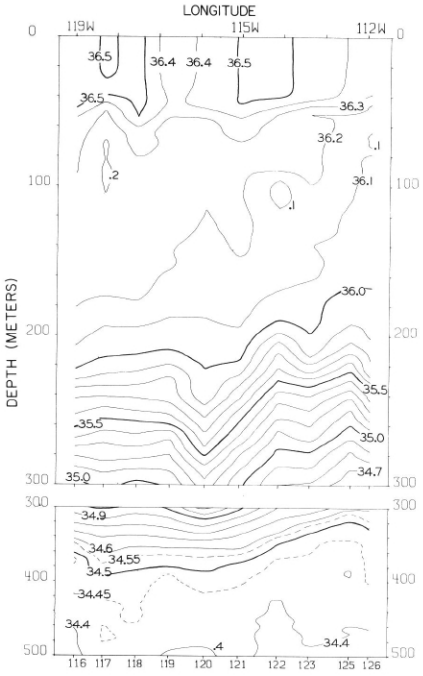


FIGURE 75-S-v3.—Vertical distribution of salinity (‰) along 20° S., March 4-7, 1968.

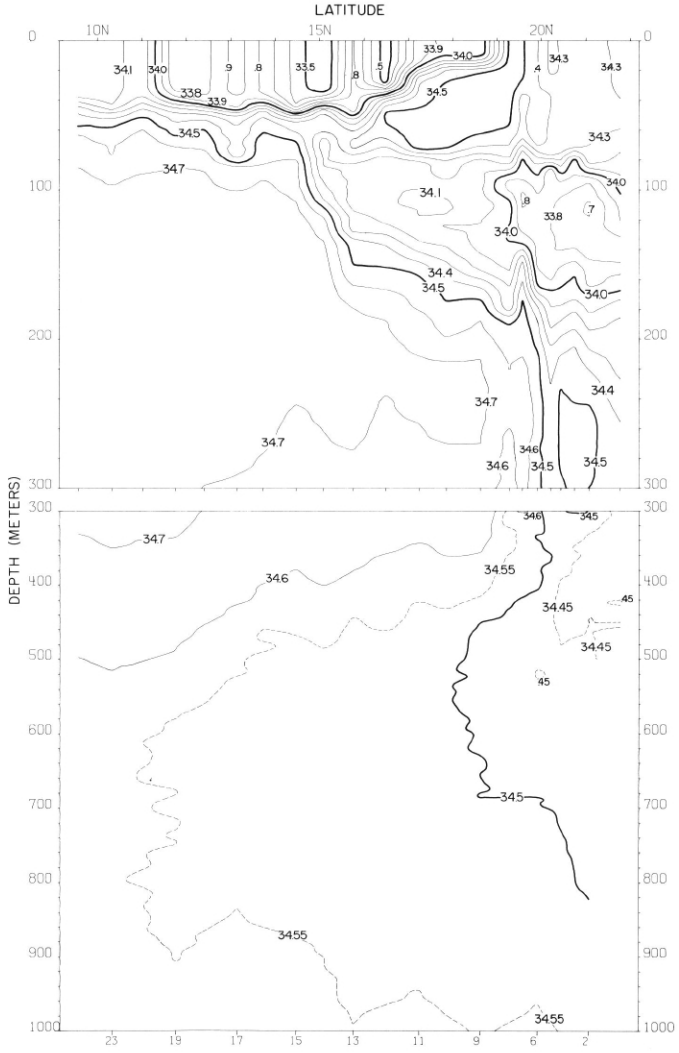


FIGURE 75-S-v1.—Vertical distribution of salinity (‰) along 119° W. from 21°46′ N. to 9°34′ N., February 18-22, 1968.

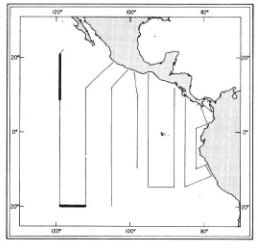

75-S-v1.

75-S-v3.

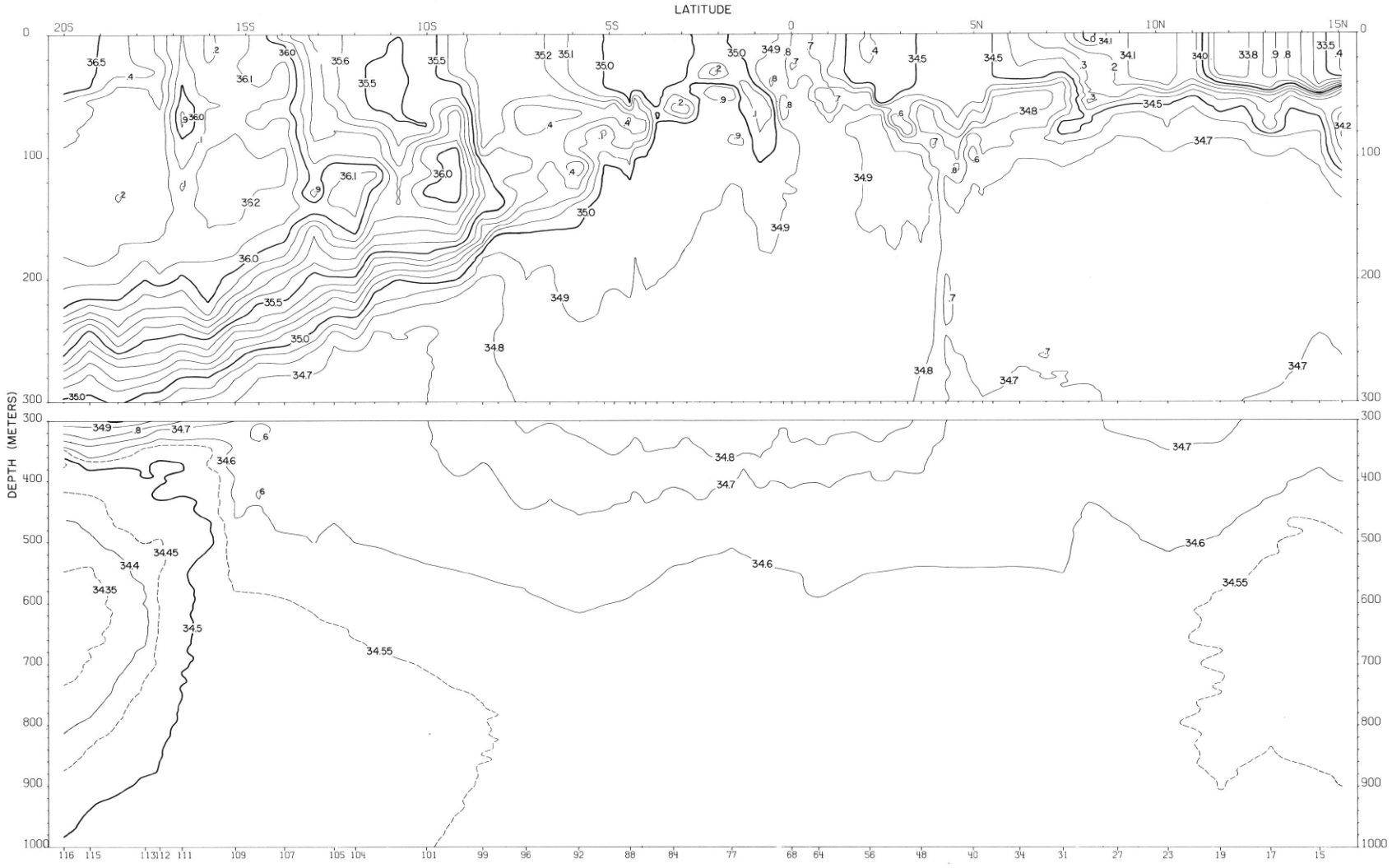


FIGURE 75-S-v2.—Vertical distribution of salinity (‰) along 119° W. from 15°05′ N. to 20°01′ S., February 20-March 4, 1968.

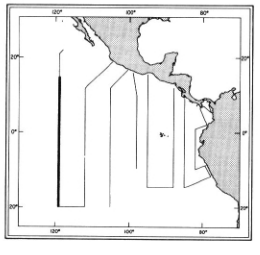

75-S-v2.

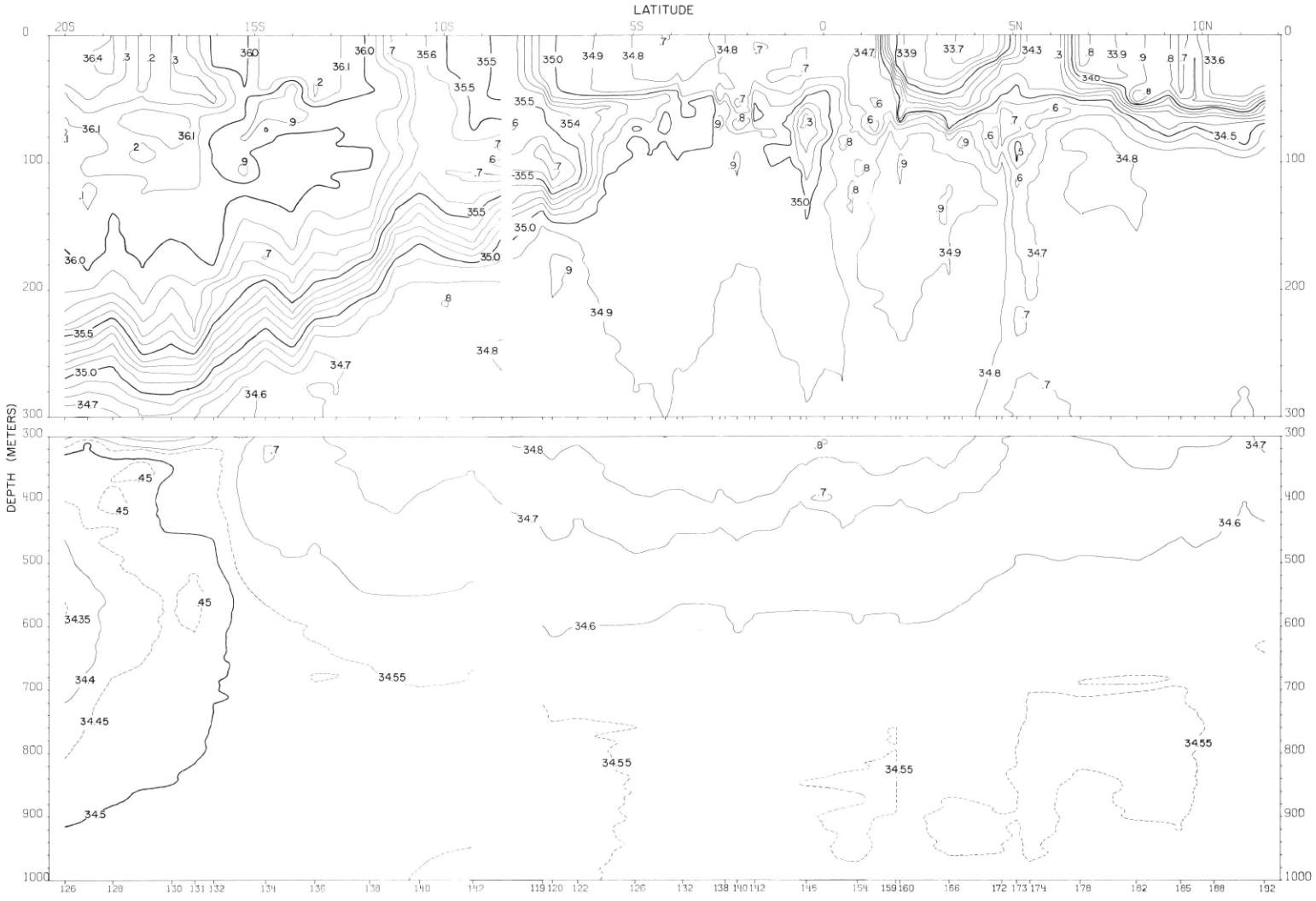


FIGURE 75-S-v4.) 76-S-v3.)—Vertical distribution of salinity (‰) along 112° W., March 1968. Southern portion of section run by *Washington*, March 7-11; northern portion by *Jordan*, March 17-26.

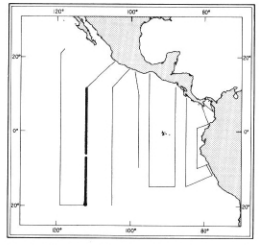

75-S-v4.
76-S-v3.

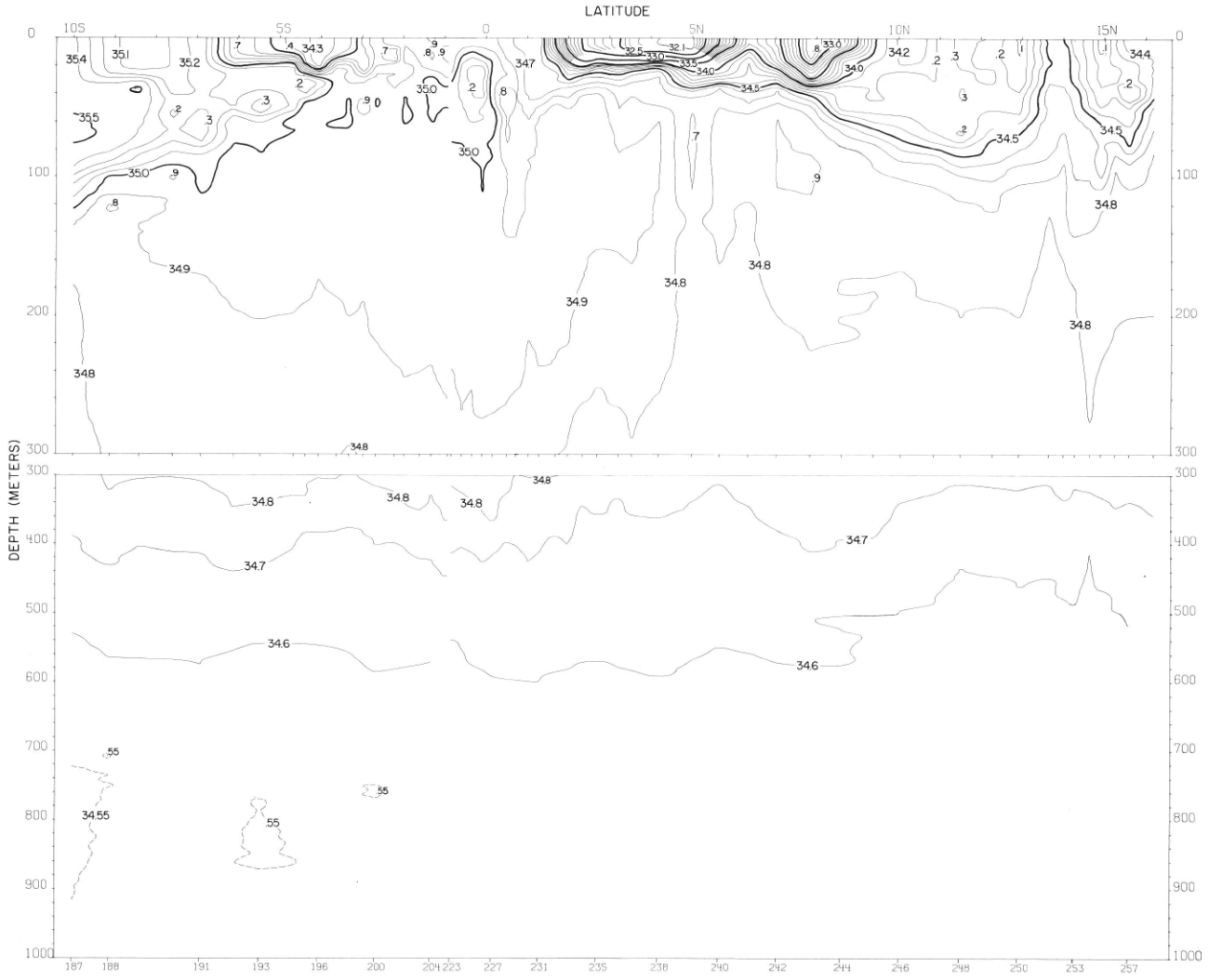


FIGURE 75-S-v5.—Vertical distribution of salinity (‰) along 98° W., March 21-April 8, 1968. The interruption in the contours indicates a 9-day interval between stations 205 and 223 in the upper (0-500m.) portion of the section, or between stations 204 and 223 in the lower portion.

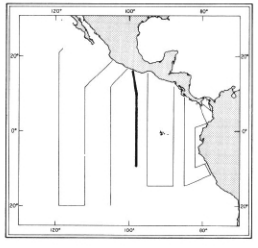

75-S-v5.

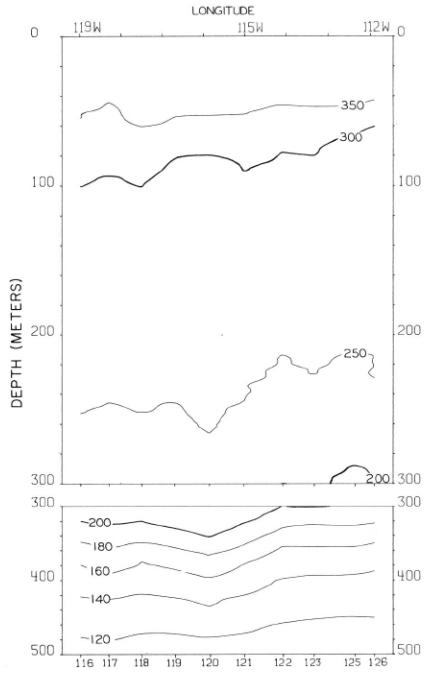


FIGURE 75-δ-v3.—Vertical distribution of thermosteric anomaly, $\delta_T$, (cl./t.) along 20° S., March 4-7, 1968.

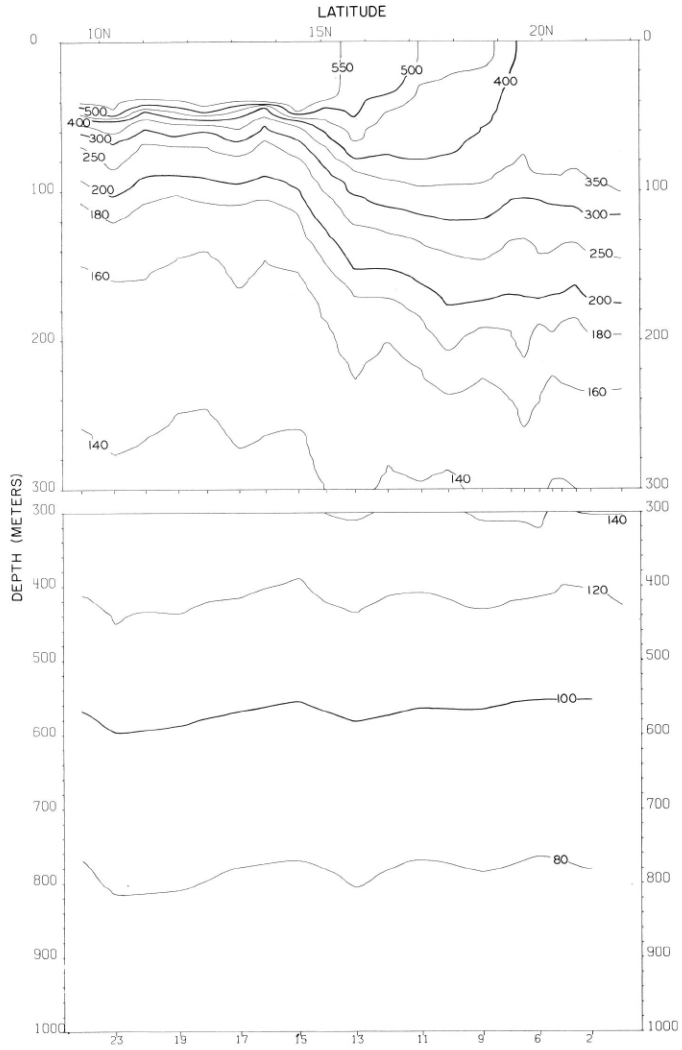


FIGURE 75-δ-v1.—Vertical distribution of thermosteric anomaly, $\delta_T$, (cl./t.) along 119° W. from 21°46′ N. to 9°34′ N., February 18-22, 1968.

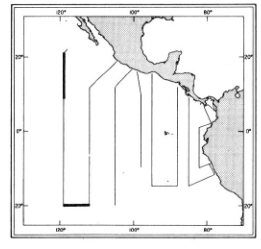

75-δ-v1.

75-δ-v3.

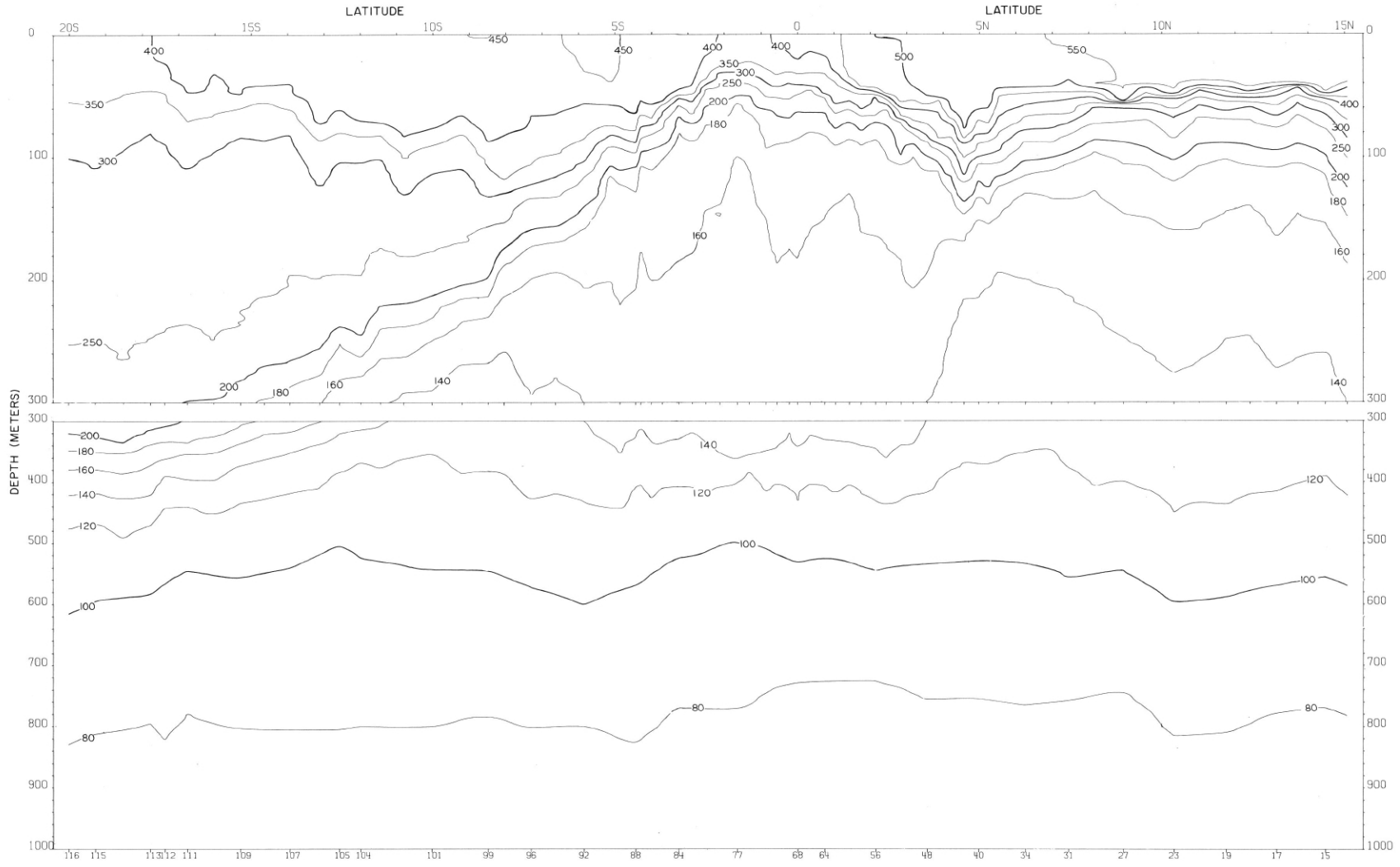


FIGURE 75-δ-v2.—Vertical distribution of thermosteric anomaly, $\delta_T$, (cl./t.) along 119° W. from 15°05′ N. to 20°01′ S., February 20-March 4, 1968.

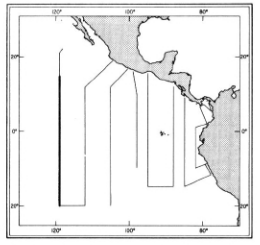

75-δ-v2.

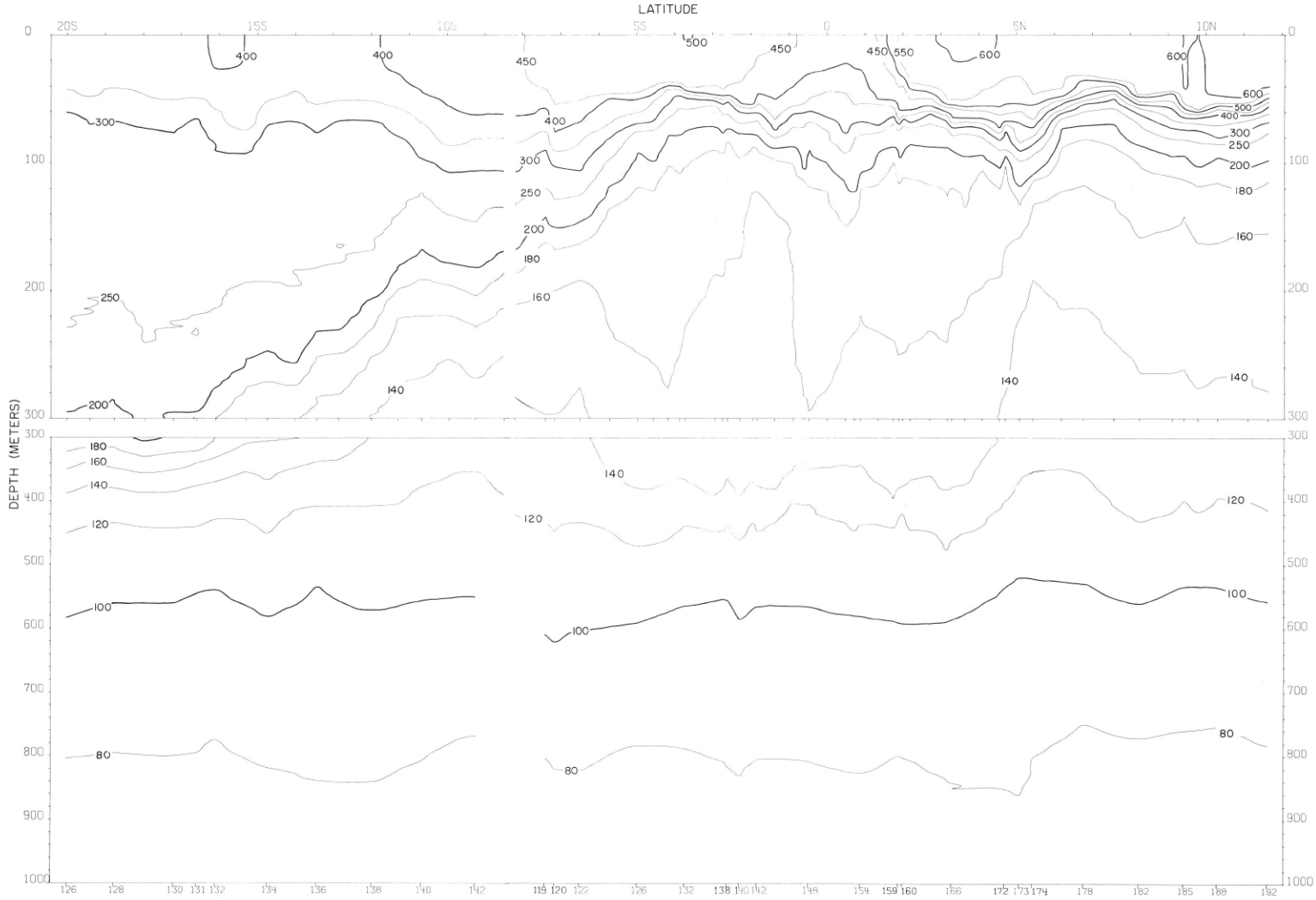


FIGURE 75-δ-v4. / 76-δ-v3. —Vertical distribution of thermosteric anomaly, $\delta_\tau$, (cl./t.) along 112° W., March 1968. Southern portion of section run by *Washington*, March 7-11; northern portion by *Jordan*, March 17-26.

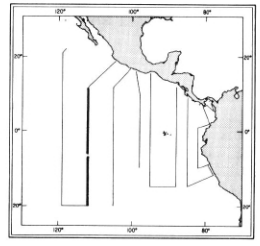

75-δ-v4.
76-δ-v3.

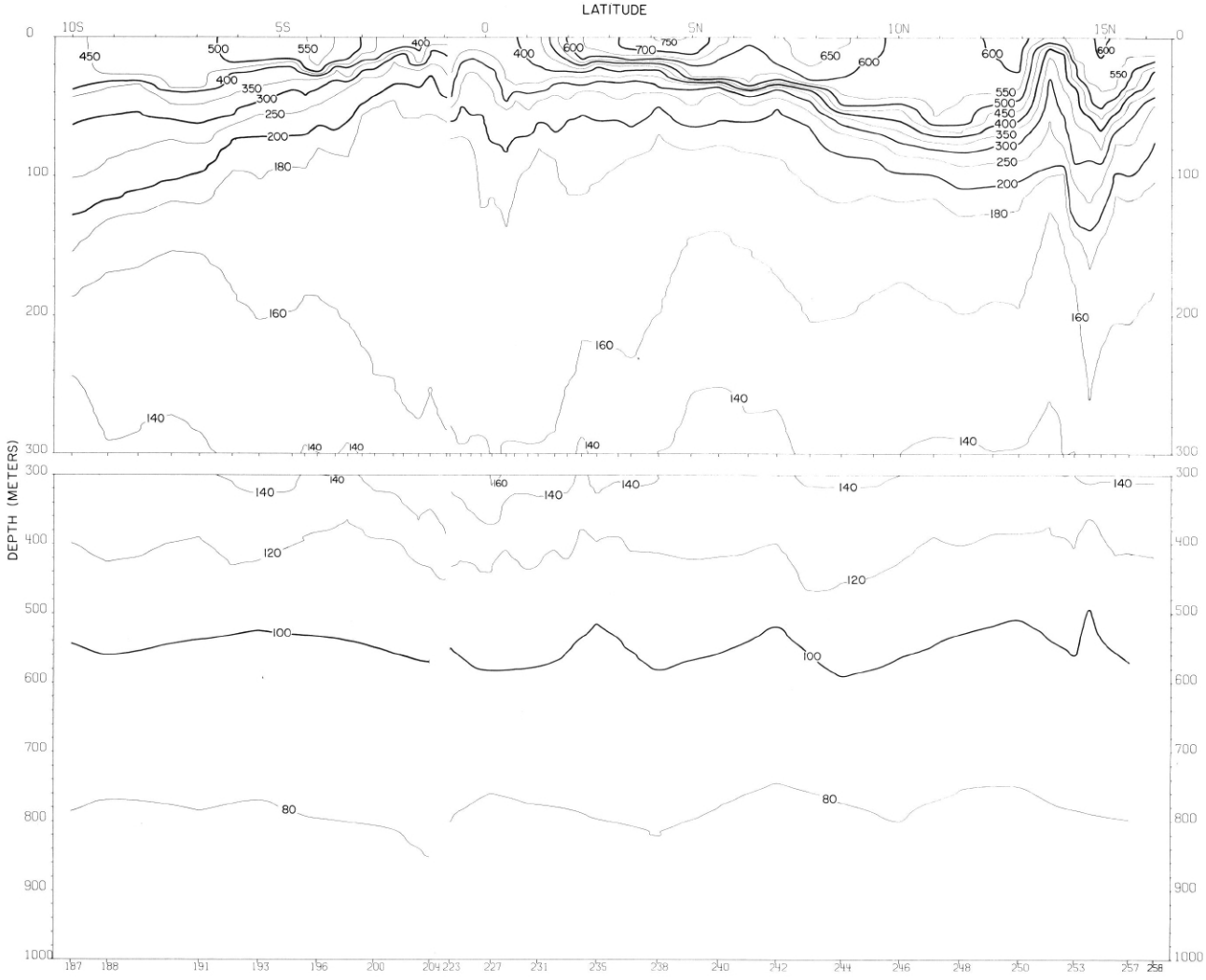


FIGURE 75-δ-v5.—Vertical distribution of thermosteric anomaly, $\delta_T$, (cl./t.) along 98° W., March 21-April 8, 1968. The interruption in the contours indicates a 9-day interval between stations 205 and 223 in the upper (0-500m.) portion of the section, or between stations 204 and 223 in the lower portion.

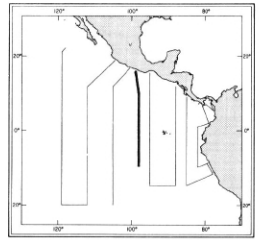

75-δ-v5.

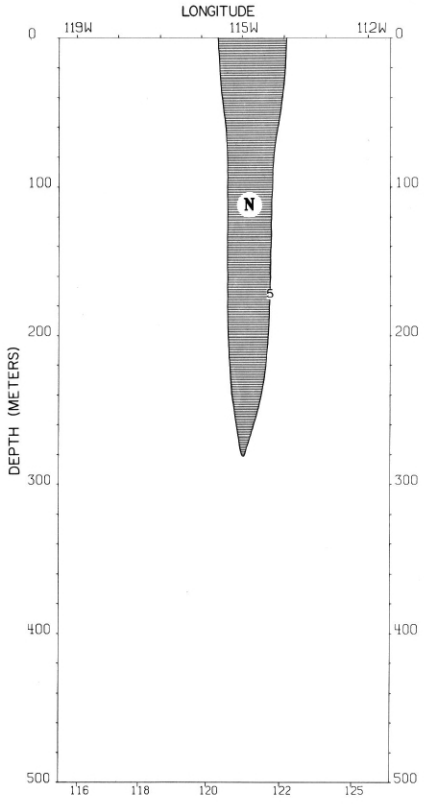


FIGURE 75-G-v3.—Vertical distribution of the meridonial component of geostrophic velocity (cm./sec.), relative to 500 db., along 20° S., March 4-6, 1968. The dark shading indicates northward flow with a velocity greater than 5 cm./sec.

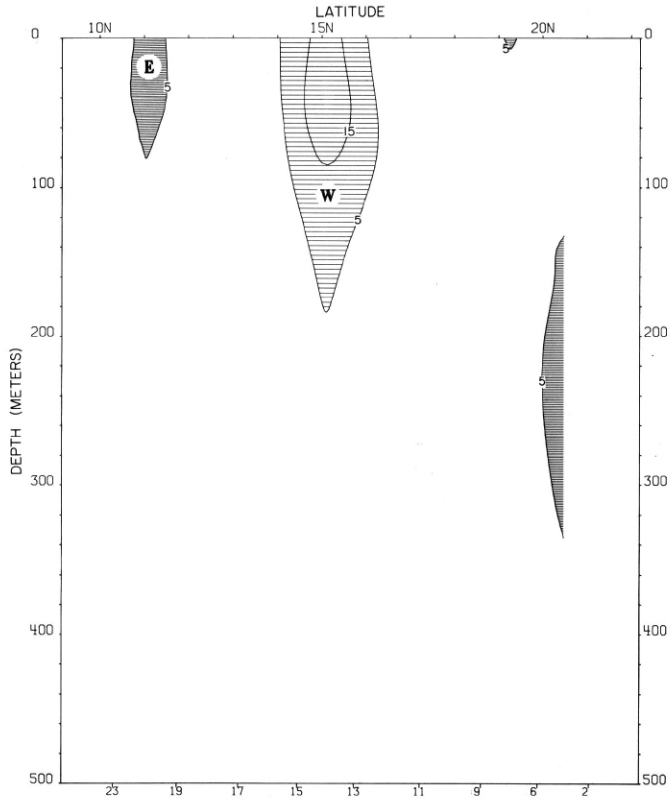


FIGURE 75-G-v1.—Vertical distribution of the zonal component of geostrophic velocity (cm./sec.), relative to 500 db., along 119° W. from 21°04′ N. to 10°19′ N., February 18-22, 1968. Dark shading indicates eastward flow with a velocity greater than 5 cm./sec.; light shading indicates westward flow with a velocity greater than 5 cm./sec.

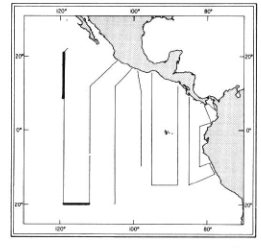

75-G-v1.

75-G-v3.

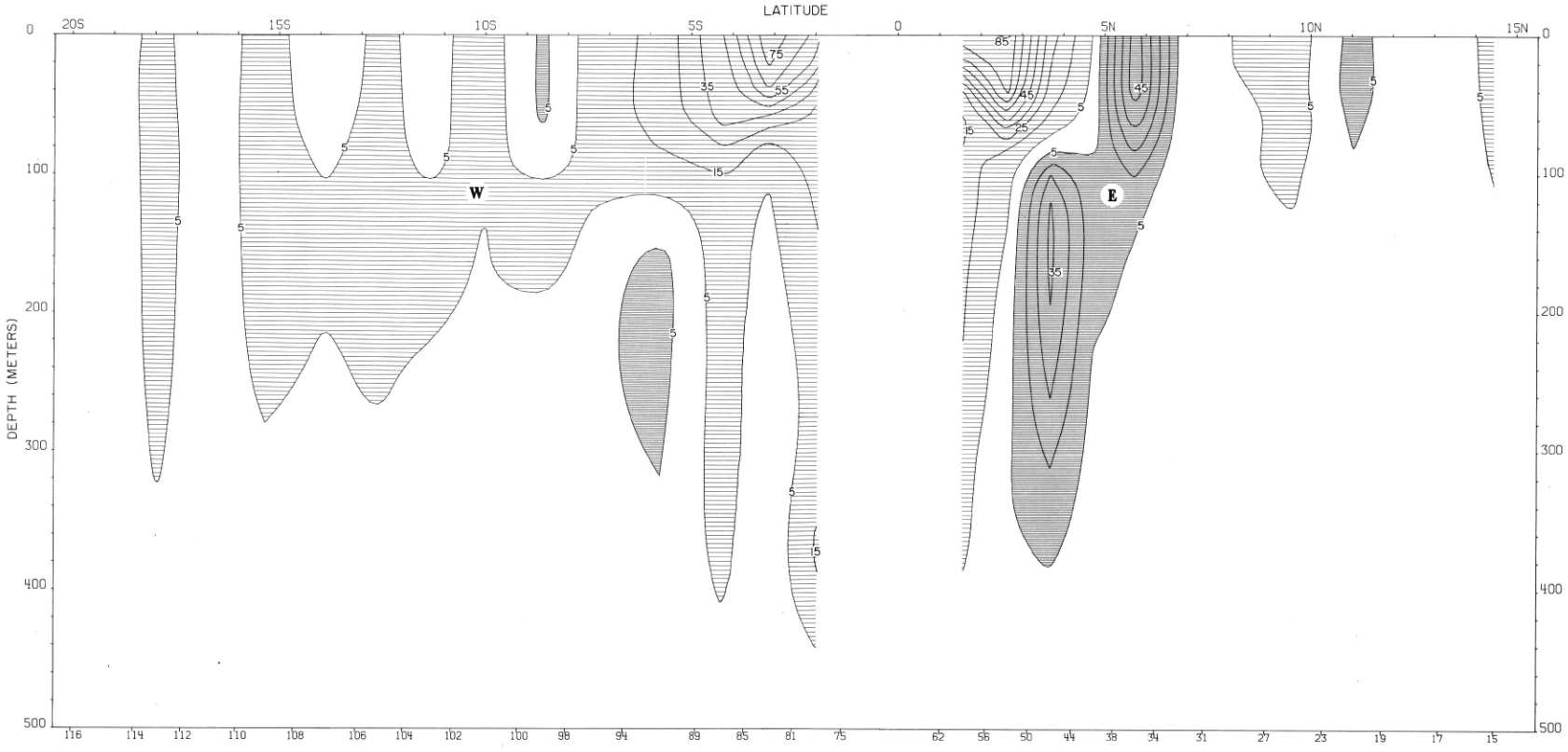


FIGURE 75-G-v2.—Vertical distribution of the zonal component of geostrophic velocity (cm./sec.), relative to 500 db., along 119° W. from 14°28′ N. to 20°01′ S., February 21-March 4, 1968. Dark shading indicates eastward flow with a velocity greater than 5 cm./sec.; light shading indicates westward flow with a velocity greater than 5 cm./sec.

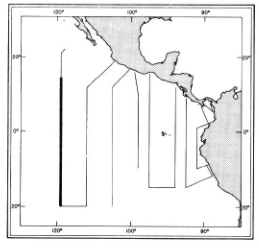

75-G-v2.

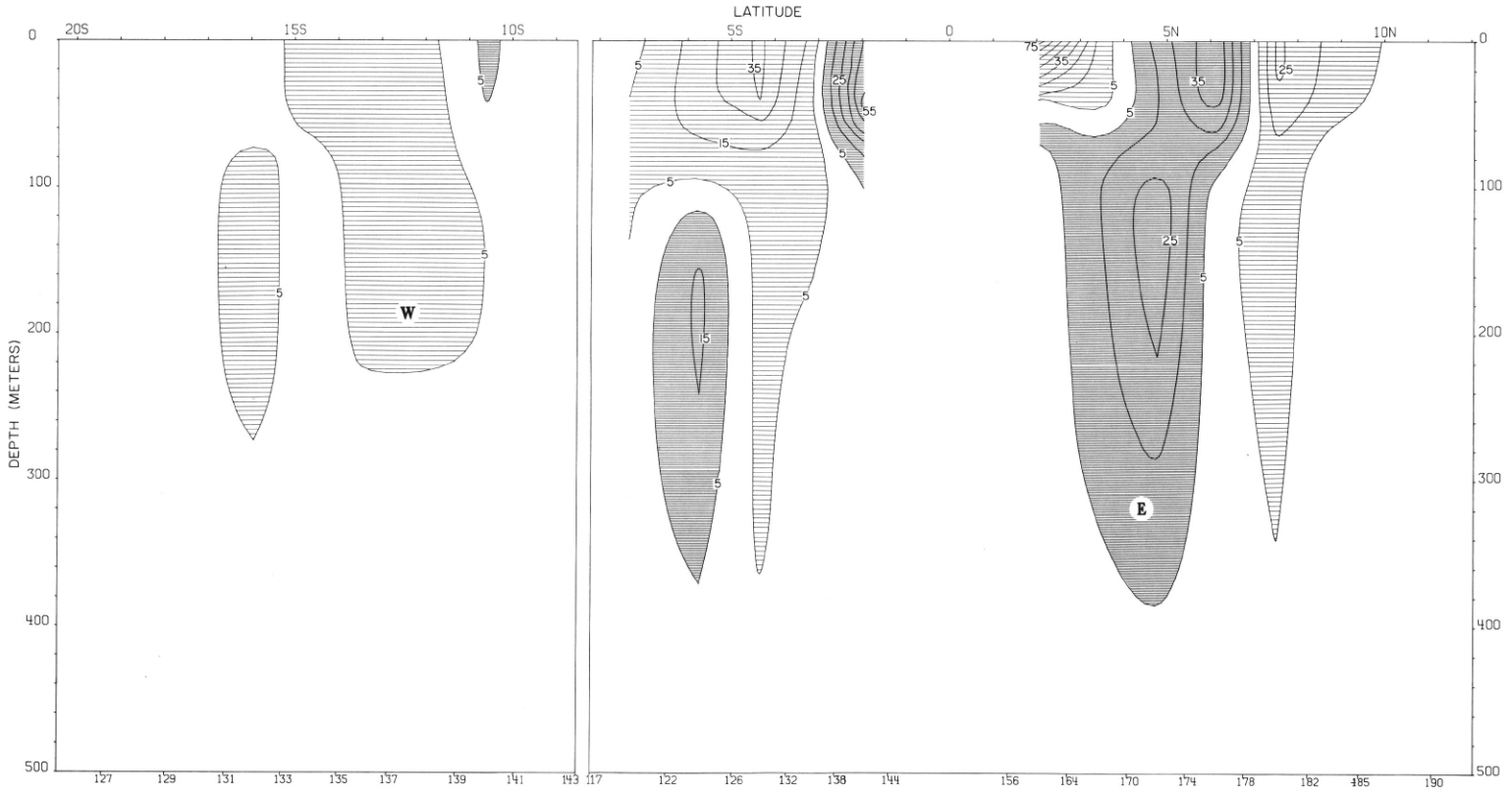


FIGURE 75-G-v4.) 76-G-v3.) —Vertical distribution of the zonal component of geostrophic velocity (cm./sec.), relative to 500 db., along 112° W., March 1968. Southern portion of section run by *Washington*, March 7-11; northern portion by *Jordan*, March 17-25. Dark shading indicates eastward flow with a velocity greater than 5 cm./sec.; light shading indicates westward flow with a velocity greater than 5 cm./sec.

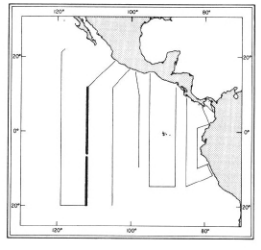

75-G-v4.
76-G-v3.

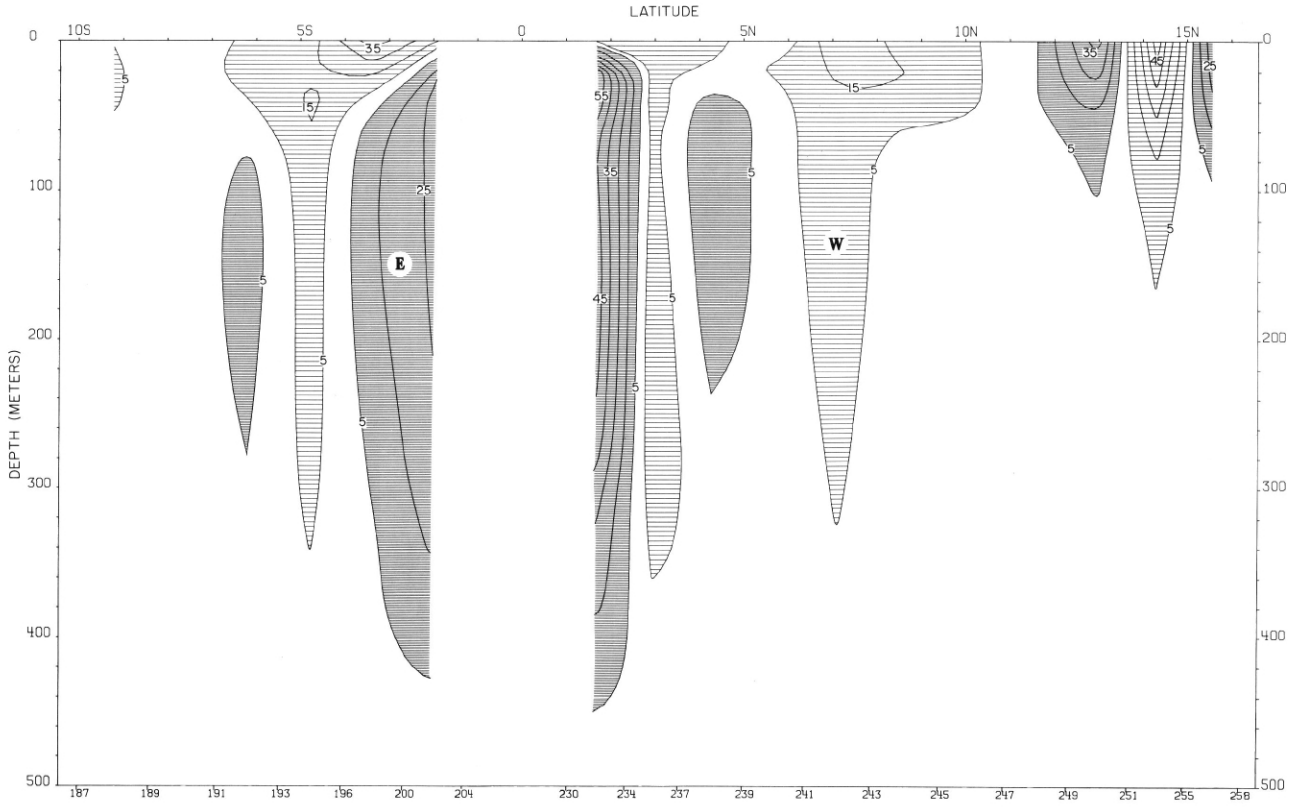


FIGURE 75-G-v5.—Vertical distribution of the zonal component of geostrophic velocity (cm./sec.), relative to 500 db., along 98° W., March 21-April 8, 1968. Dark shading indicates eastward flow with a velocity greater than 5 cm./sec.; light shading indicates westward flow with a velocity greater than 5 cm./sec.

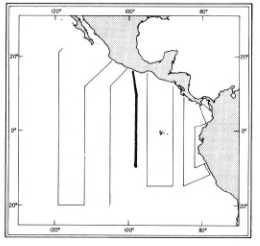

75-G-v5.

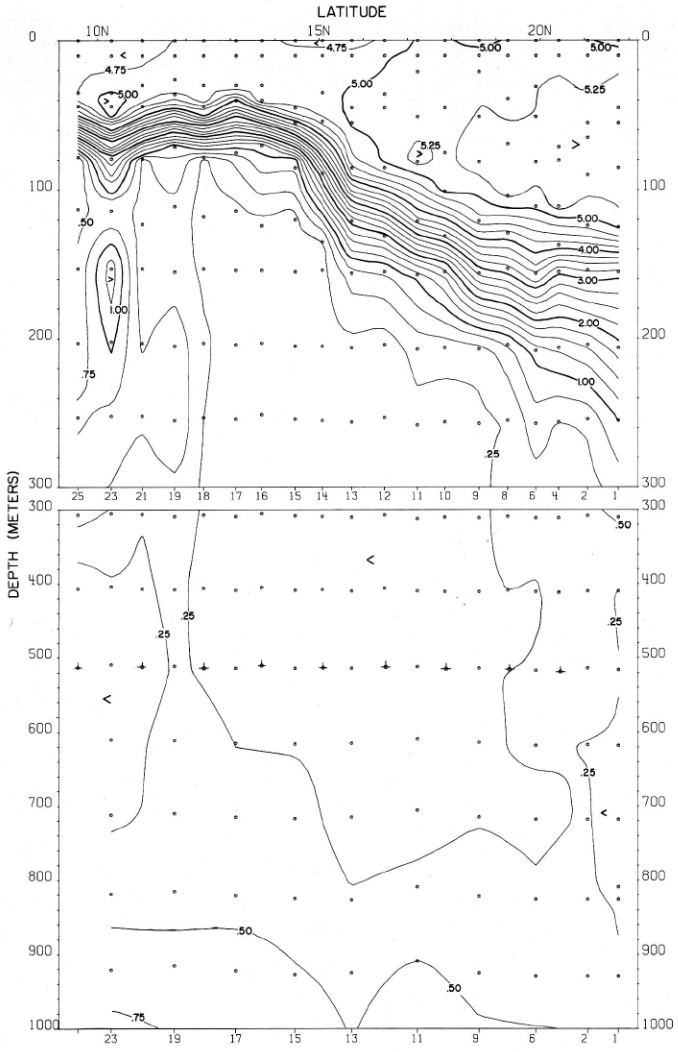


FIGURE 75-O2-v1.—Vertical distribution of oxygen (ml./l.) along 119° W. from 21°46′ N. to 9°34′ N., February 18-22, 1968.

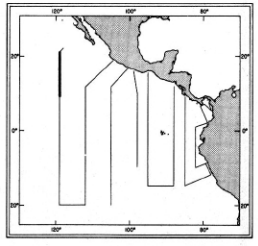

75-O2-v1.

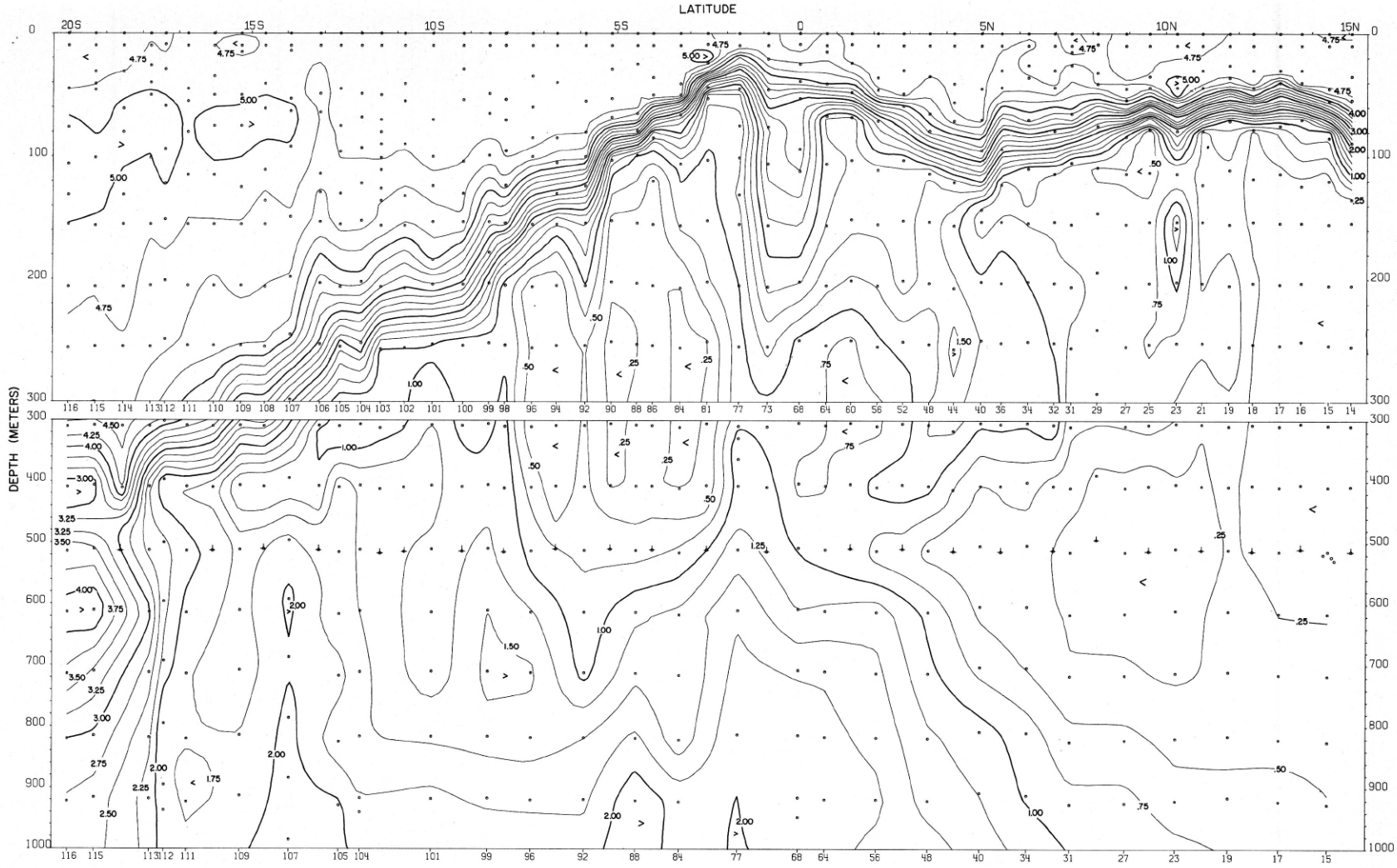


FIGURE 75-O₂-v2.—Vertical distribution of oxygen (ml./l.) along 119° W. from 15°05′ N. to 20°01′ S., February 20-March 4, 1968.

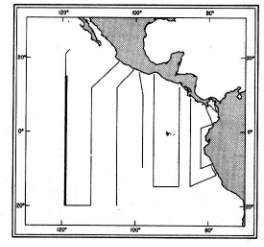

75-O₂-v2.

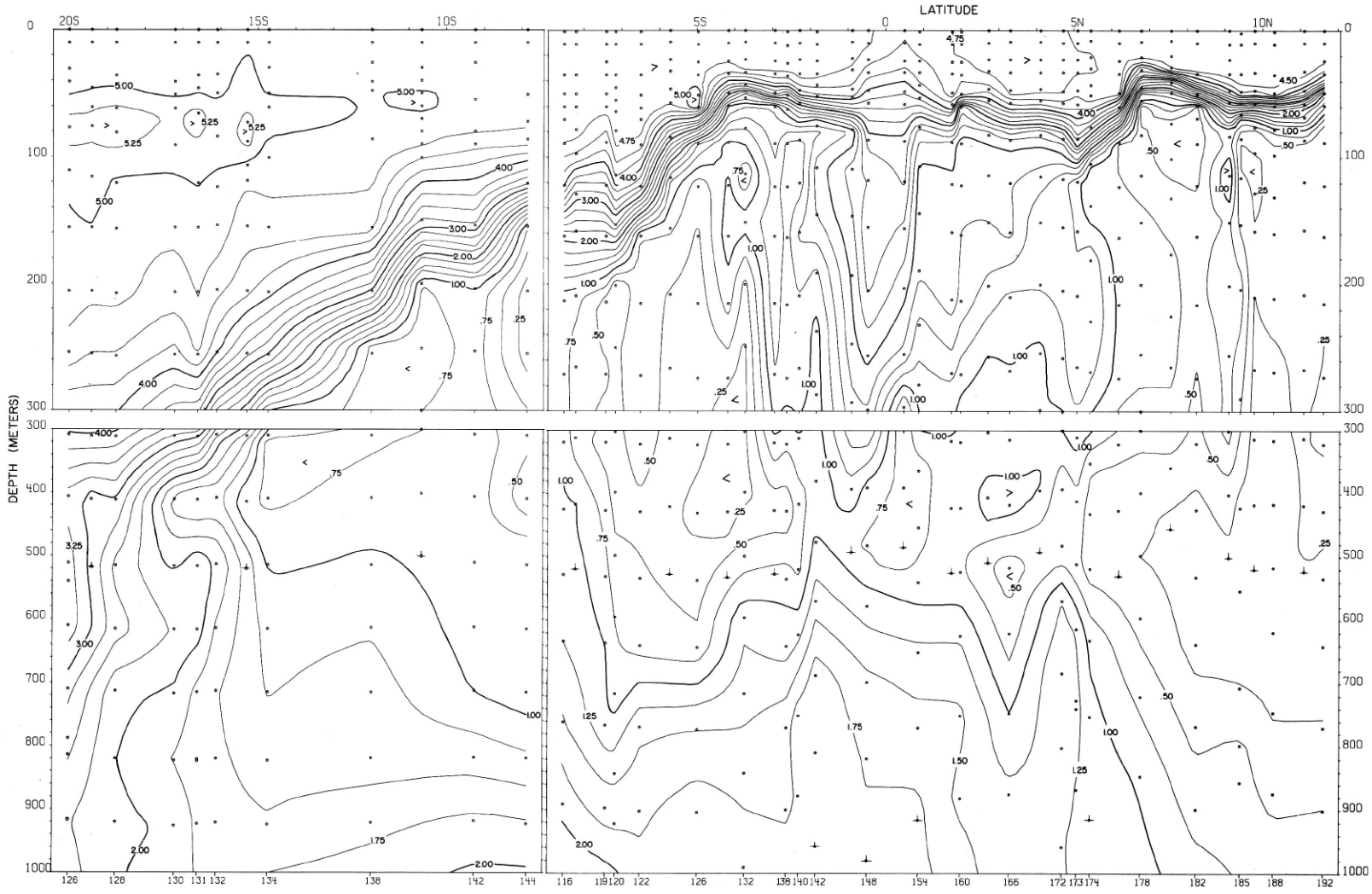


FIGURE 75-$O_2$-v4.}—Vertical distribution of oxygen (ml./l.) along 112° W., March 1968. Southern portion of section run by *Washington*, March 7-11; northern portion by *Jordan*, March 17-26.
FIGURE 76-$O_2$-v3.}

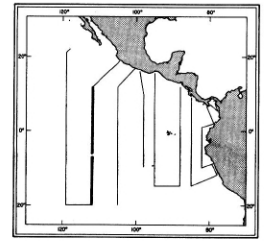

75-$O_2$-v4.
76-$O_2$-v3.

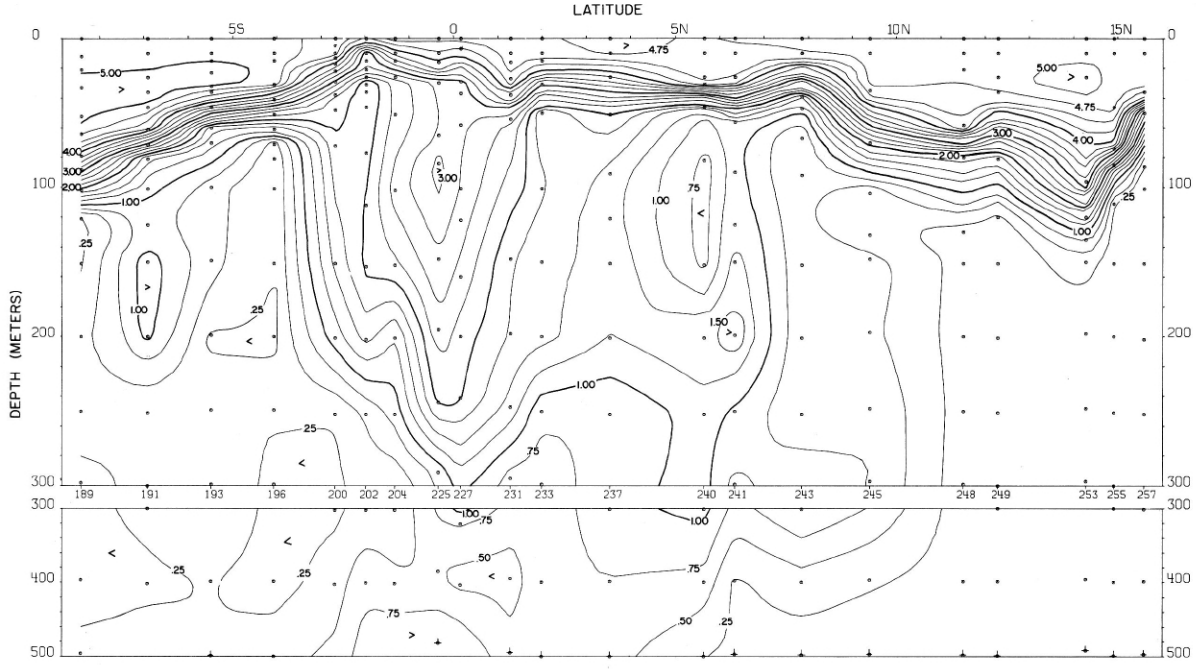


FIGURE 75-$O_2$-v5.—Vertical distribution of oxygen (ml./l.) along 98° W., March 21-April 8, 1968. The interruption in the contours indicates a 9-day interval between stations 205 and 223.

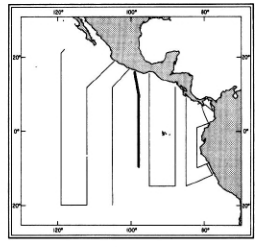

75-$O_2$-v5.

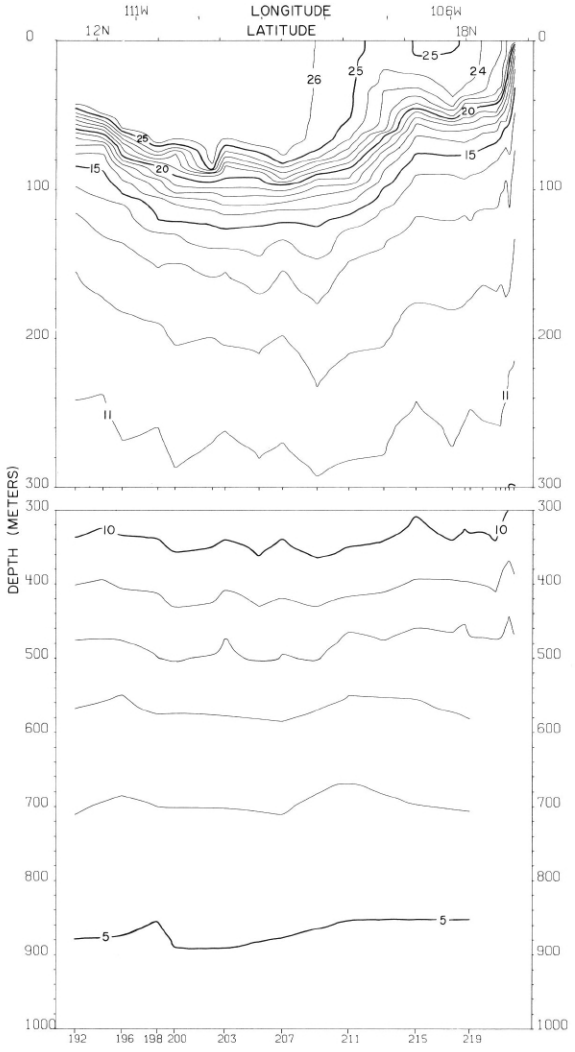


FIGURE 76-T-v4.—Vertical distribution of temperature (°C.) along a section from 12° N., 112° W. to Manzanillo, March 26-30, 1968.

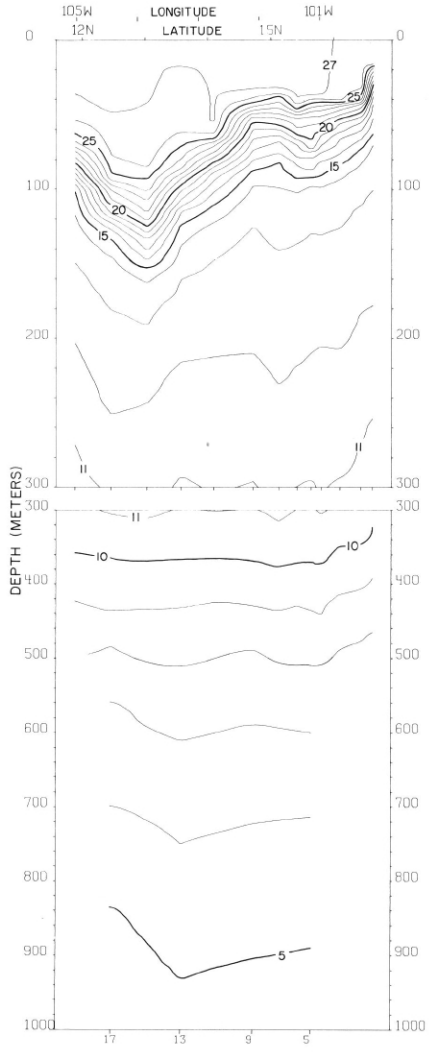


FIGURE 76-T-v1.—Vertical distribution of temperature (°C.) along a section from Acapulco to 12° N., 105° W., February 26-28, 1968.

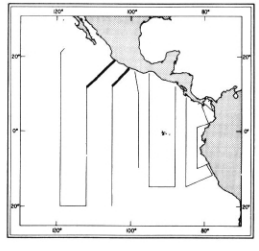

76-T-v1.

76-T-v4.

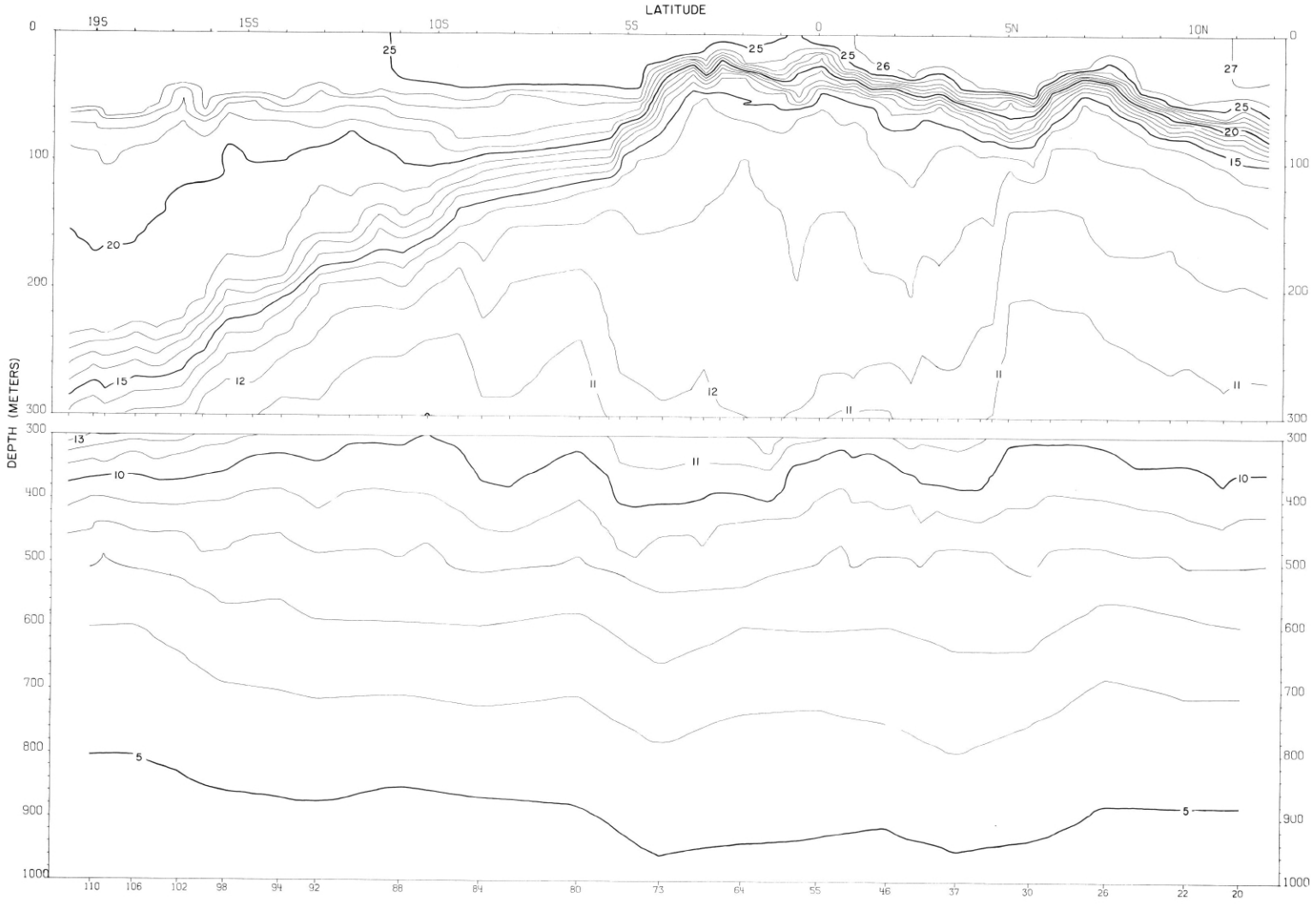


FIGURE 76-T-v2.—Vertical distribution of temperature (°C.) along 105° W. February 28-March 14, 1968.

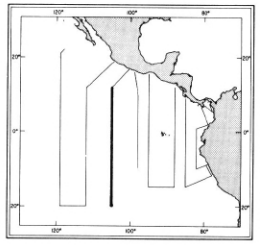

76-T-v2.

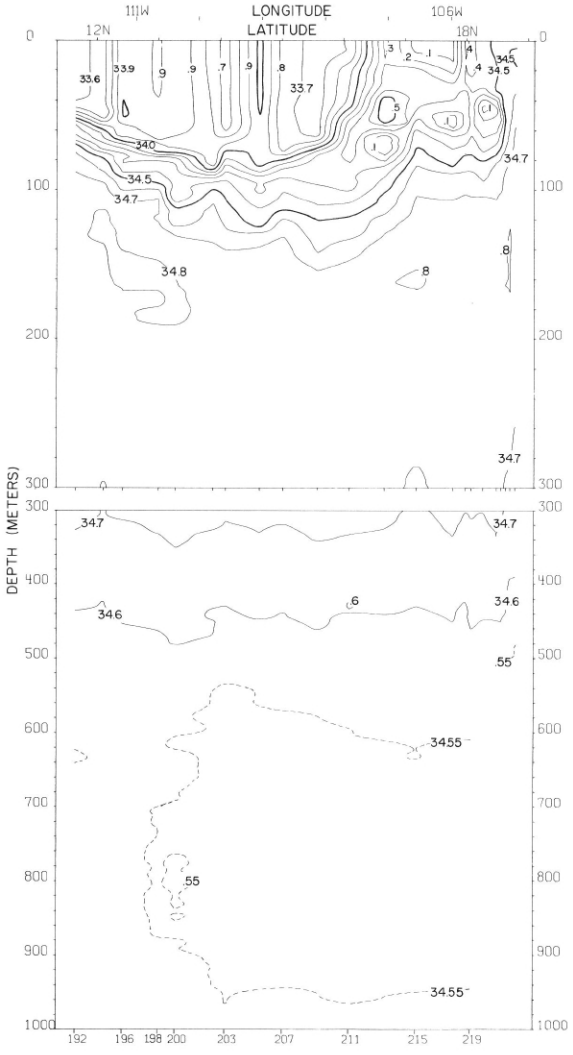


FIGURE 76-S-v4.—Vertical distribution of salinity (‰) along a section from 12° N., 112° W. to Manzanillo, March 26-30, 1968.

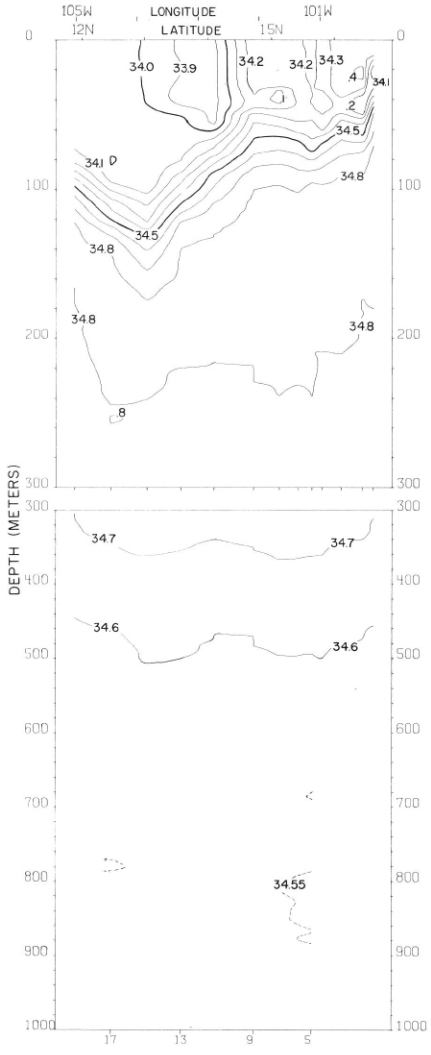


FIGURE 76-S-v1.—Vertical distribution of salinity (‰) along a section from Acapulco to 12° N., 105° W., February 26-28, 1968.

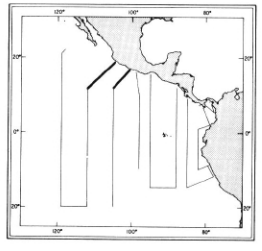

76-S-v1.

76-S-v4.

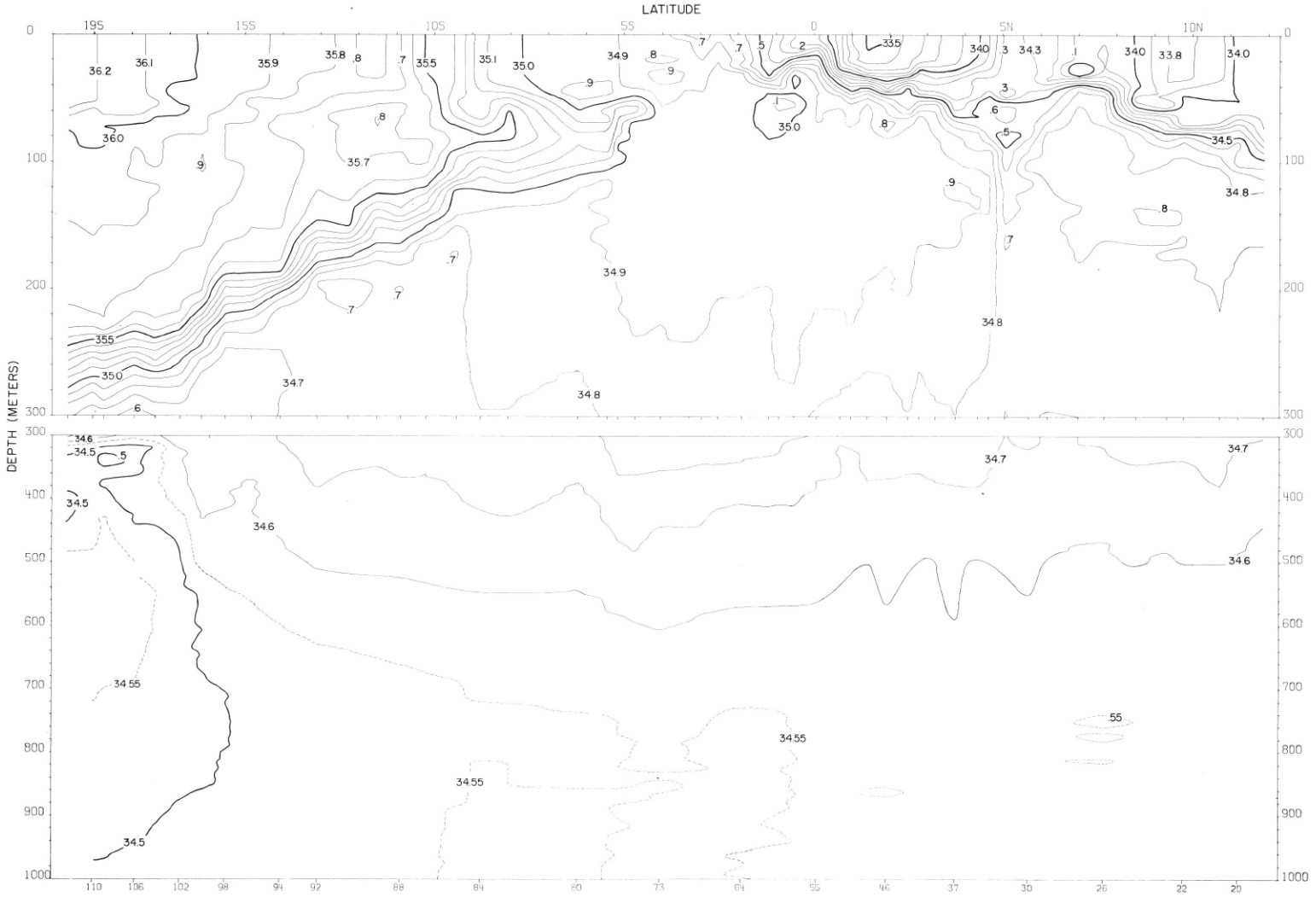


FIGURE 76-S-v2.—Vertical distribution of salinity (‰) along 105° W., February 28-March 14, 1968.

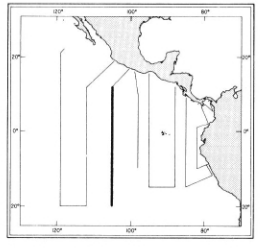

76-S-v2.

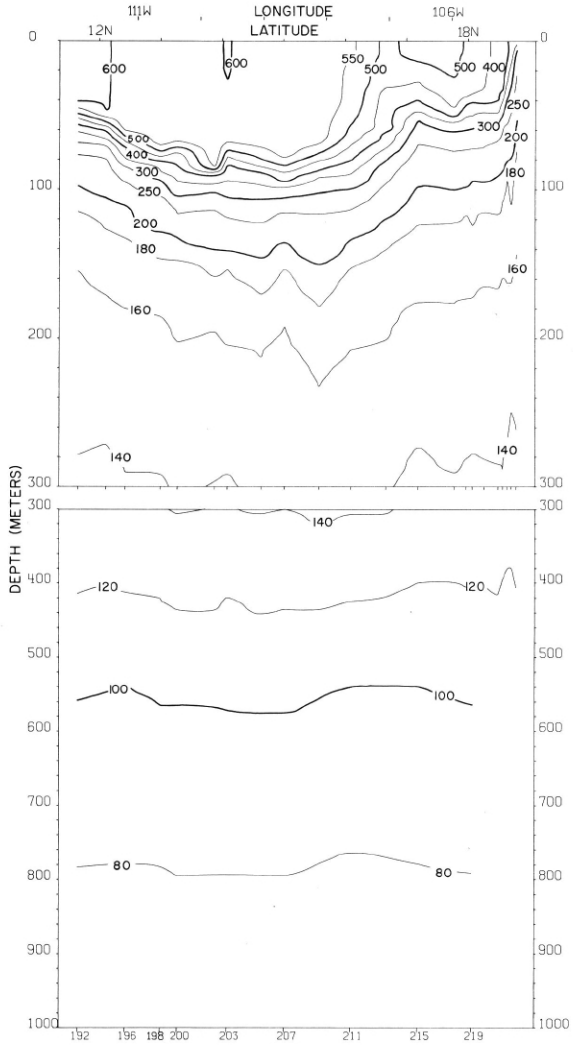


FIGURE 76-δ-v4.—Vertical distribution of thermosteric anomaly, $\delta_T$, (cl./t.) along a section from 12° N., 112° W. to Manzanillo, March 26-30, 1968.

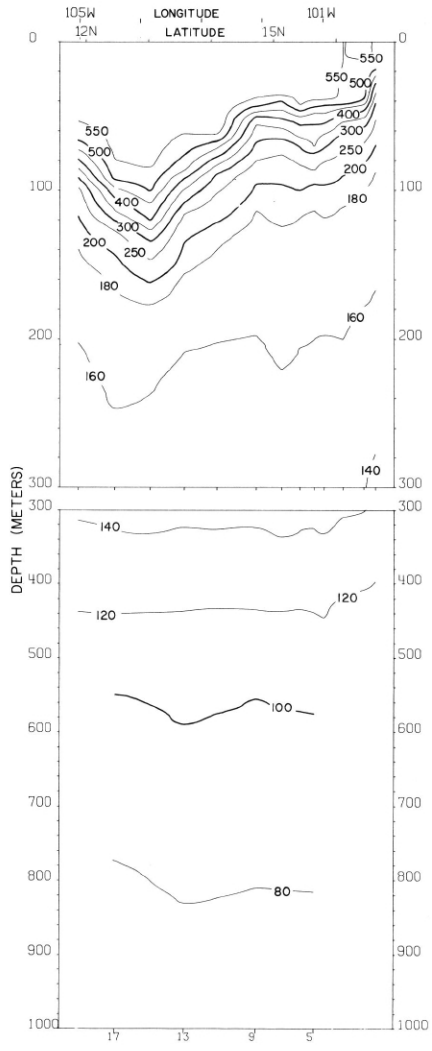


FIGURE 76-δ-v1.—Vertical distribution of thermosteric anomaly, $\delta_T$, (cl./t.) along a section from Acapulco to 12° N., 105° W., February 26-28, 1968.

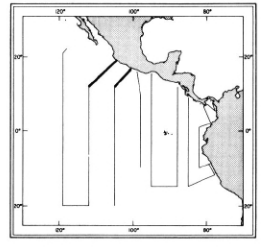

76-δ-v1.

76-δ-v4.

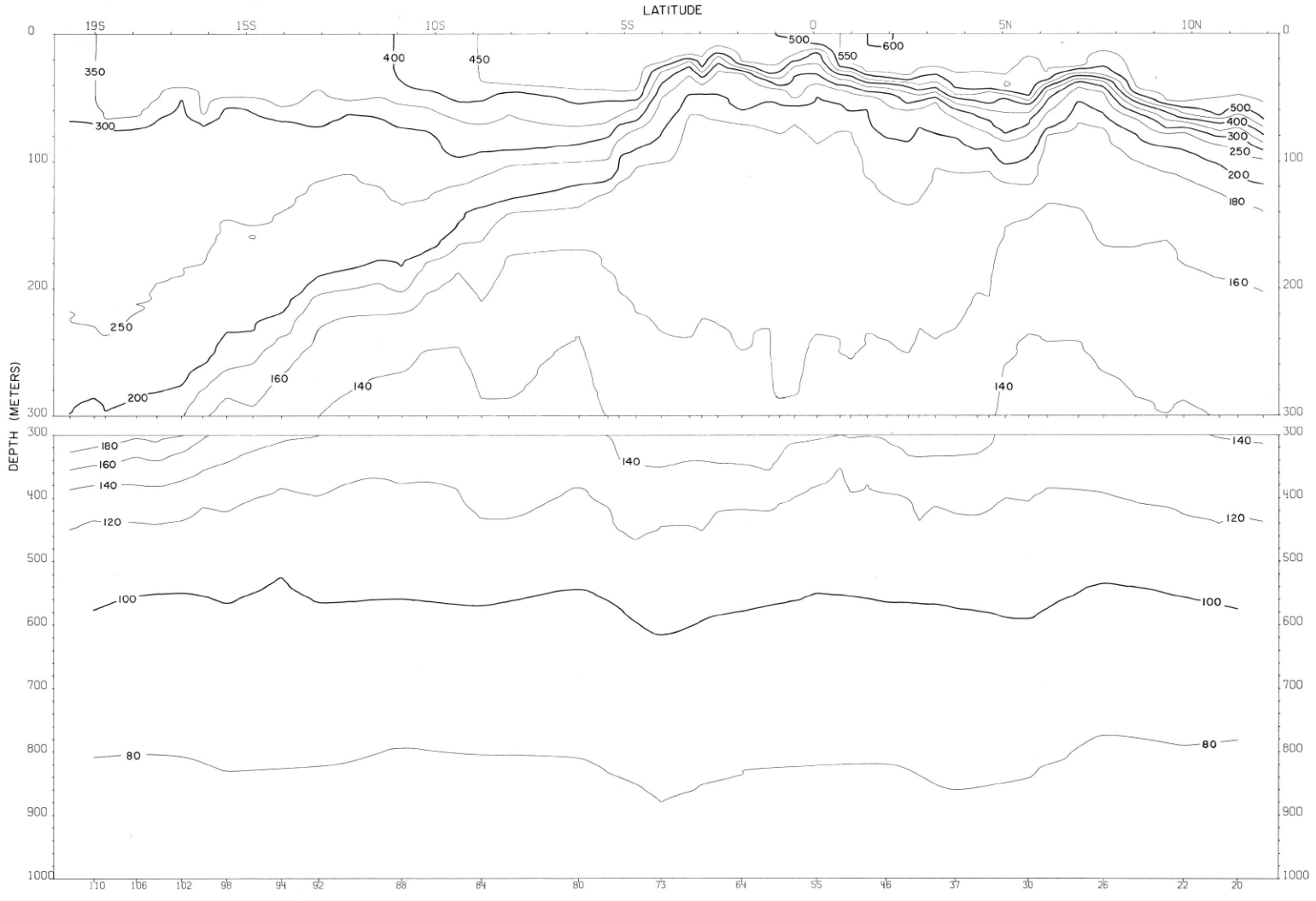


FIGURE 76-δ-v2.—Vertical distribution of thermosteric anomaly, $\delta_T$, (cl./t.) along 105° W., February 28-March 14,1968.

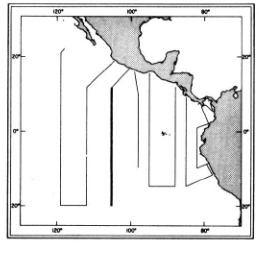

76-δ-v2.

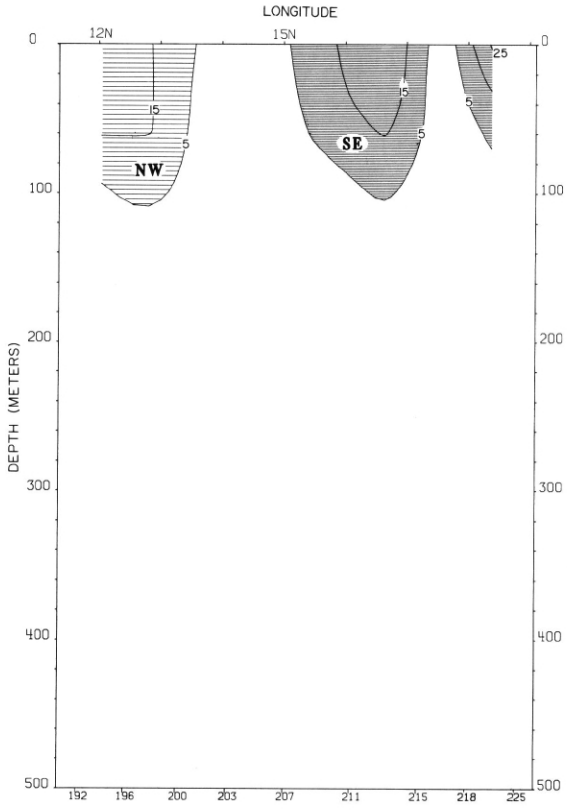


FIGURE 76-G-v4.—Vertical distribution of the component of geostrophic velocity (cm./sec.), relative to 500 db., normal to a section from 12° N., 112° W. to Manzanillo, March 26-30, 1968. Dark shading indicates flow toward the southeast with a velocity greater than 5 cm./sec.; light shading indicates flow toward the northwest with a velocity greater than 5 cm./sec.

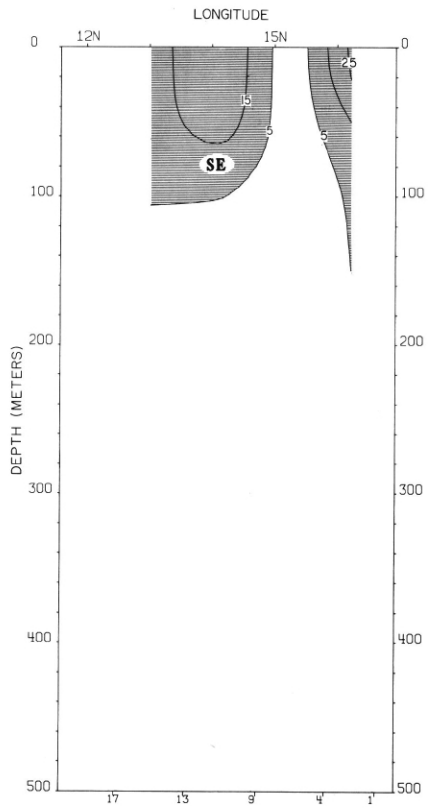


FIGURE 76-G-v1.—Vertical distribution of the component of geostrophic velocity (cm./sec.), relative to 500 db., normal to a section from Acapulco to 12° N., 105° W., February 26-28, 1968. The dark shading indicates flow toward the southeast with a velocity greater than 5 cm./sec.

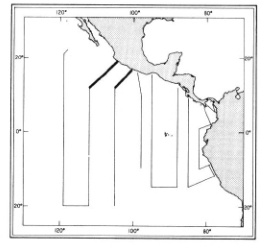

76-G-v1.

76-G-v4.

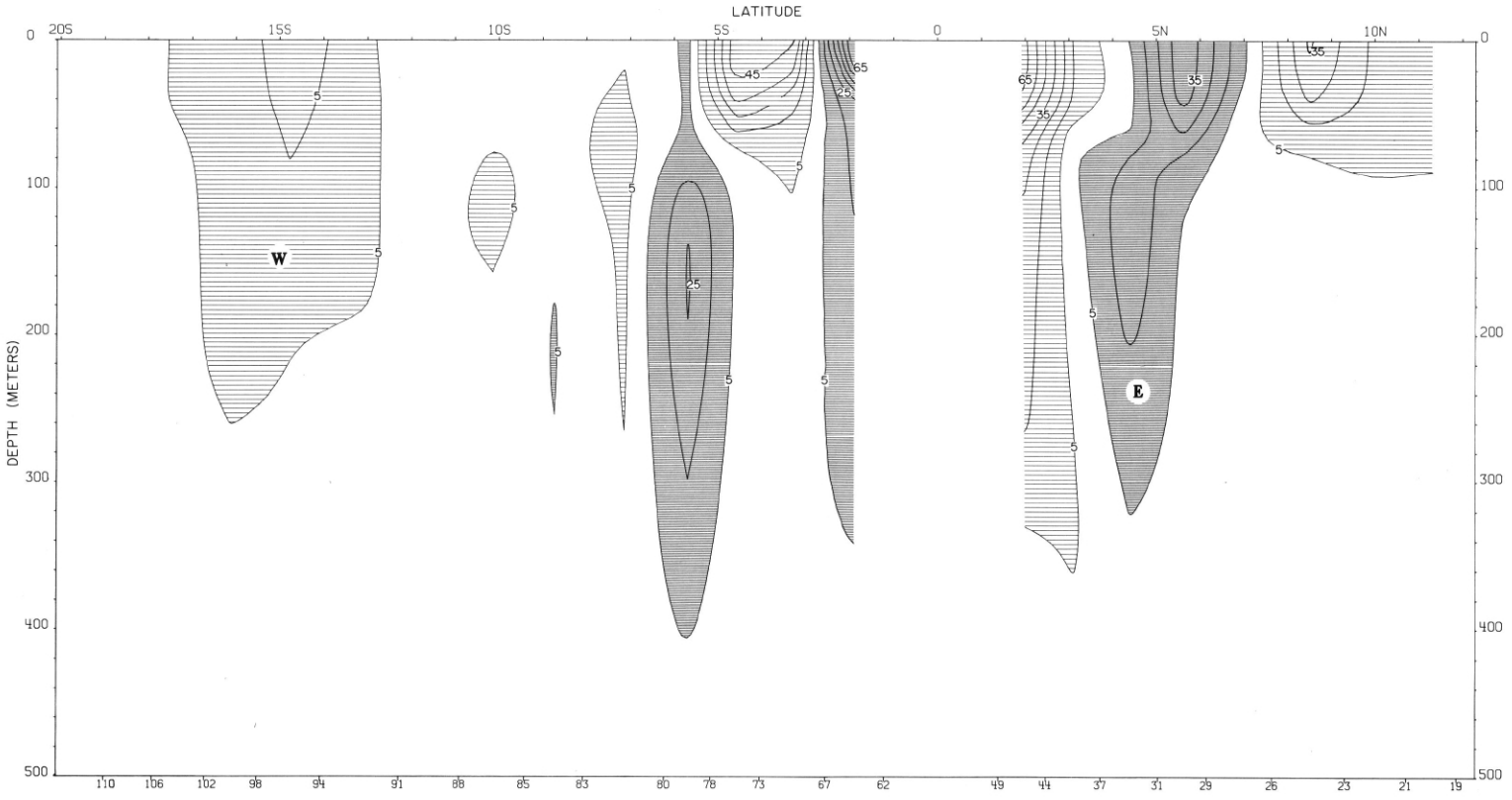


FIGURE 76-G-v2.—Vertical distribution of the zonal component of geostrophic velocity (cm./sec.), relative to 500 db., along 105° W., February 28-March 14, 1968. Dark shading indicates eastward flow with a velocity greater than 5 cm./sec.; light shading indicates westward flow with a velocity greater than 5 cm./sec.

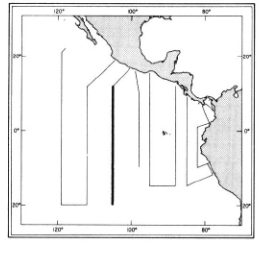

76-G-v2.

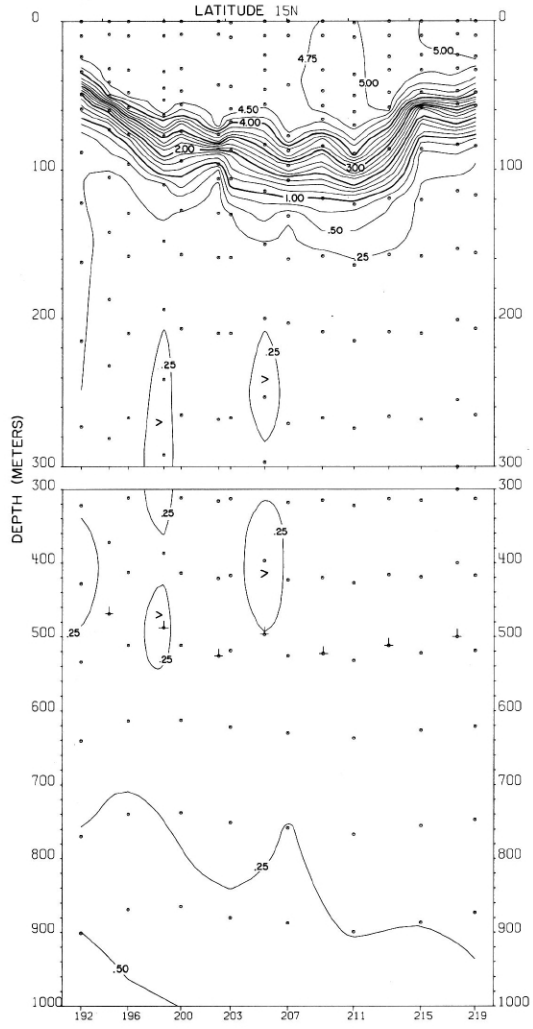


FIGURE 76-O₂-v4.—Vertical distribution of oxygen (ml./l.) along a section from 12° N., 112° W. to Manzanillo, March 26-30, 1968.

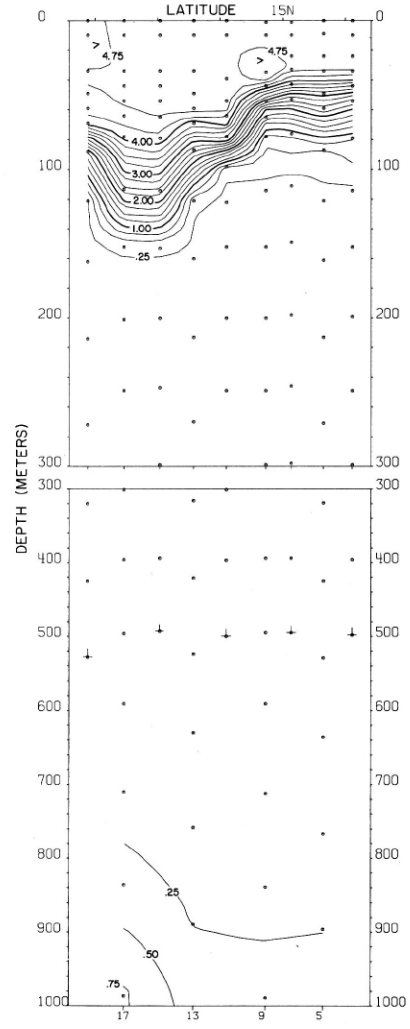


FIGURE 76-O₂-v1.—Vertical distribution of oxygen (ml./l.) along a section from Acapulco to 12° N., 105° W., February 26-28, 1968.

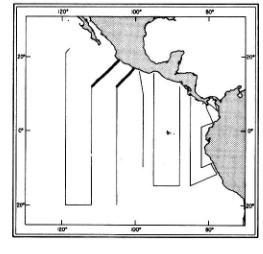

76-O₂-v1.

76-O₂-v4.

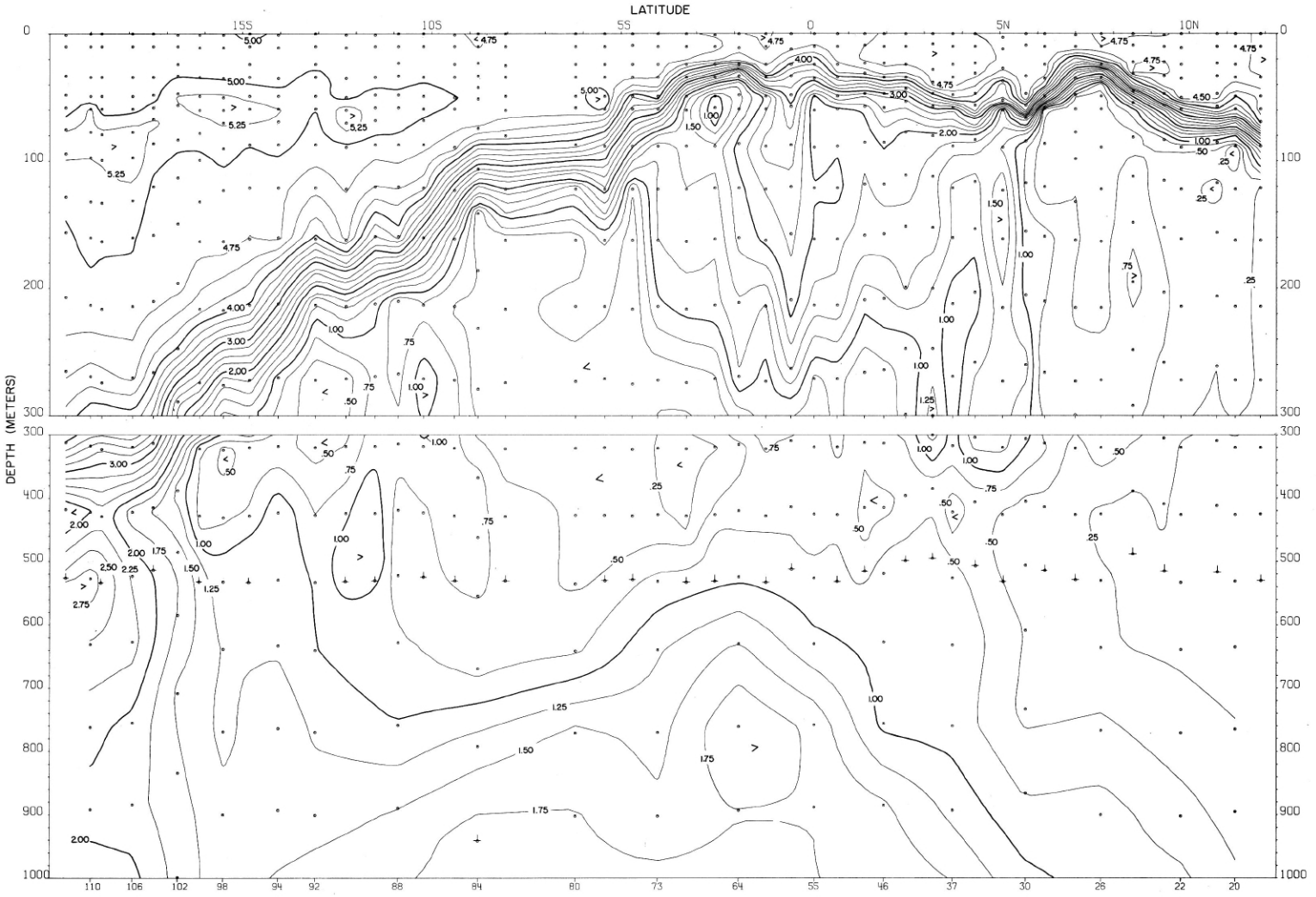


FIGURE 76-O₂-v2.—Vertical distribution of oxygen (ml./l.) along 105° W., February 28-March 14, 1968.

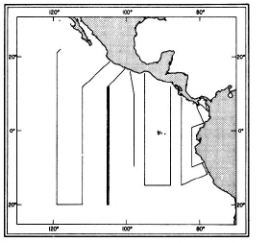

76-O₂-v2.

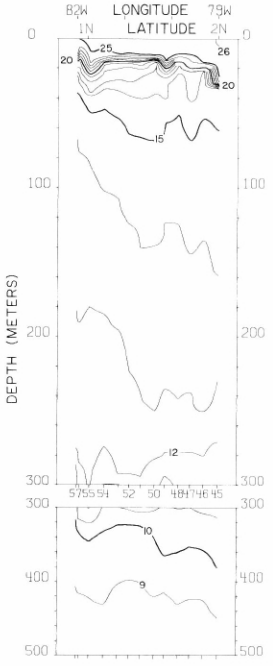


FIGURE 77-T-v5.—Vertical distribution of temperature (°C.) along a northeast-southwest section from the coast of Colombia to 0°54′ N., 82°00′ W., February 4-9, 1968.

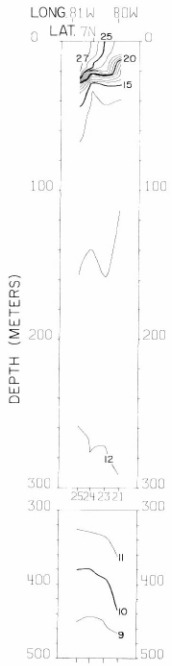


FIGURE 77-T-v3.—Vertical distribution of temperature (°C.) along the coast of Panama from 79°57′ W. to 80°53′ W., February 1, 1968.

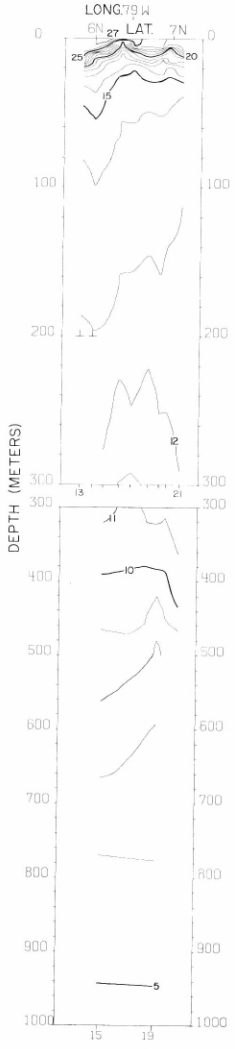


FIGURE 77-T-v2.—Vertical distribution of temperature (°C.) across the northern portion of the Panama Bight from the coast of Colombia to Cabo Mala, Panama, January 31-February 1, 1968.

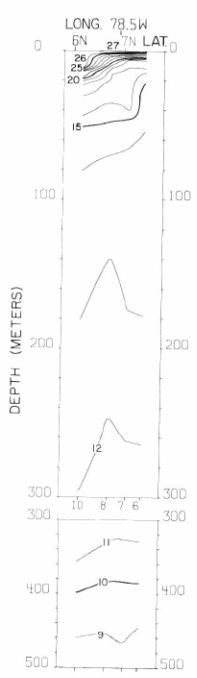


FIGURE 77-T-v1.—Vertical distribution of temperature (°C.) along a section in the Panama Bight near the coasts of Panama and Colombia from 7°25′ N. to 6°10′ N., January 30-31, 1968.

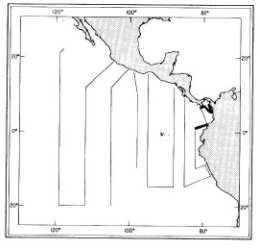

77-T-v1.

77-T-v2.

77-T-v3.

77-T-v5.

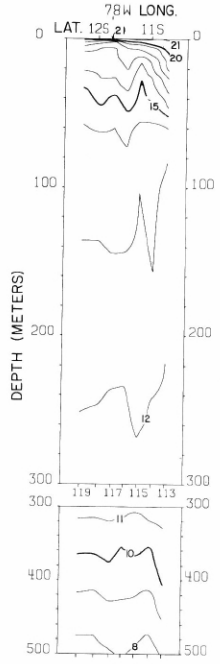


FIGURE 77-T-v8.—Vertical distribution of temperature (°C.) along the coast of Peru from 10°40′ S. to 12°17′ S., February 12-13, 1968.

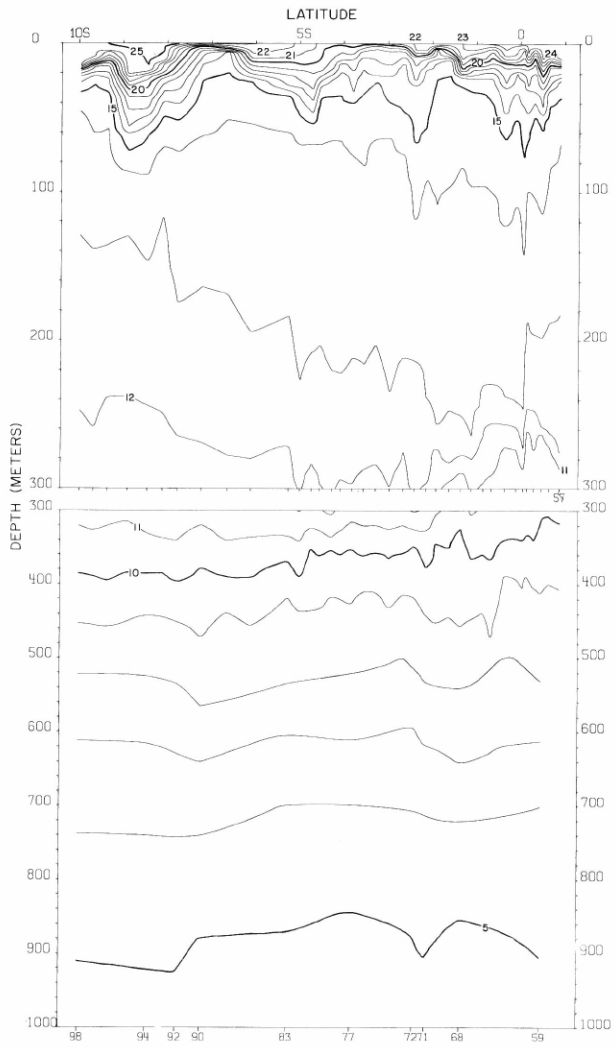


FIGURE 77-T-v6.—Vertical distribution of temperature (°C.) along 82° W., February 4-9, 1968.

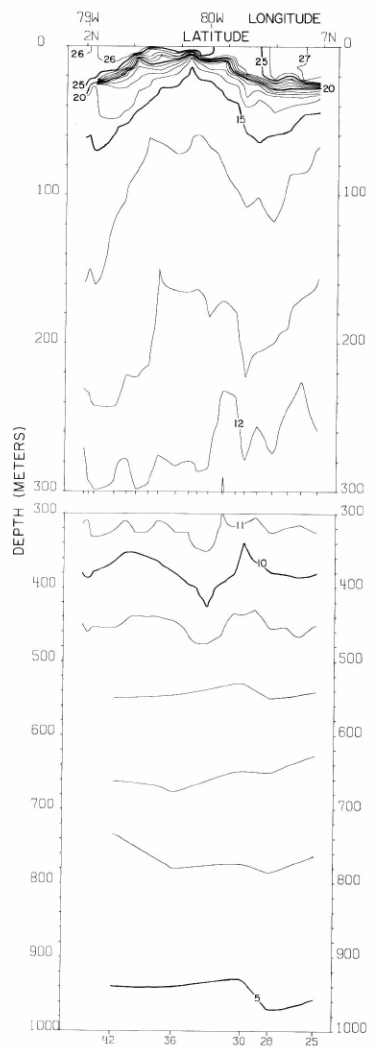


FIGURE 77-T-v4.—Vertical distribution of temperature (°C.) along a northwest-southeast section across the Panama Bight from Peninsula de Azuero, Panama, to the coast of Colombia, February 1-3, 1968.

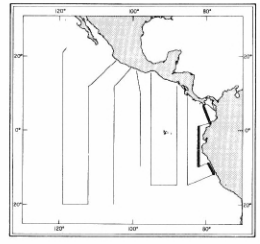

77-T-v4.

77-T-v6.

77-T-v8.

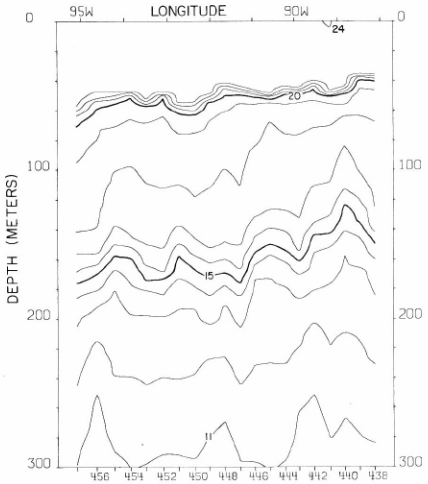


FIGURE 77-T-v12.—Vertical distribution of temperature (°C.) along 15° S., April 8-9, 1968.

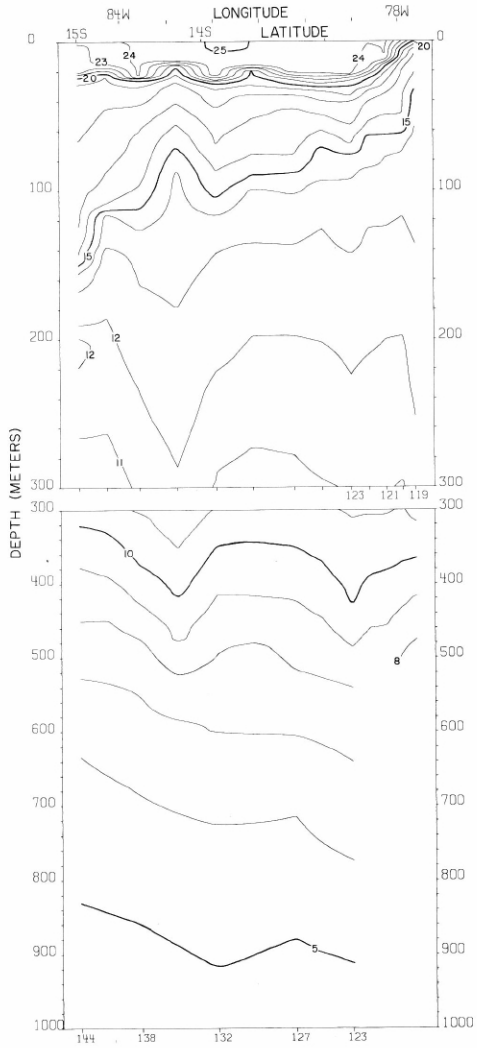


FIGURE 77-T-v9.—Vertical distribution of temperature (°C.) along a northeast-southwest section from the coast of Peru to 14°59'S., 84°56'W., February 13-15, 1968.

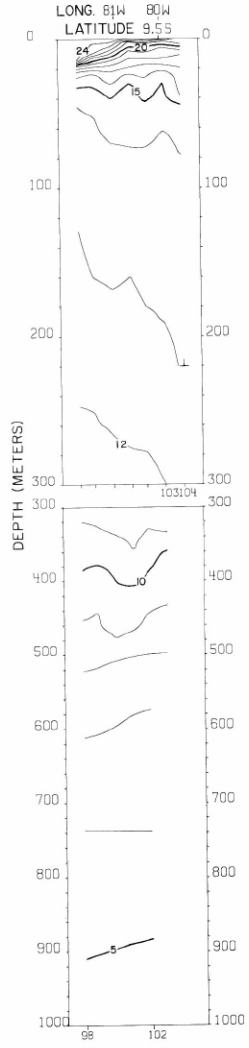


FIGURE 77-T-v7.—Vertical distribution of temperature (°C.) along a southwest-northeast section from 9°57'S., 81°49'W. to the coast of Peru, February 9, 1968.

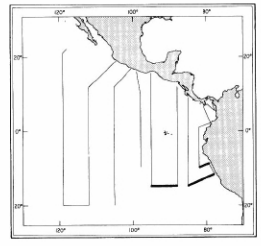

77-T-v7.

77-T-v9.

77-T-v12.

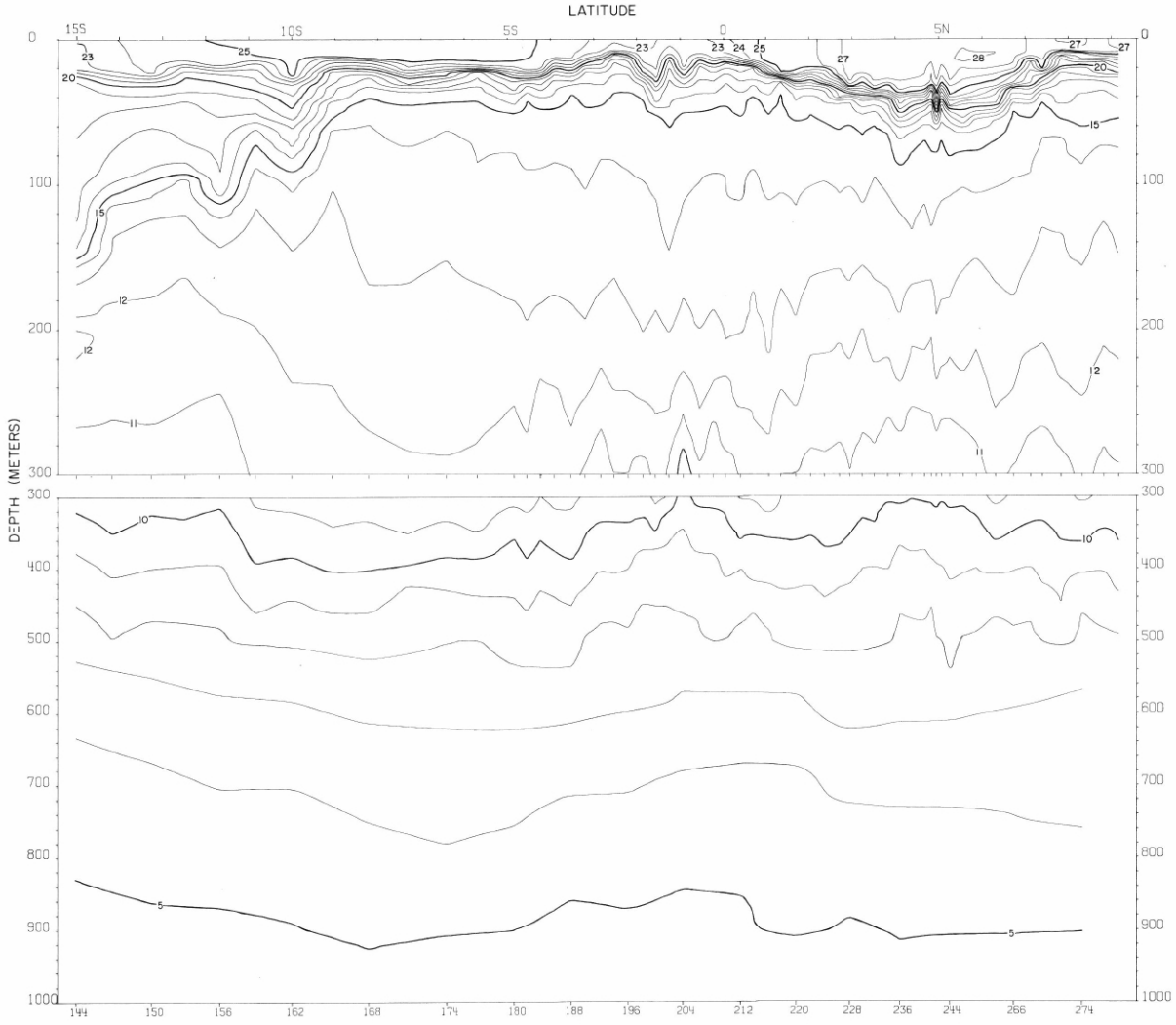


FIGURE 77-T-v10.—Vertical distribution of temperature (°C.) along 85° W., February 15-25, 1968.

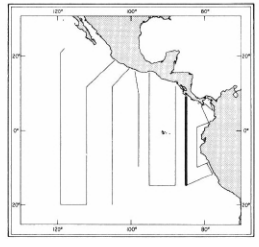

77-T-v10.

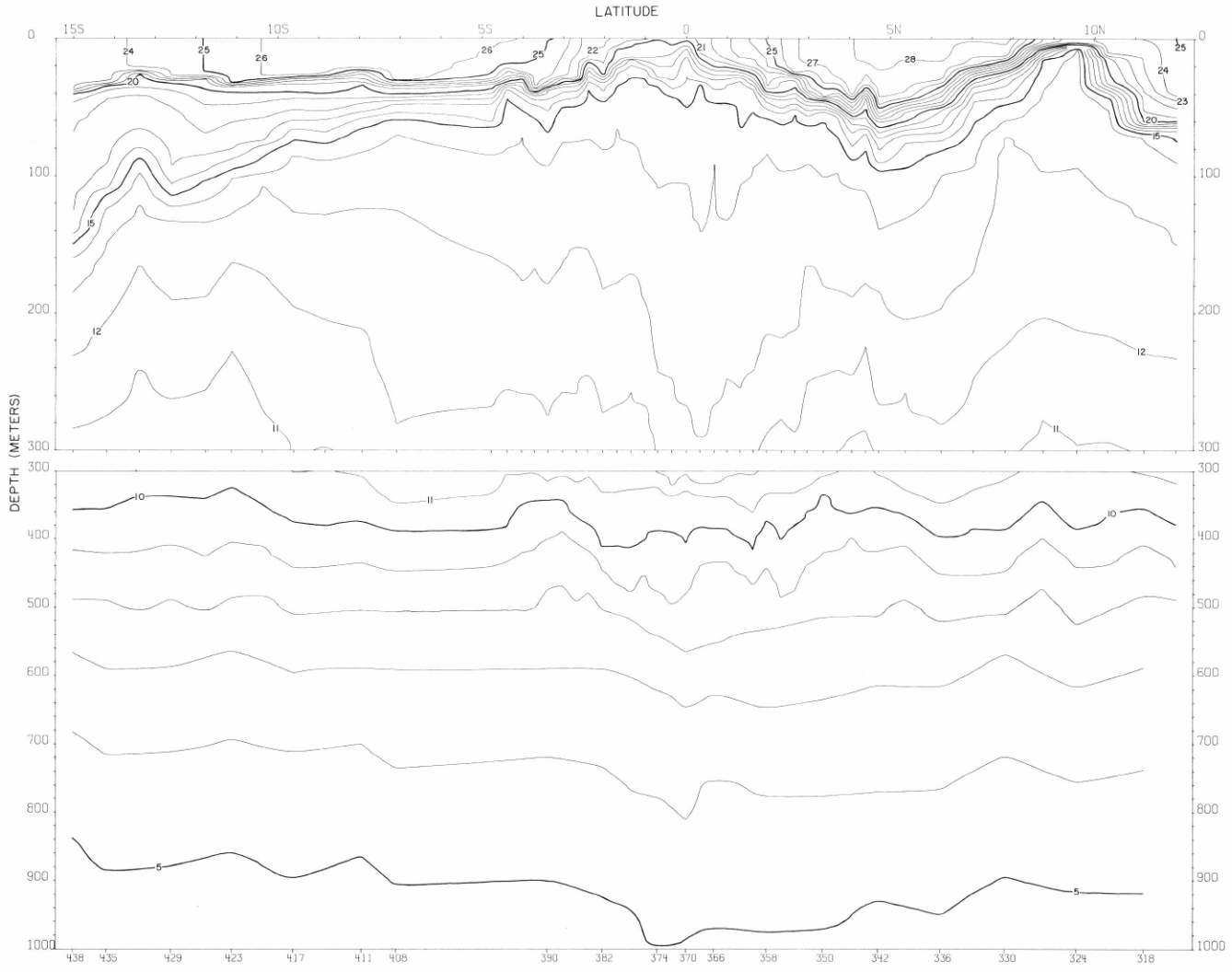


FIGURE 77-T-v11.—Vertical distribution of temperature (°C.) along 88° W., March 30-April 8, 1968.

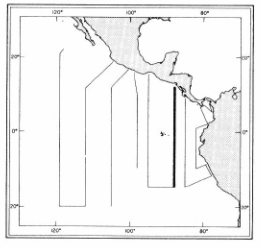

77-T-v11.

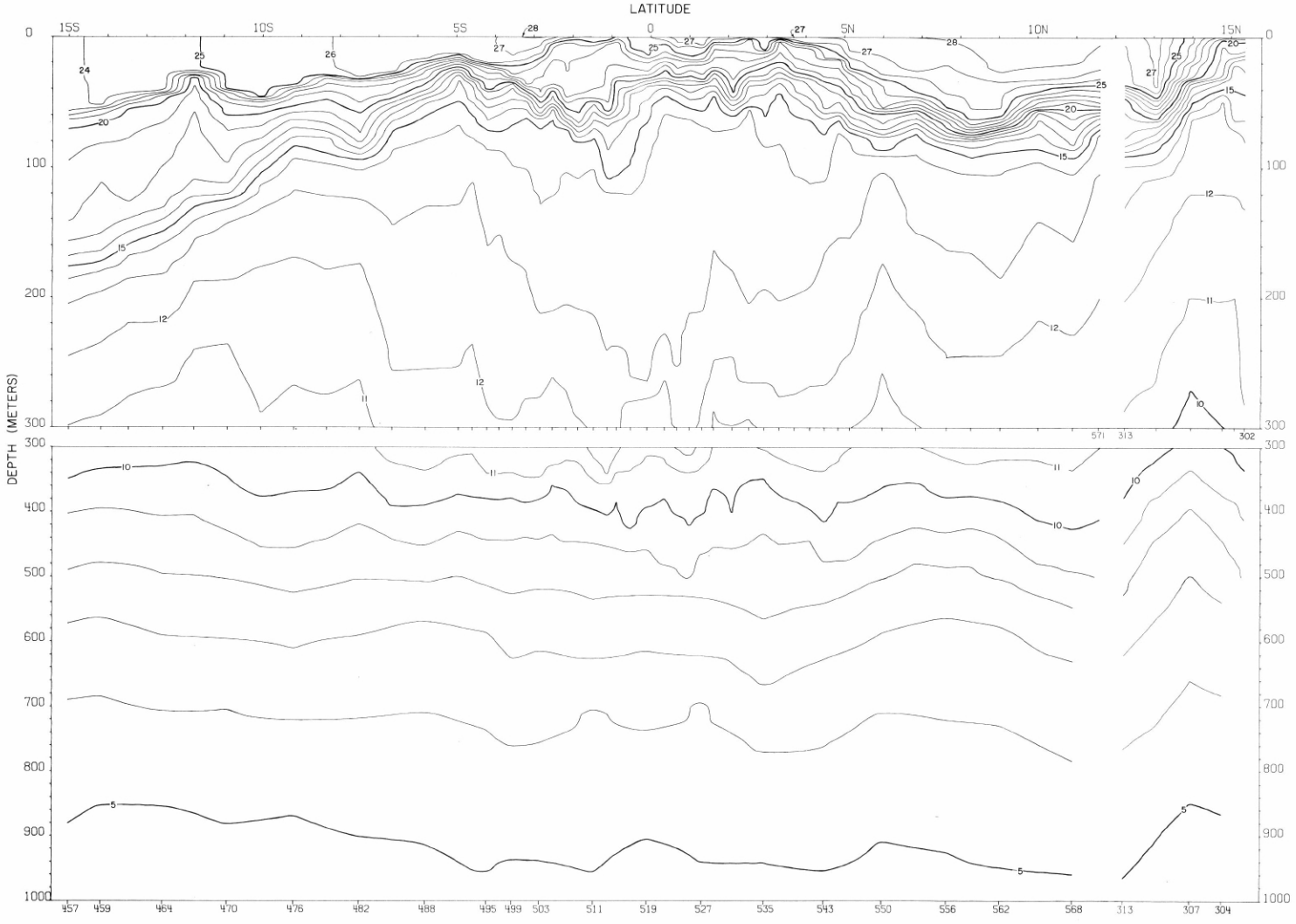


FIGURE 77-T-v13.—Vertical distribution of temperature (°C.) along 95° W., March-April 1968. Stations 302-313 were occupied on March 3-4, Stations 457-571 on April 9-18. The interruption in the contours indicates the 44½-day interval between Stations 313 and 571.

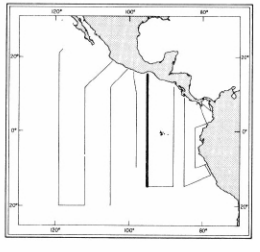

77-T-v13.

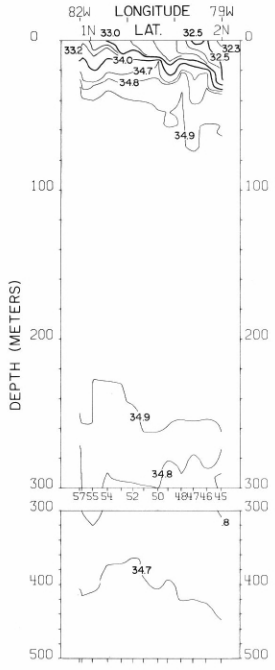


FIGURE 77-S-v5.—Vertical distribution of salinity (‰) along a northeast-southwest section from the coast of Colombia to 0°54′ N., 82°00′ W., February 3-4, 1968. Some contours in the range 32.4 to 34.6 ‰ have been omitted in order to avoid excessive crowding near the top of the chart.

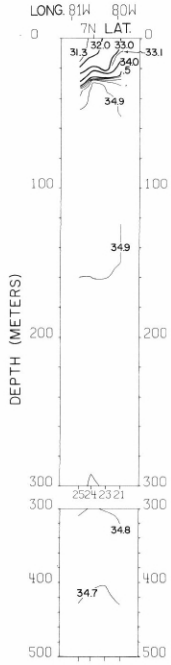


FIGURE 77-S-v3.—Vertical distribution of salinity (‰) along the coast of Panama from 79°57′ W. to 80°53′ W., February 1, 1968. Some contours in the range 31.4 to 34.4 ‰ have been omitted in order to avoid excessive crowding near the top of the chart.

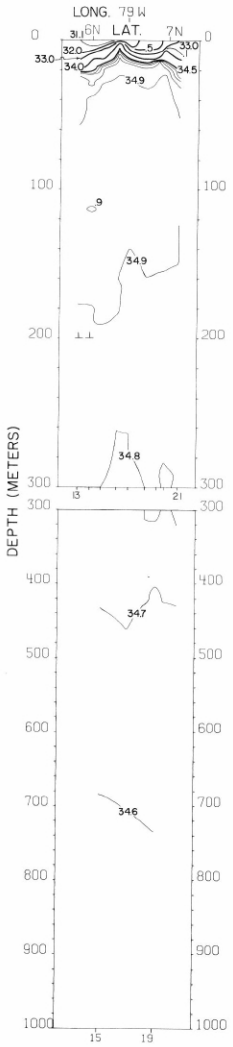


FIGURE 77-S-v2.—Vertical distribution of salinity (‰) across the northern portion of the Panama Bight from the coast of Colombia to Cabo Mala, Panama, January 31-February 1, 1968.

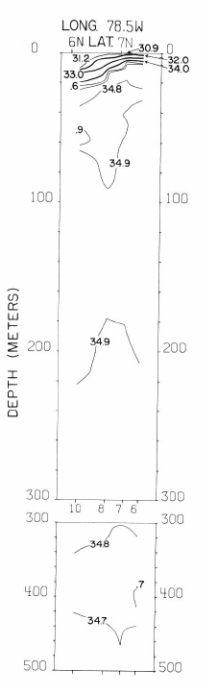


FIGURE 77-S-v1.—Vertical distribution of salinity (‰) along a section in the Panama Bight near the coasts of Panama and Colombia from 7°25′ N. to 6°10′ N., January 30-31, 1968. Some contours in the range 31.0 to 34.5 ‰ have been omitted in order to avoid excessive crowding near the top of the chart.

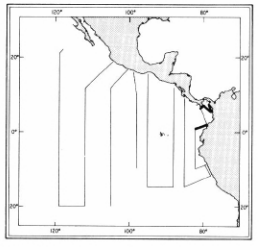

77-S-v1.

77-S-v2.

77-S-v3.

77-S-v5.

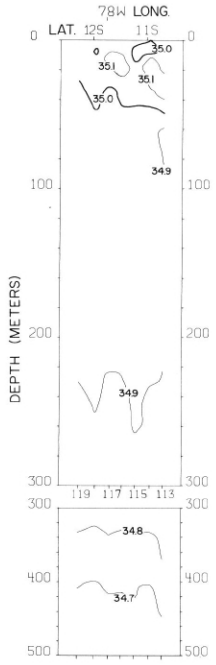


FIGURE 77-S-v8.—Vertical distribution of salinity (‰) along the coast of Peru from 10°40′ S. to 12°17′ S., February 12-13, 1968.

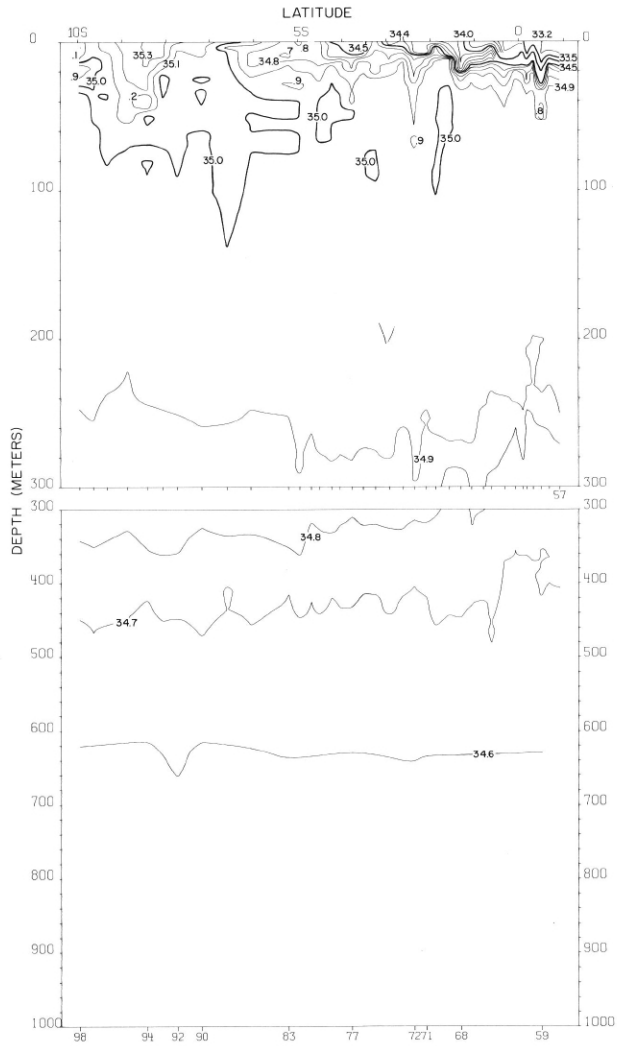


FIGURE 77-S-v6.—Vertical distribution of salinity (‰) along 82° W., February 4-9, 1968.

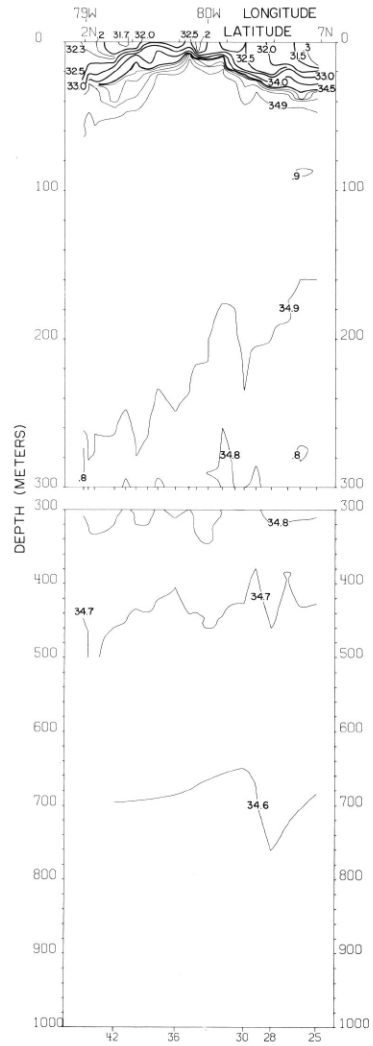


FIGURE 77-S-v4.—Vertical distribution of salinity (‰) along a northwest-southeast section across the Panama Bight from Peninsula de Azuero, Panama, to the coast of Colombia, February 1-3, 1968. Some contours in the range 31.4 to 34.4 ‰ have been omitted in order to avoid excessive crowding near the top of the chart.

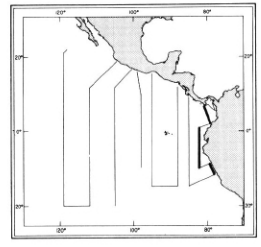

77-S-v4.

77-S-v6.

77-S-v8.

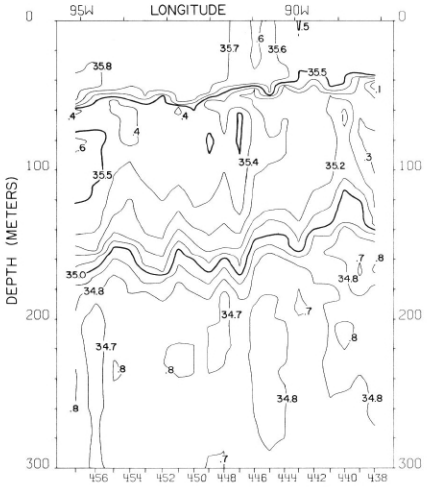


FIGURE 77-S-v12.—Vertical distribution of salinity (‰) along 15° S., April 8-9, 1968.

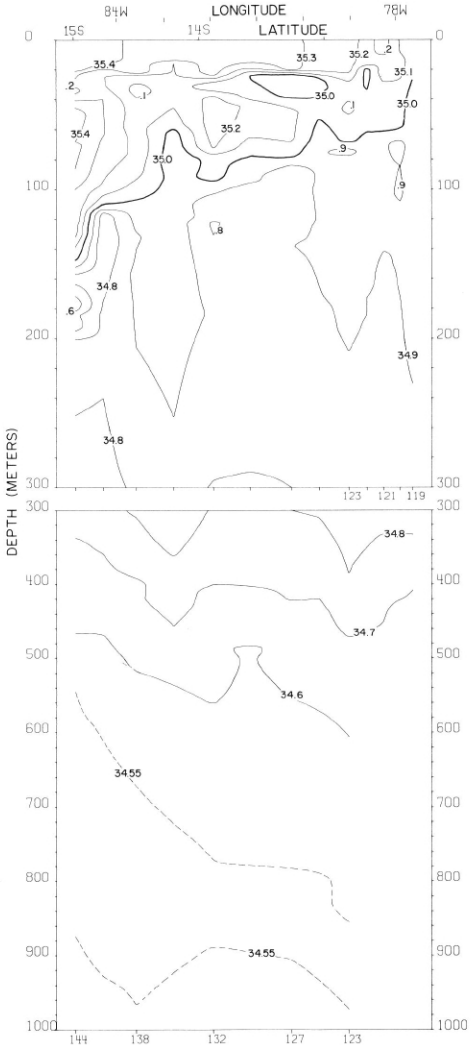


FIGURE 77-S-v9.—Vertical distribution of salinity (‰) along a northeast-southwest section from the coast of Peru to 14°59′ S., 84°56′ W., February 13-15, 1968.

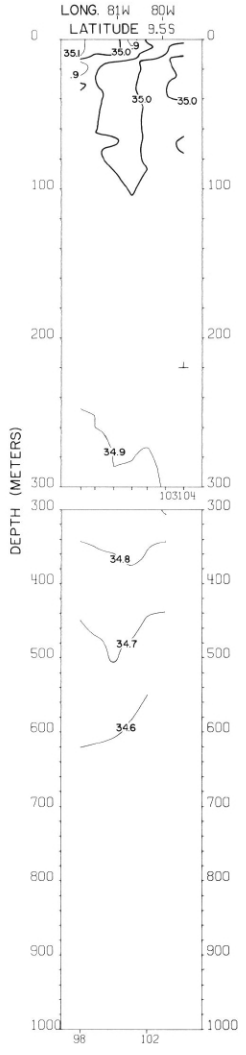


FIGURE 77-S-v7.—Vertical distribution of salinity (‰) along a southwest-northeast section from 9°57′ S., 81°49′ W. to the coast of Peru, February 9, 1968.

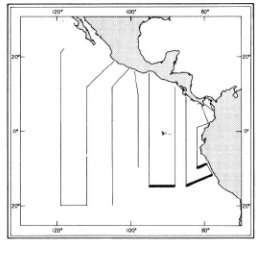

77-S-v7.

77-S-v9.

77-S-v12.

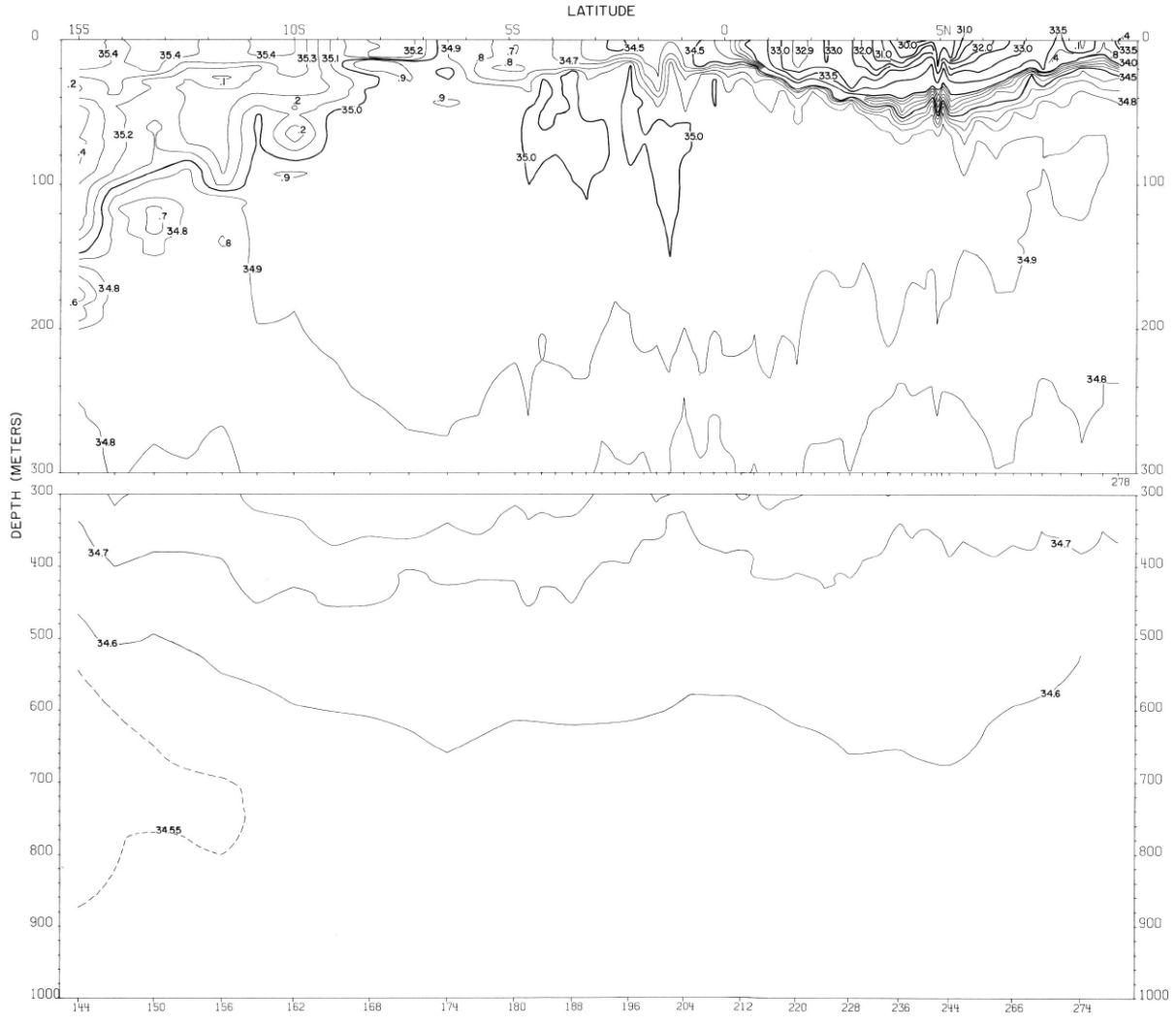


FIGURE 77-S-v10.—Vertical distribution of salinity (‰) along 85° W., February 15-25, 1968.

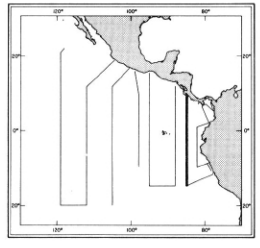

77-S-v10.

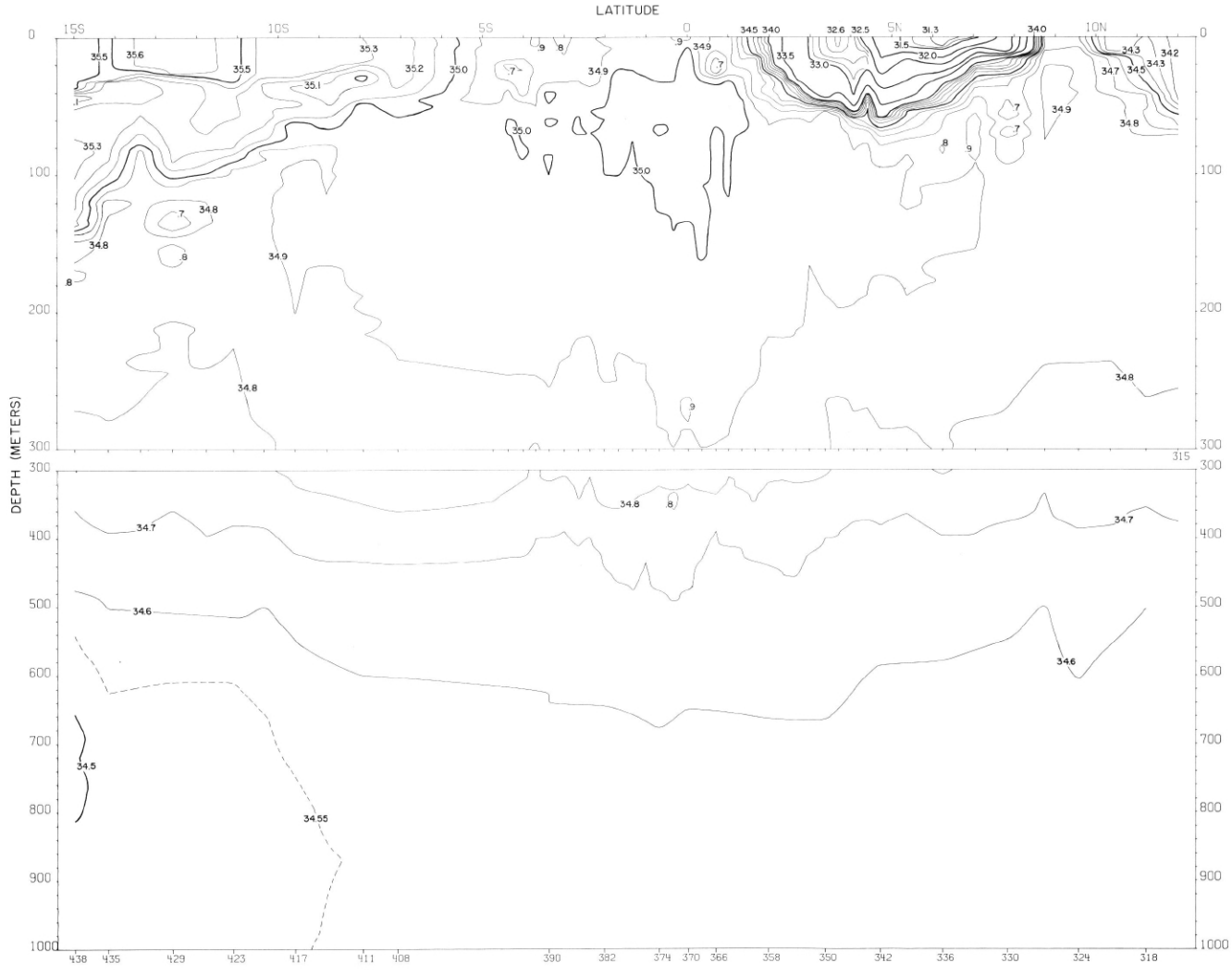


FIGURE 77-S-v11.—Vertical distribution of salinity (‰) along 88° W., March 30-April 8, 1968.

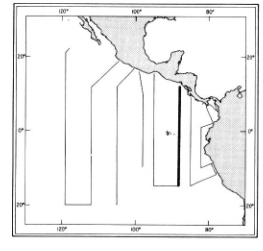

77-S-v11.

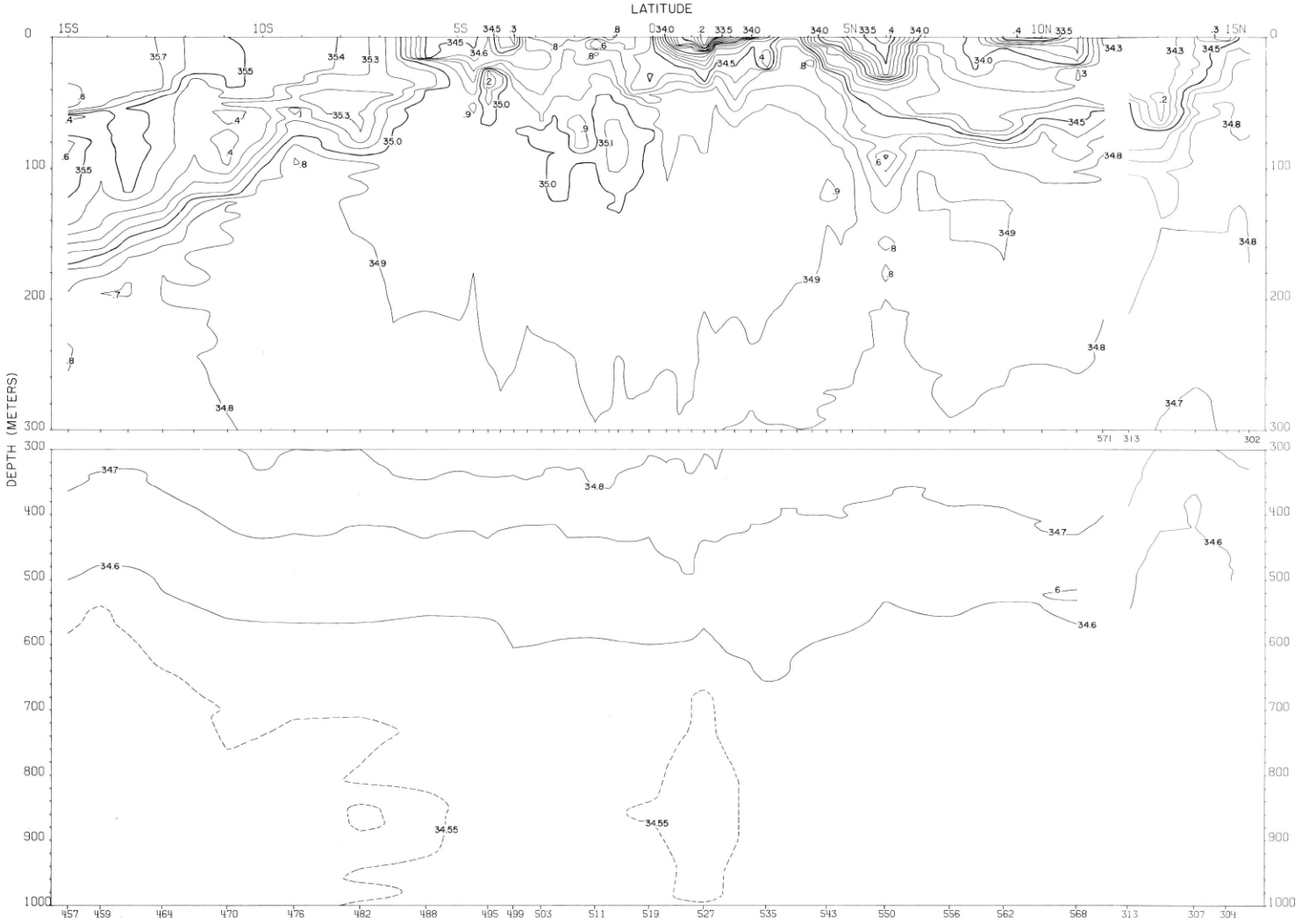


FIGURE 77-S-v13.—Vertical distribution of salinity (‰) along 95° W., March-April 1968. Stations 302-313 were occupied on March 3-4, Stations 457-571 on April 9-18. The interruption in the contours indicates the 44½-day interval between Stations 313 and 571.

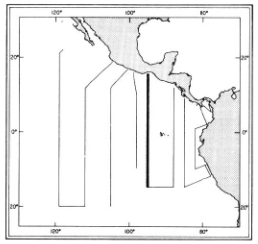

77-S-v13.

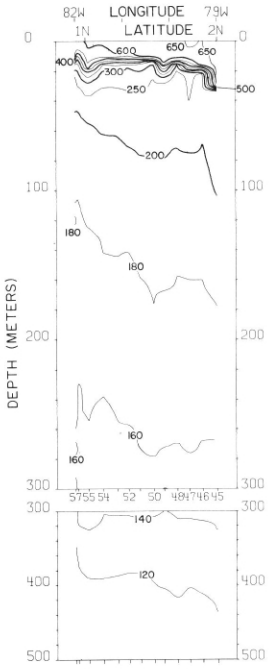


FIGURE 77-$\delta$-v5.—Vertical distribution of thermosteric anomaly, $\delta_T$, (cl./t.) along a northeast-southwest section from the coast of Colombia to 0°54′ N., 82°00′ W., February 4-9, 1968.

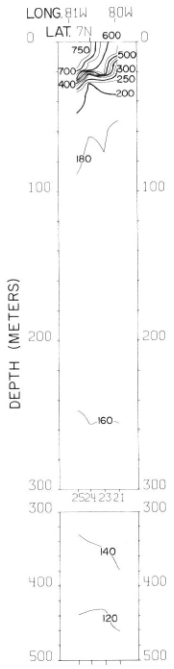


FIGURE 77-$\delta$-v3.—Vertical distribution of thermosteric anomaly, $\delta_T$, (cl./t.) along the coast of Panama from 79°57′ W. to 80°53′ W., February 1, 1968.

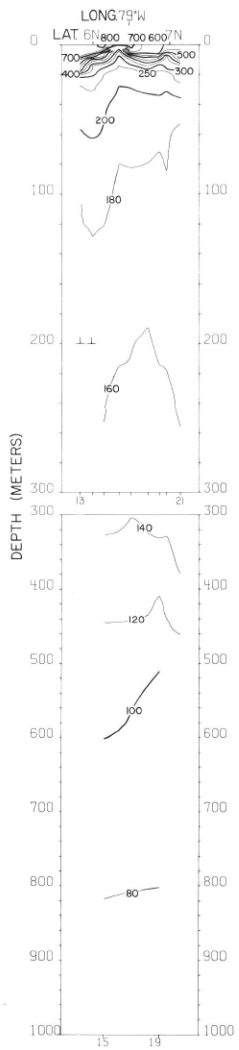


FIGURE 77-$\delta$-v2.—Vertical distribution of thermosteric anomaly, $\delta_T$, (cl./t.) across the northern portion of the Panama Bight from the coast of Colombia to Cabo Mala, Panama, January 31-February 1, 1968.

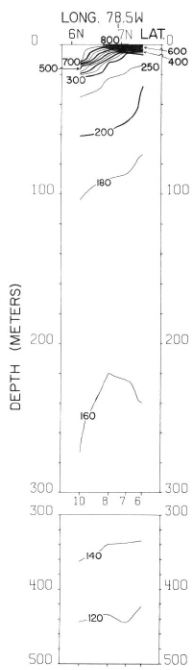


FIGURE 77-$\delta$-v1.—Vertical distribution of thermosteric anomaly, $\delta_T$ (cl./t.) along a section in the Panama Bight near the coasts of Panama and Colombia from 7°25′ N. to 6°10′ N., January 30-31, 1968.

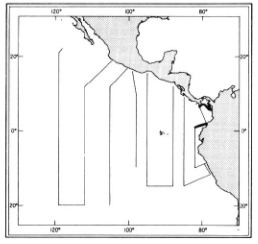

77-$\delta$-v1.

77-$\delta$-v2.

77-$\delta$-v3.

77-$\delta$-v5.

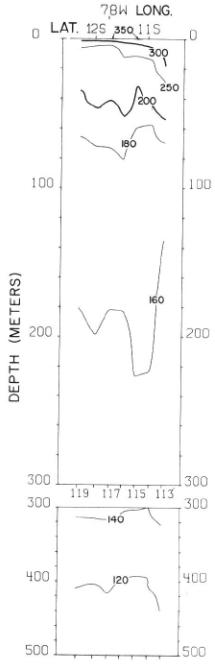


FIGURE 77-$\delta$-v8.—Vertical distribution of thermosteric anomaly, $\delta_T$, (cl./t.) along the coast of Peru from 10°40′ S. to 12°17′S., February 12-13, 1968.

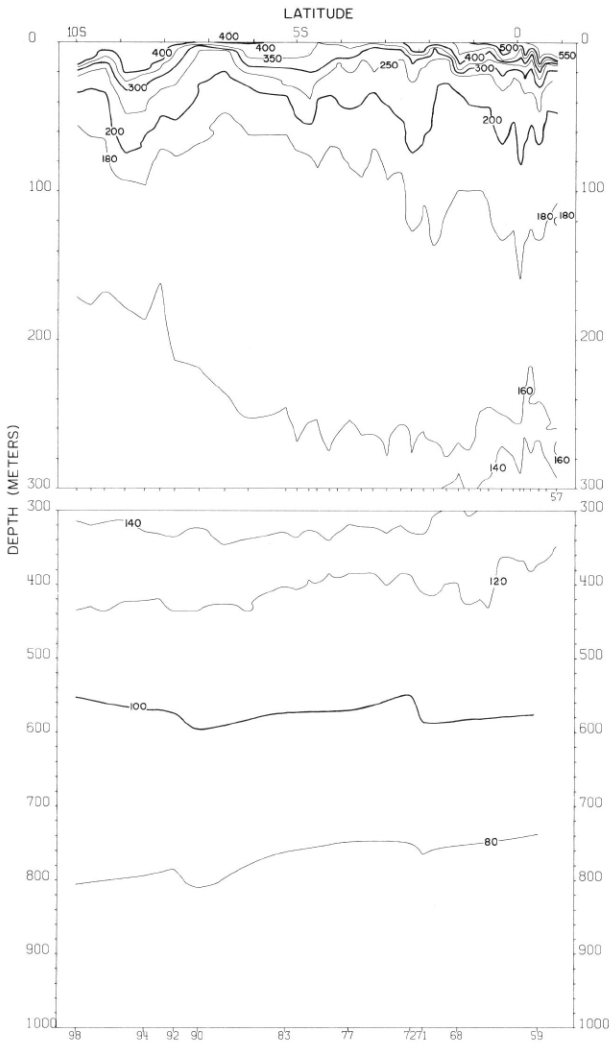


FIGURE 77-$\delta$-v6.—Vertical distribution of thermosteric anomaly, $\delta_T$, (cl./t.) along 82° W., February 4-9, 1968.

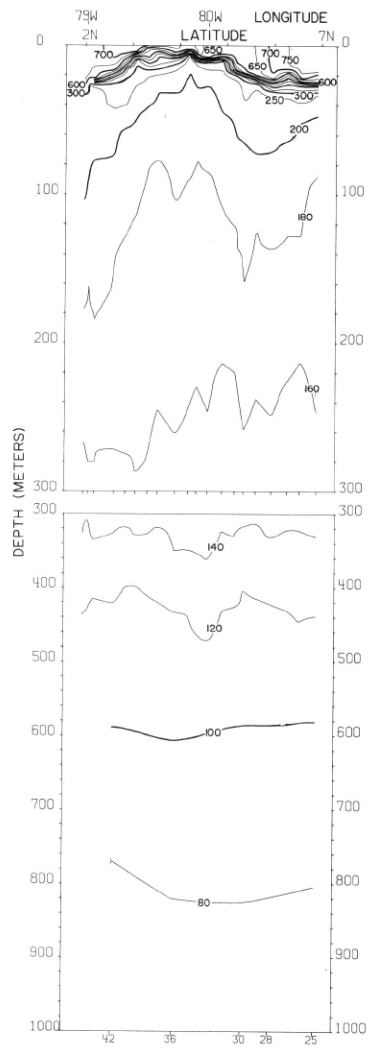


FIGURE 77-$\delta$-v4.—Vertical distribution of thermosteric anomaly, $\delta_T$, (cl./t.) along a northwest-southeast section across the Panama Bight from Peninsula de Azuero, Panama, to the coast of Colombia, February 1-3, 1968.

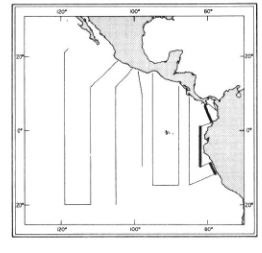

77-$\delta$-v4.

77-$\delta$-v6.

77-$\delta$-v8.

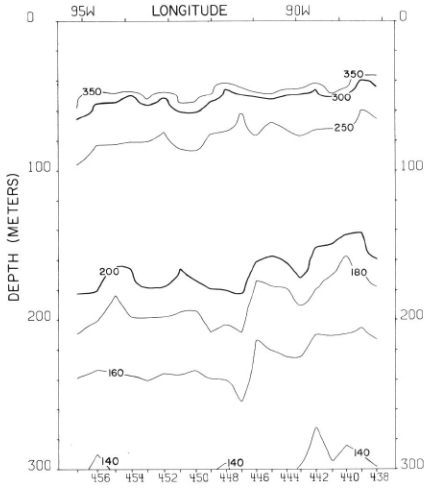


FIGURE 77-δ-v12.—Vertical distribution of thermosteric anomaly, $\delta_T$, (cl./t.) along 15° S., April 8-9, 1968.

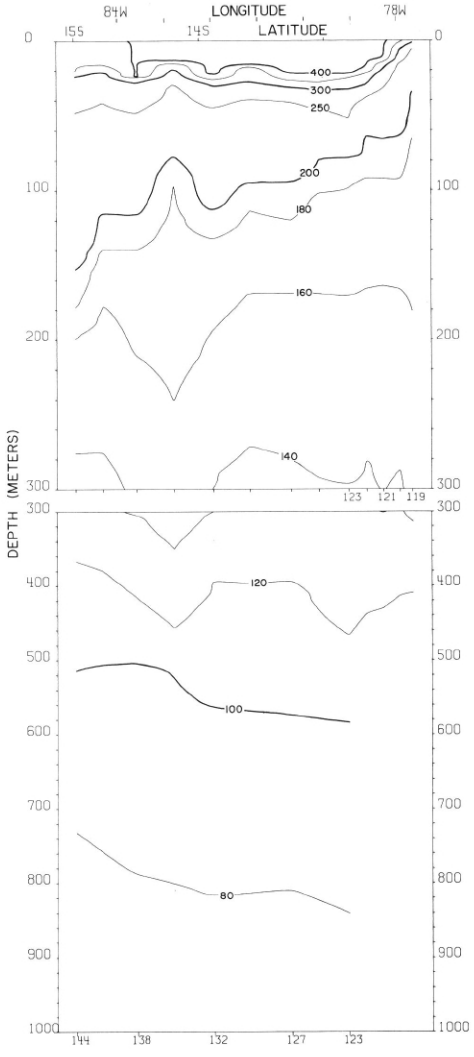


FIGURE 77-δ-v9.—Vertical distribution of thermosteric anomaly, $\delta_T$, (cl./t.) along a northeast-southwest section from the coast of Peru to 14°59′ S., 84°56′ W., February 13-15, 1968.

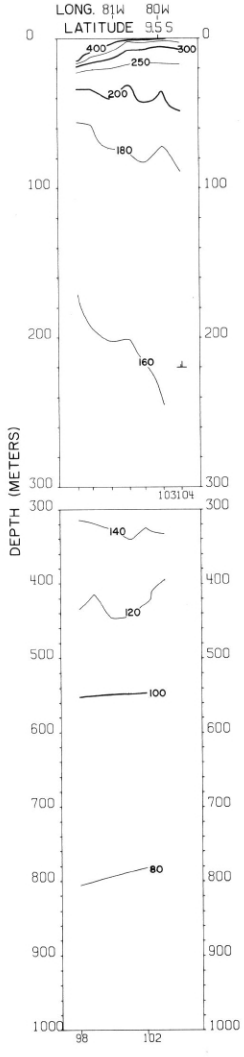


FIGURE 77-δ-v7.—Vertical distribution of thermosteric anomaly, $\delta_T$, (cl./t.) along a southwest-northeast section from 9°57′ S., 81°49′ W. to the coast of Peru, February 9, 1968.

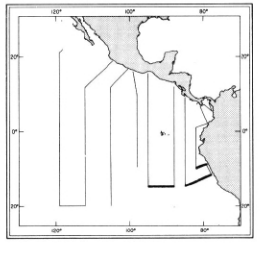

77-δ-v7.

77-δ-v9.

77-δ-v12.

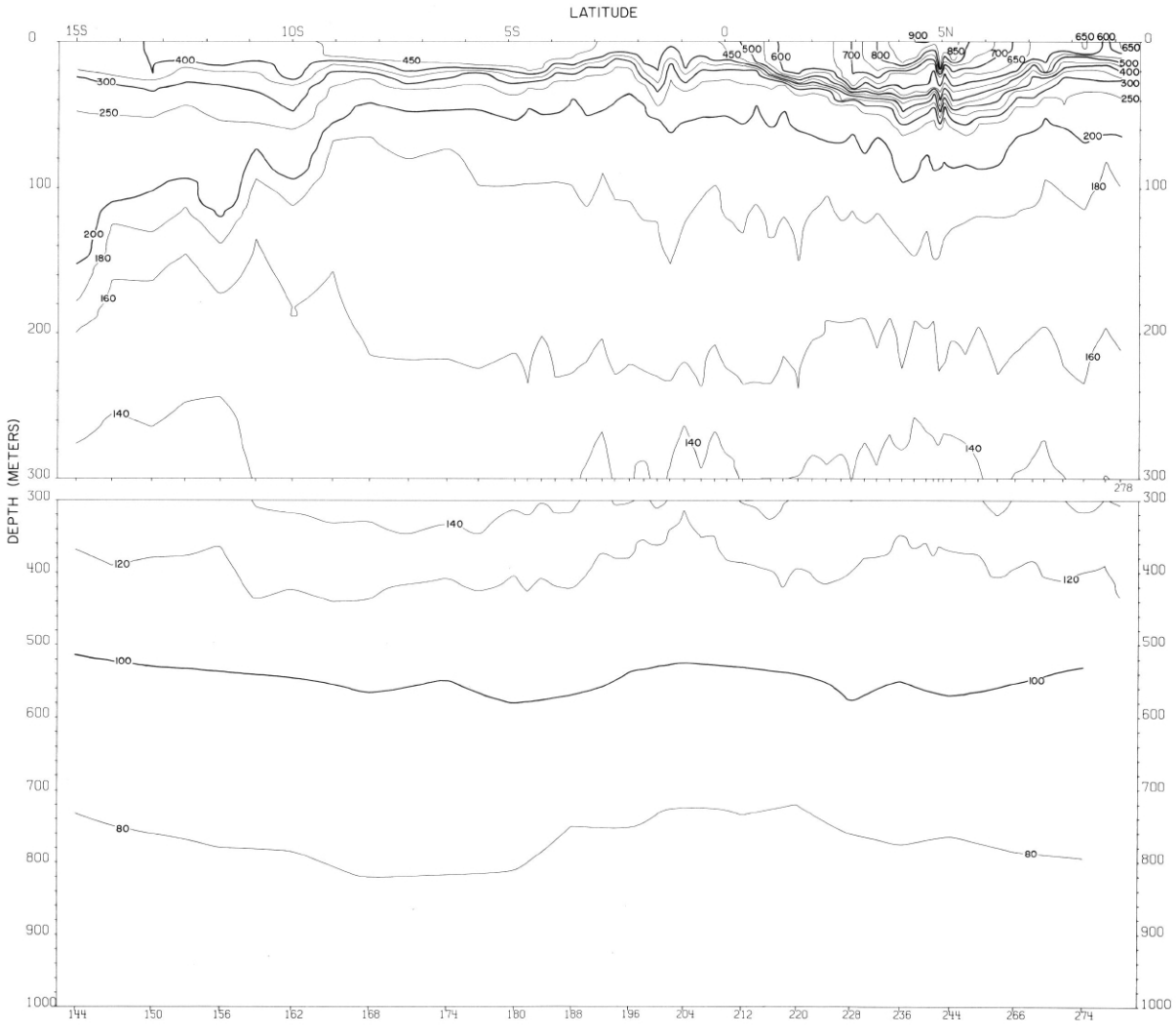


FIGURE 77-δ-v10.—Vertical distribution of thermosteric anomaly, $\delta_s$, (cl./t.) along 85° W., February 15-25, 1968.

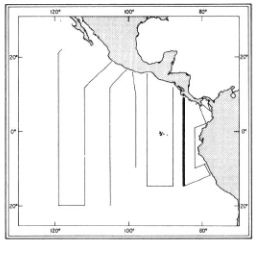

77-δ-v10.

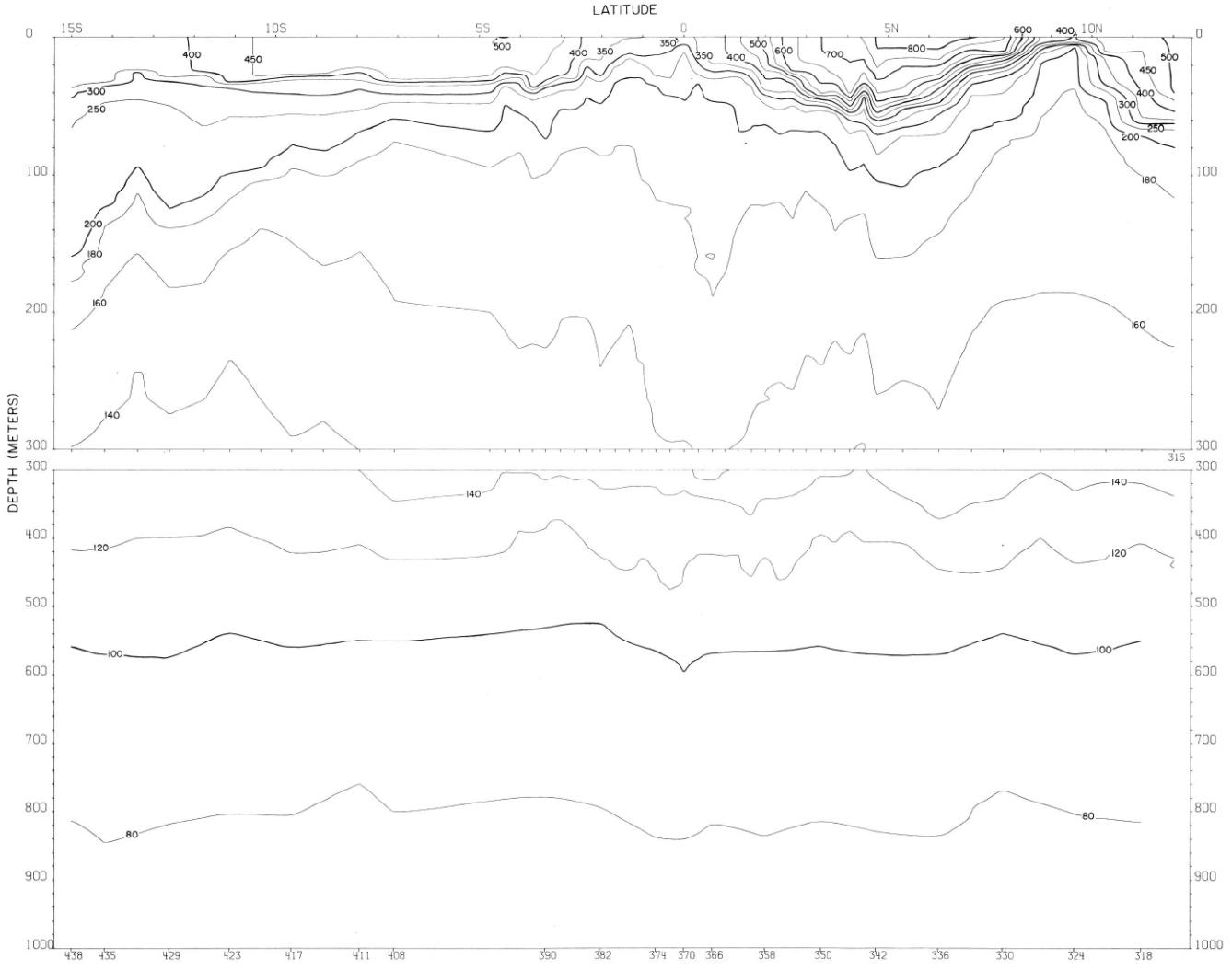


FIGURE 77-δ-v11.—Vertical distribution of thermosteric anomaly, $\delta_T$, (cl./t.) along 88° W., March 30-April 8, 1968.

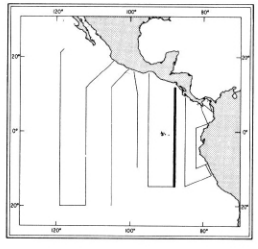

77-δ-v11.

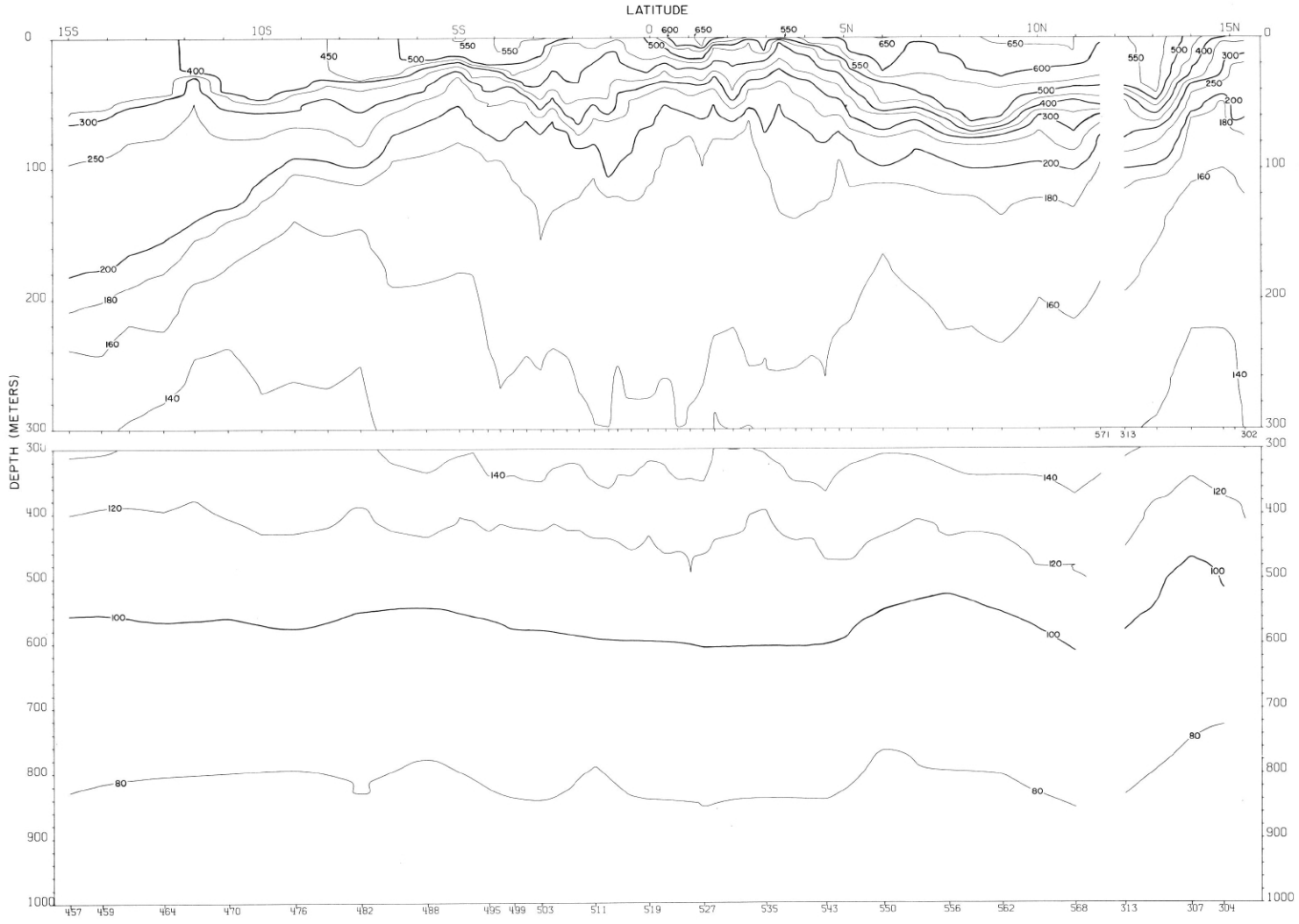


FIGURE 77-δ-v13.—Vertical distribution of thermosteric anomaly, $\delta_T$, (cl./t.) along 95° W., March-April 1968. Stations 302-313 were occupied on March 3-4, stations 457-571 on April 9-18. The interruption in the contours indicates the 44½-day interval between stations 313 and 571.

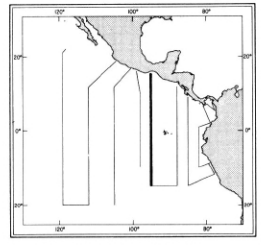

77-δ-v13.

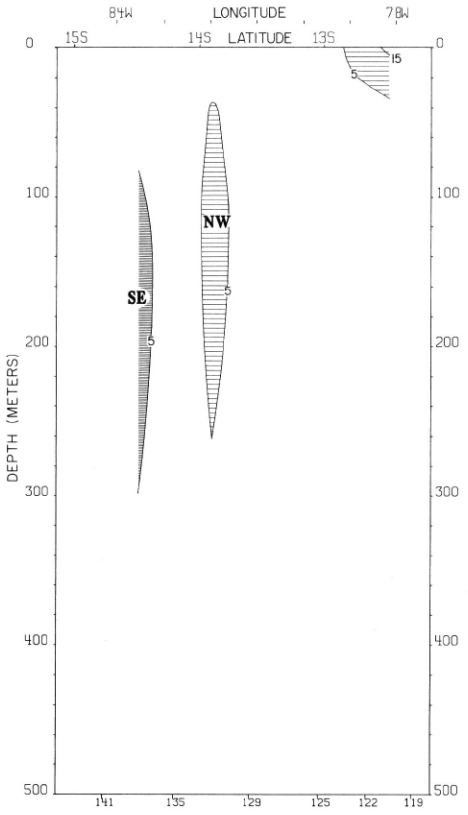


FIGURE 77-G-v9.—Vertical distribution of the component of geostrophic velocity (cm./sec.), relative to 500 db., normal to a northeast-southwest section from the coast of Peru to 14°46′ S., 84°20′ W., February 13-15, 1968. Dark shading indicates flow toward the southeast with a velocity greater than 5 cm./sec.; light shading indicates flow toward the northwest with a velocity greater than 5 cm./sec.

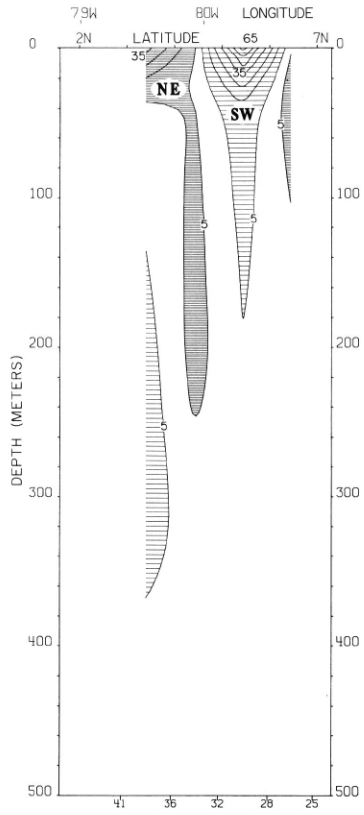


FIGURE 77-G-v4.—Vertical distribution of the component of geostrophic velocity (cm./sec.), relative to 500 db., normal to a northwest-southeast section across the Panama Bight from Peninsula de Azuero, Panama, to the coast of Colombia, February 1-3, 1968. Dark shading indicates flow toward the northeast with a velocity greater than 5 cm./sec.; light shading indicates flow toward the southwest with a velocity greater than 5 cm./sec.

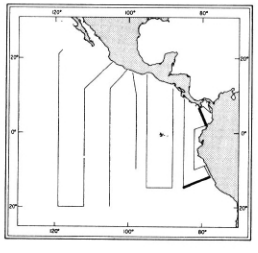

77-G-v4.

77-G-v9.

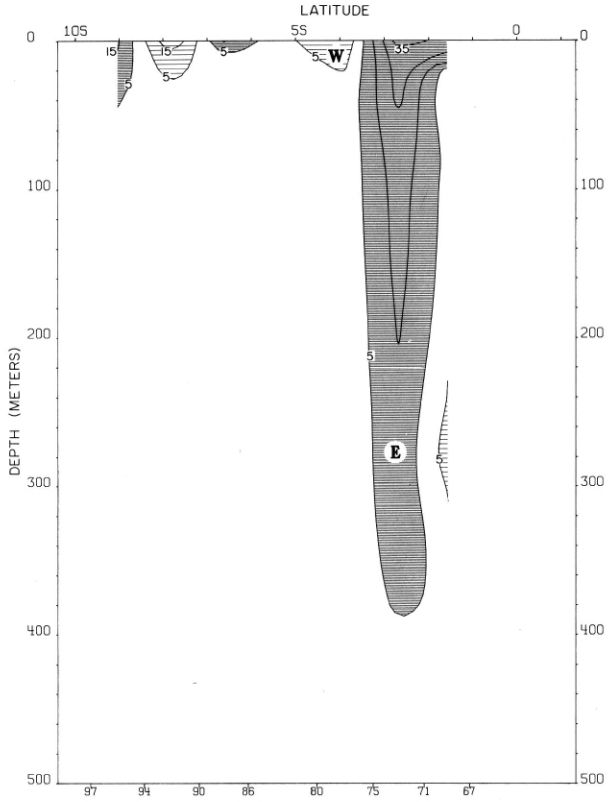


FIGURE 77-G-v6.—Vertical distribution of the zonal component of geostrophic velocity (cm./sec.), relative to 500 db., along 82° W., February 6-9, 1968. Dark shading indicates eastward flow with a velocity greater than 5 cm./sec.; light shading indicates westward flow with a velocity greater than 5 cm./sec.

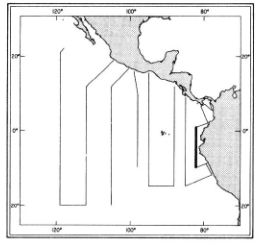

77-G-v6.

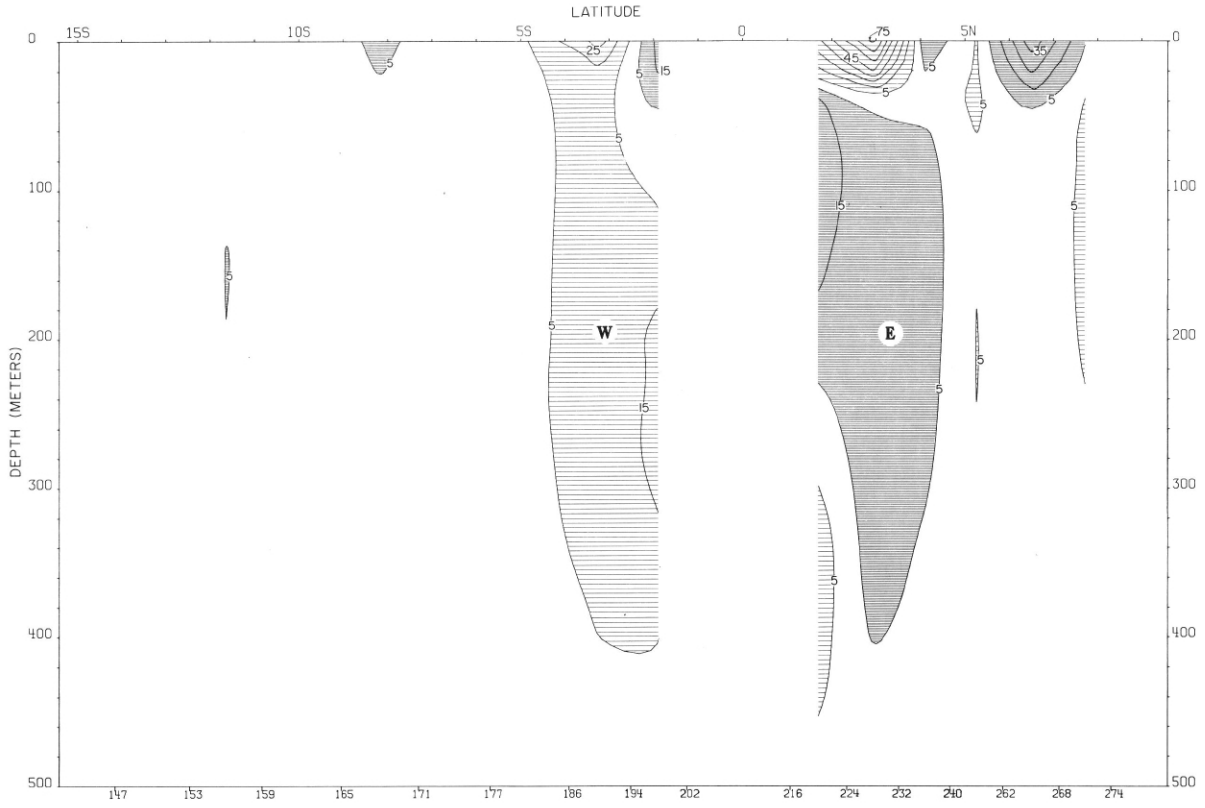


FIGURE 77-G-v10.—Vertical distribution of the zonal component of geostrophic velocity (cm./sec.), relative to 500 db., along 85° W., February 15-24, 1968. Dark shading indicates eastward flow with a velocity greater than 5 cm./sec.; light shading indicates westward flow with a velocity greater than 5 cm./sec.

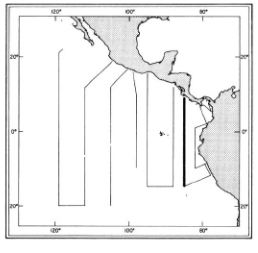

77-G-v10.

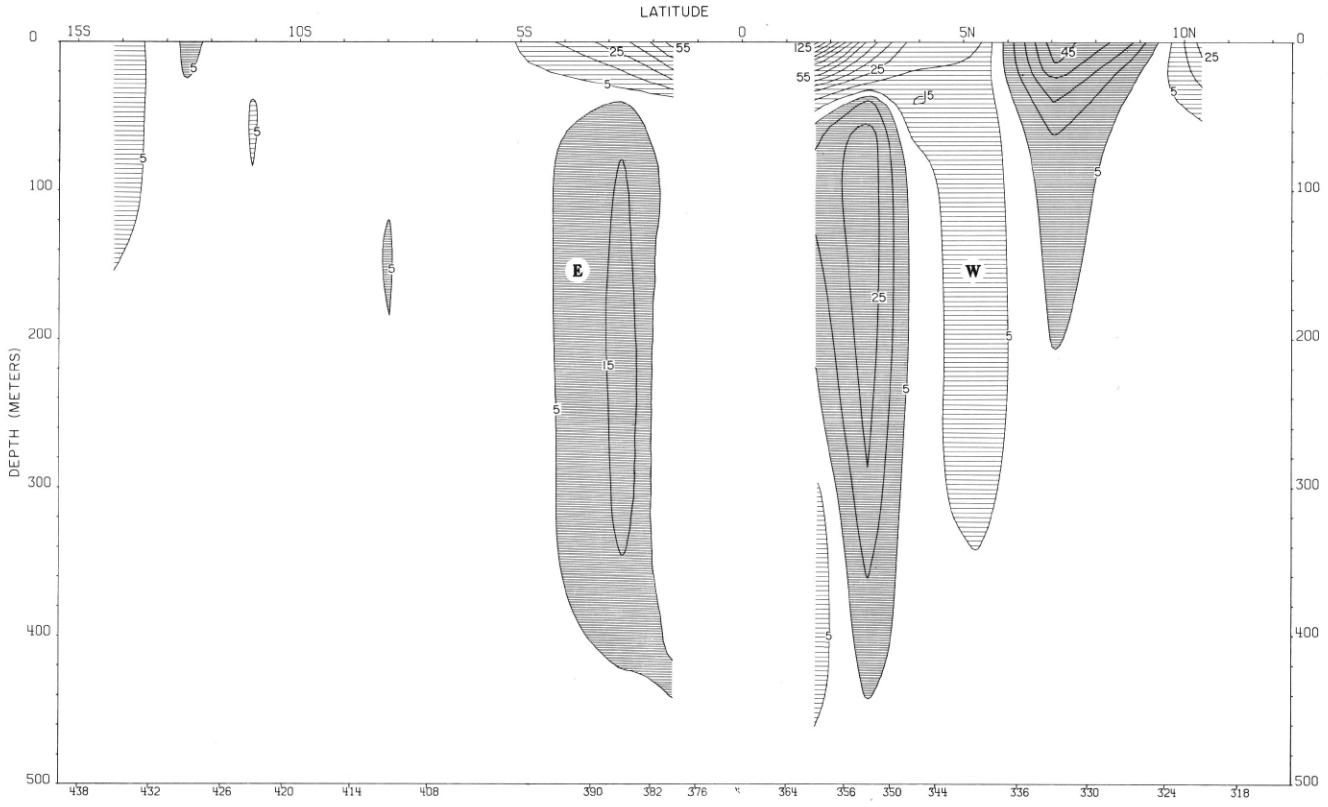


FIGURE 77-G-v11.—Vertical distribution of the zonal component of geostrophic velocity (cm./sec.), relative to 500 db., along 88° W., March 30-April 8, 1968. Dark shading indicates eastward flow with a velocity greater than 5 cm./sec.; light shading indicates westward flow with a velocity greater than 5 cm./sec.

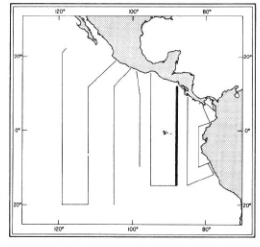

77-G-v11.

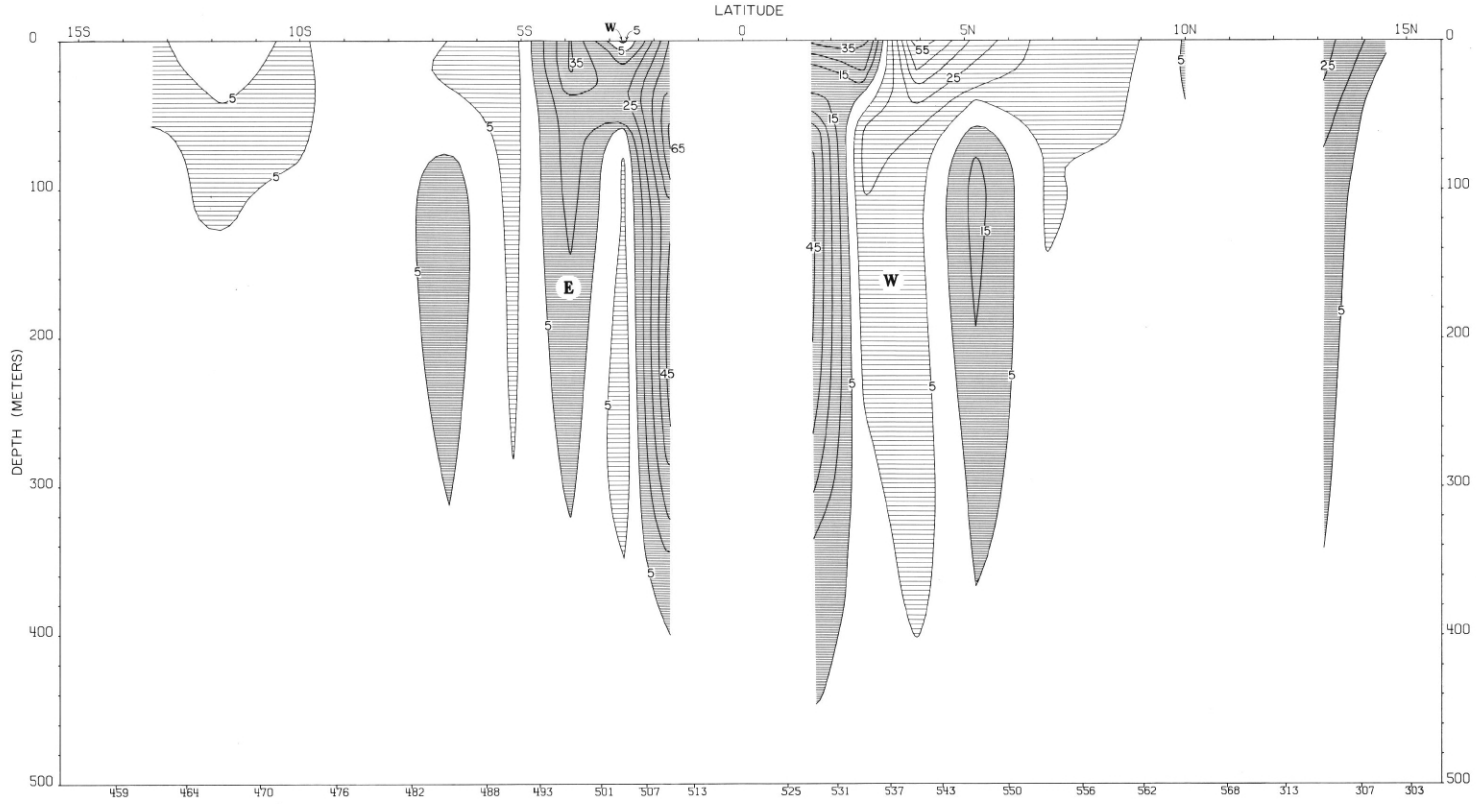


FIGURE 77-G-v13.—Vertical distribution of the zonal component of geostrophic velocity (cm./sec.) relative to 500 db., along 95° W., March-April 1968. Dark shading indicates eastward flow with a velocity greater than 5 cm./sec.; light shading indicates westward flow with a velocity greater than 5 cm./sec. Stations 303-313 were occupied on March 3-4, Stations 459-568 on April 10-18. The interruption in the contours and shading in the vicinity of 12° N. indicates the 44½-day interval between Stations 313 and 568.

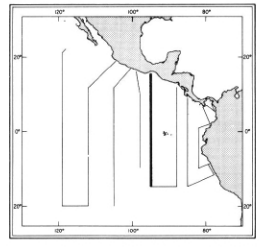

77-G-v13.

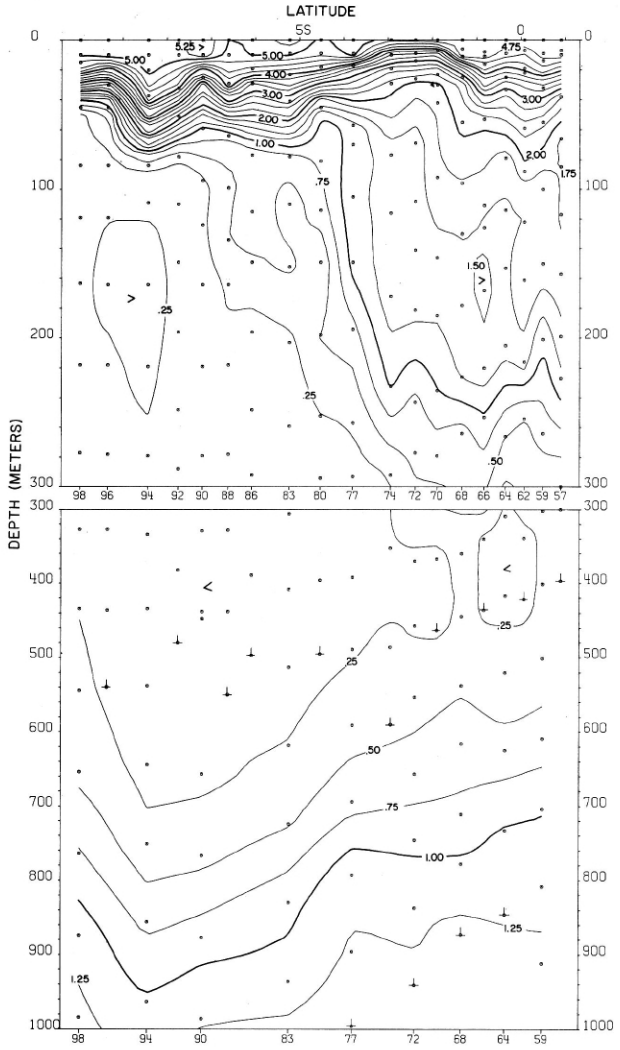


FIGURE 77-$O_2$-v6.—Vertical distribution of oxygen (ml./l.) along 82° W., February 4-9, 1968.

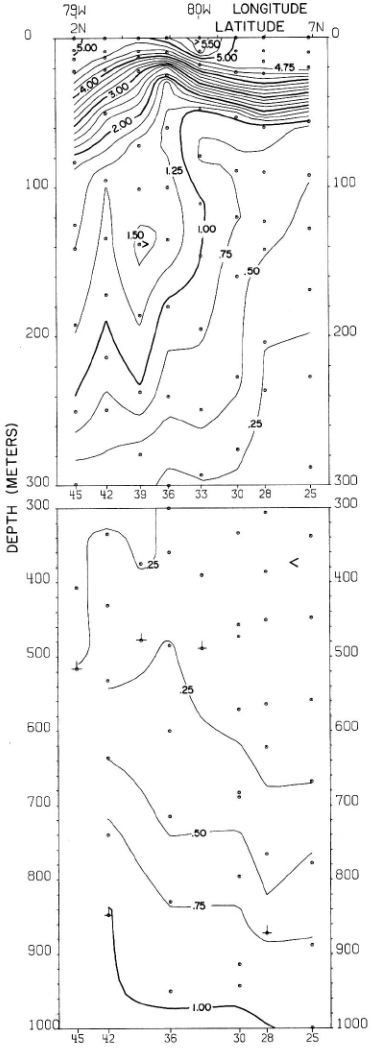


FIGURE 77-$O_2$-v4.—Vertical distribution of oxygen (ml./l.) along a northwest-southeast section across the Panama Bight from Peninsula de Azuero, Panama, to the coast of Colombia, February 1-3, 1968.

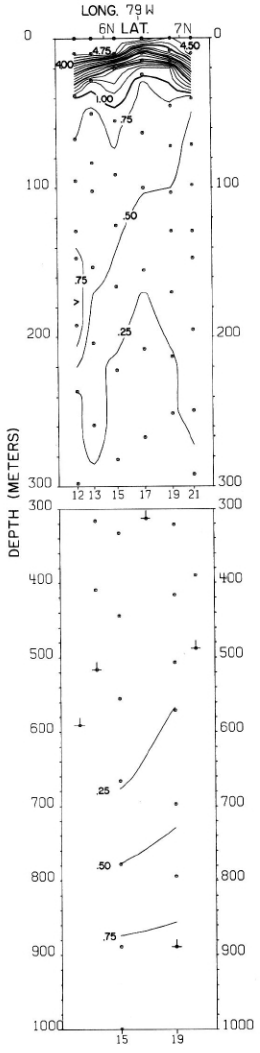


FIGURE 77-$O_2$-v2.—Vertical distribution of oxygen (ml./l.) across the northern portion of the Panama Bight from the coast of Colombia to Cabo Mala, Panama, January 31-February 1, 1968.

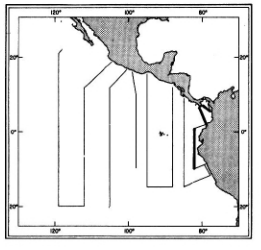

77-$O_2$-v2.

77-$O_2$-v4.

77-$O_2$-v6.

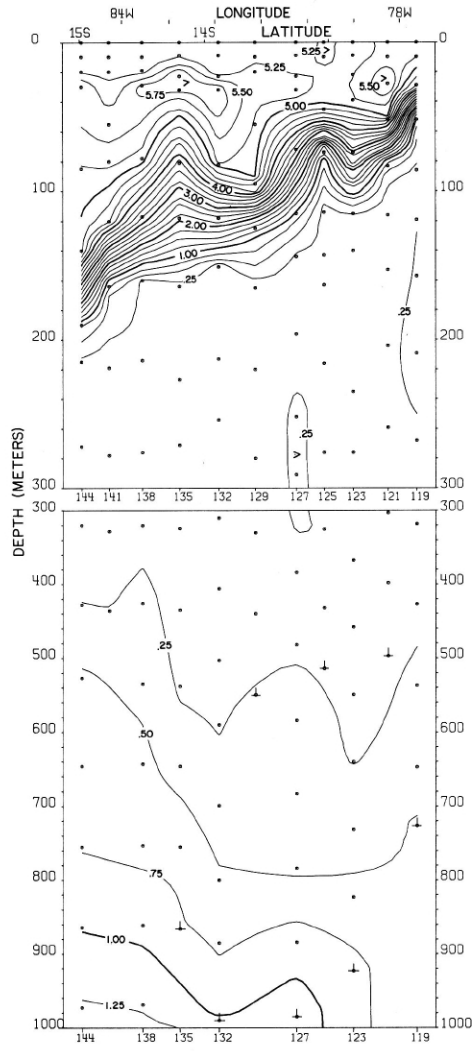


FIGURE 77-$O_2$-v9.—Vertical distribution of oxygen (ml./l.) along a northeast-southwest section from the coast of Peru to 14°59′ S., 84°56′ W., February 13-15, 1968.

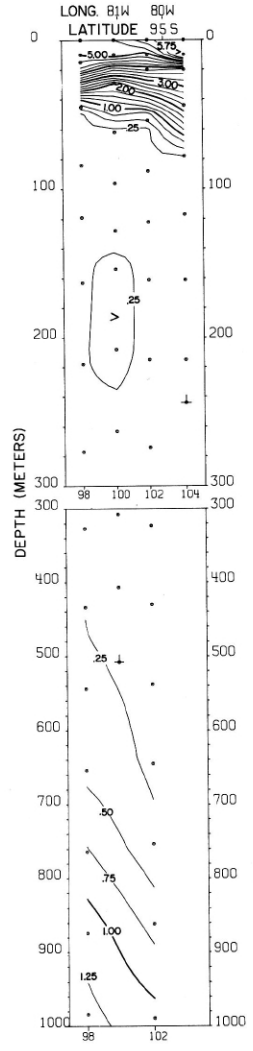


FIGURE 77-$O_2$-v7.—Vertical distribution of oxygen (ml./l.) along a southwest-northeast section from 9°57′ S., 81°49′ W. to the coast of Peru, February 9, 1968.

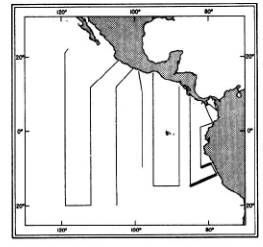

77-$O_2$-v7.

77-$O_2$-v9.

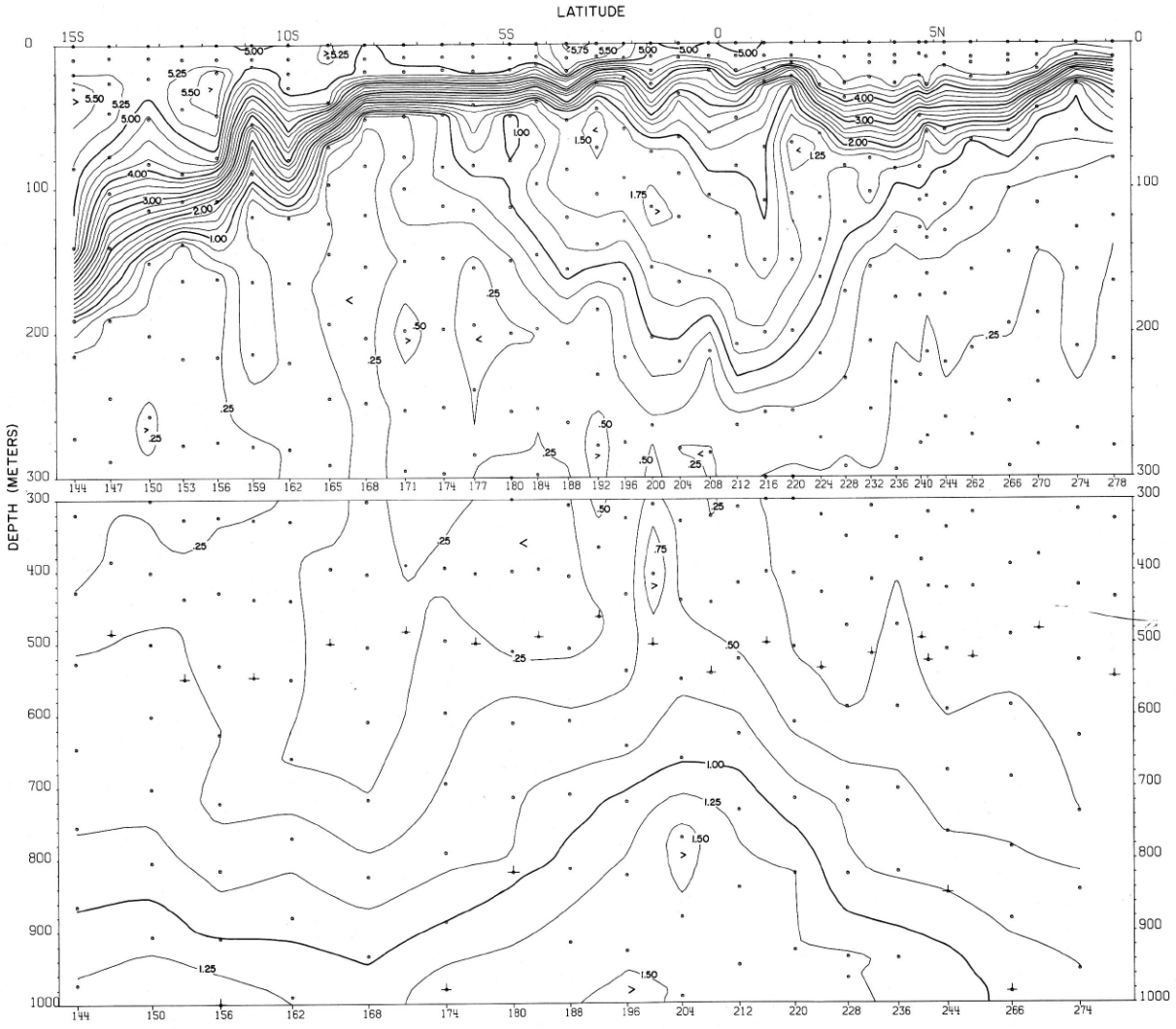


FIGURE 77-$O_2$-v10.—Vertical distribution of oxygen (ml./l.) along 85° W., February 15-25, 1968.

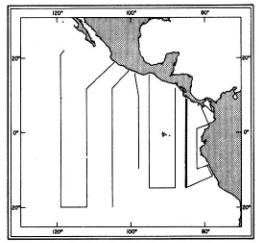

77-$O_2$-v10.

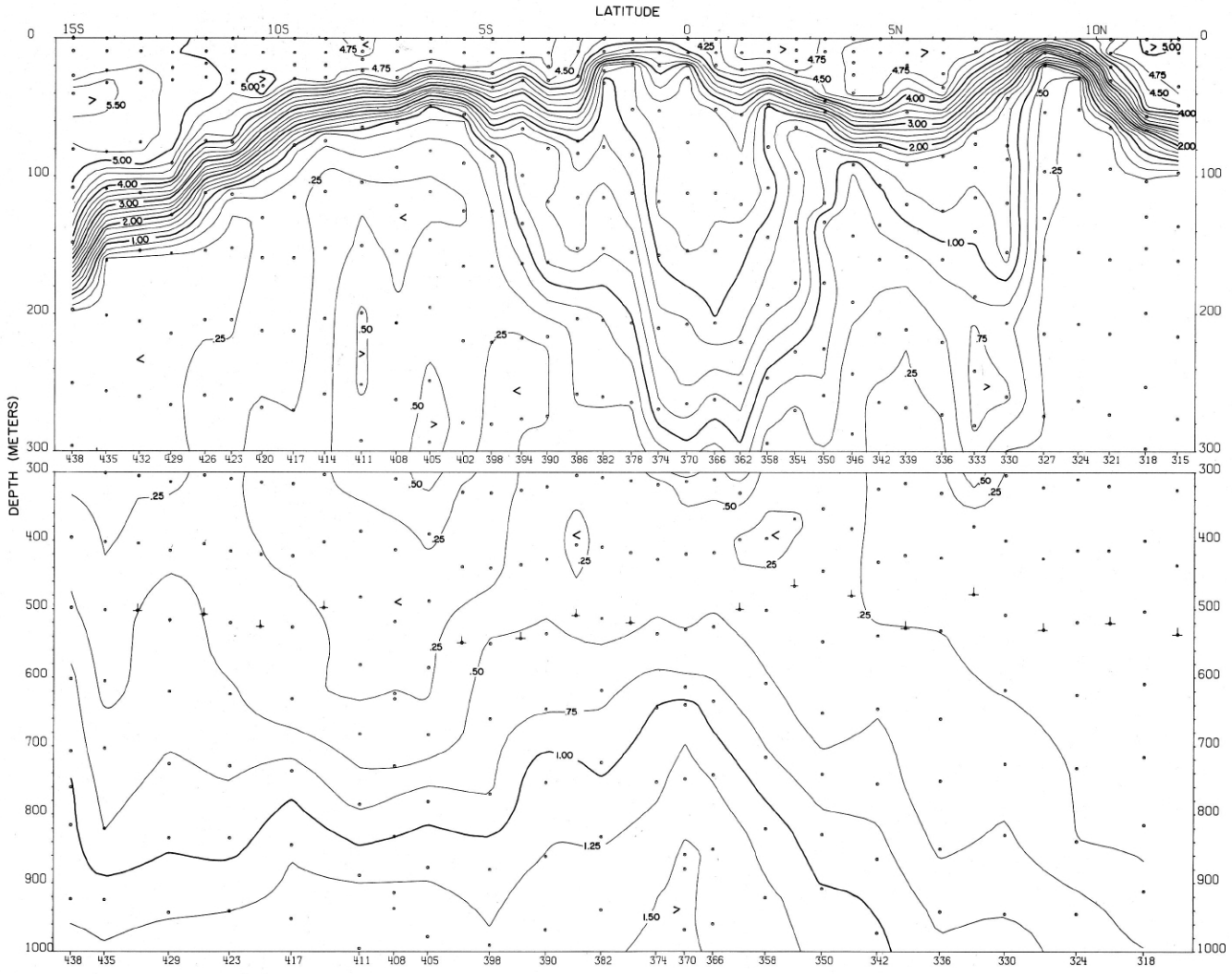


FIGURE 77-O₂-v11.—Vertical distribution of oxygen (ml./l.) along 88° W., March 30-April 8, 1968.

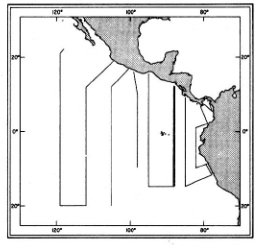

77-O₂-v11.

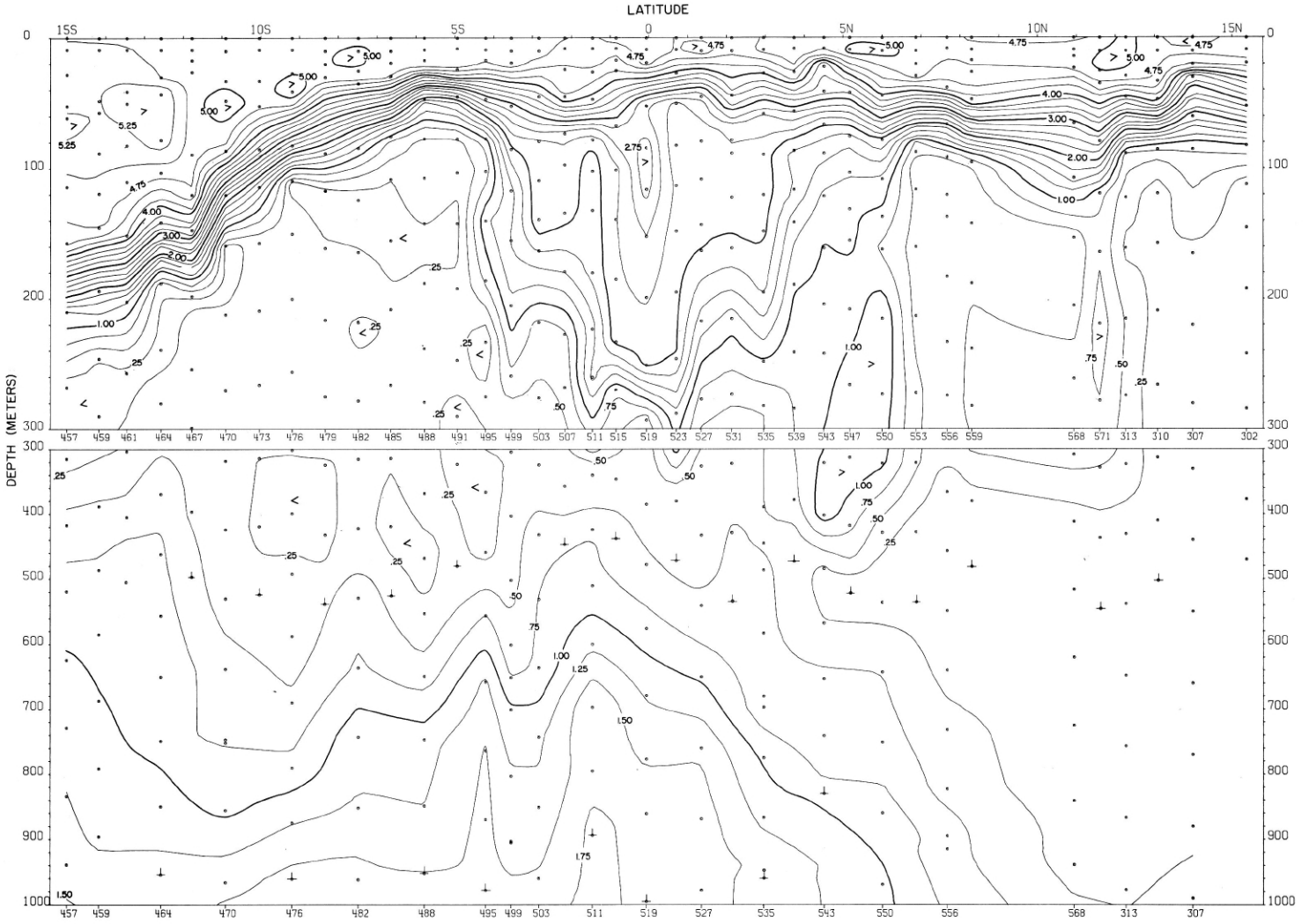


FIGURE 77-O₂-v13.—Vertical distribution of oxygen (ml./l.) along 95° W., March-April 1968. Stations 302-313 were occupied on March 3-4, Stations 457-571 on April 9-18. The interruption in the contours indicates the 44½-day interval between Stations 313 and 571.

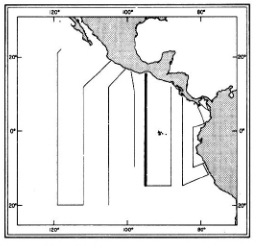

77-O₂-v13.

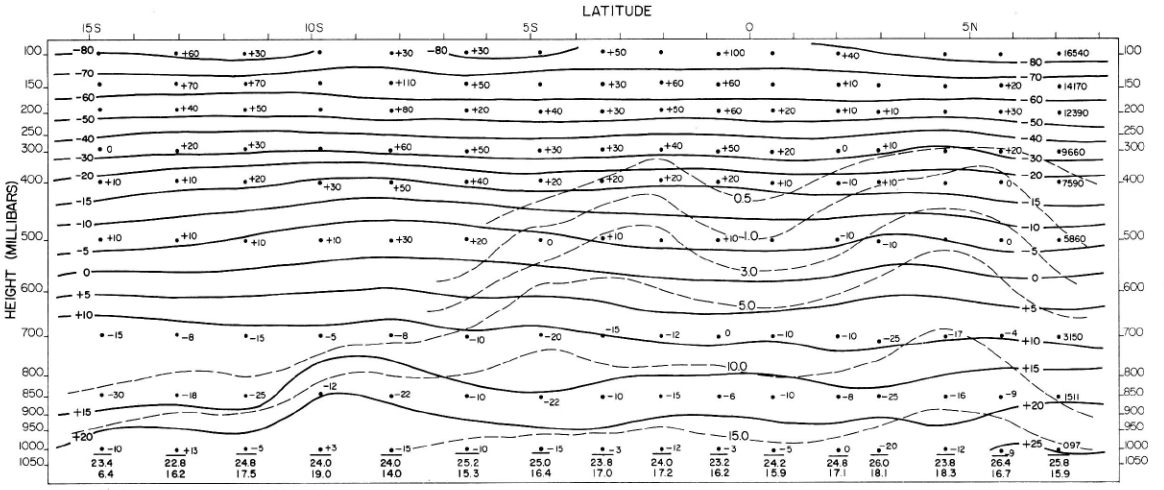


FIGURE 77-UA-v10.—Vertical section of the atmosphere along 85° W., February 16-24, 1968. Solid lines are isotherms of air temperature (°C.). Dashed lines are isopleths of mixing ratio of the air (g./kg.). Surface air temperature is plotted above surface mixing ratio and below a base line representing the surface pressure (mb.). The computed height (m.) of each standard pressure surface is plotted for the northernmost radiosonde station of the section. At other stations the difference of computed height minus the corresponding height at the northern station is shown at each standard level.

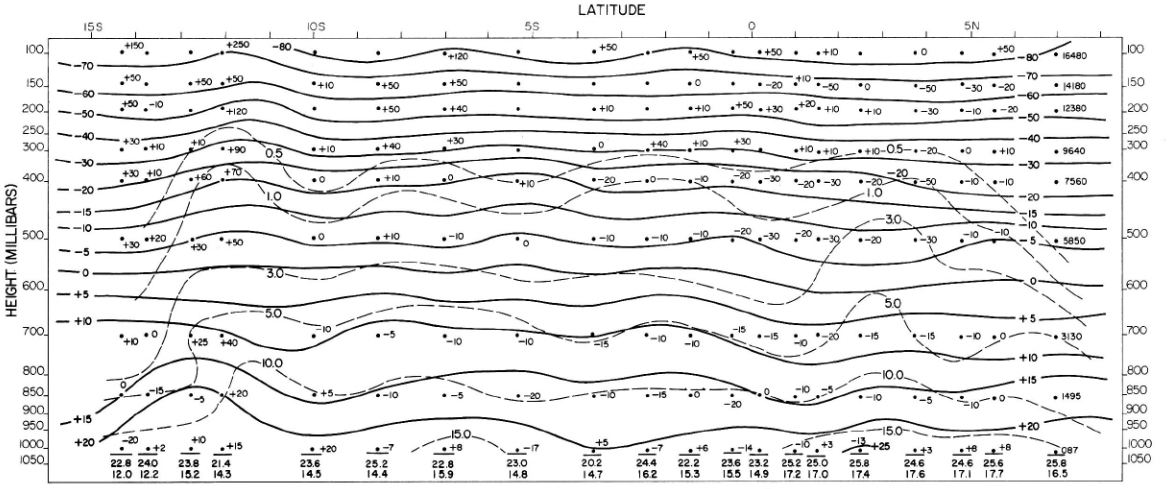


FIGURE 77-UA-v6.—Vertical section of the atmosphere along 82° W., February 1-15, 1968. Solid lines are isotherms of air temperature (°C.). Dashed lines are isopleths of mixing ratio of the air (g./kg.). Surface air temperature is plotted above surface mixing ratio and below a base line representing the surface pressure (mb.). The computed height (m.) of each standard pressure surface is plotted for the northernmost radiosonde station of the section. At other stations the difference of computed height minus the corresponding height at the northern station is shown at each standard level.

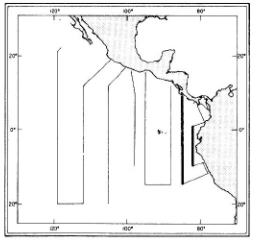

77-UA-v6.

77-UA-v10.

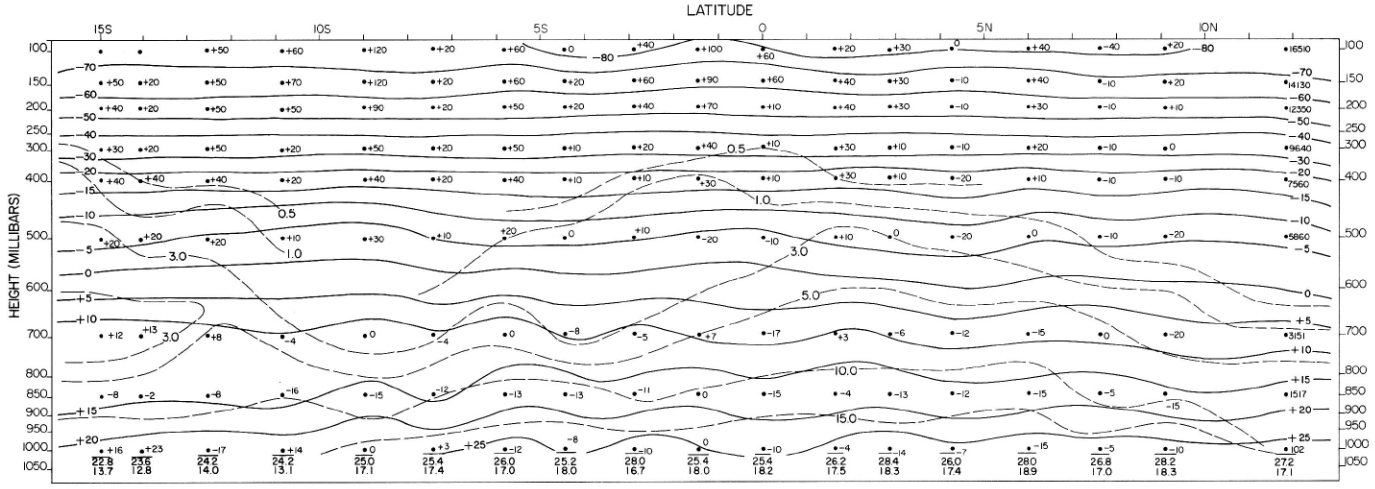


FIGURE 77-UA-v13.—Vertical section of the atmosphere along 95° W., April 10-18, 1968. Solid lines are isotherms of air temperature (°C.). Dashed lines are isopleths of mixing ratio of the air (g./kg.). Surface air temperature is plotted above surface mixing ratio and below a base line representing the surface pressure (mb.). The computed height (m.) of each standard pressure surface is plotted for the northernmost radiosonde station of the section. At other stations the difference of computed height minus the corresponding height at the northern station is shown at each standard level.

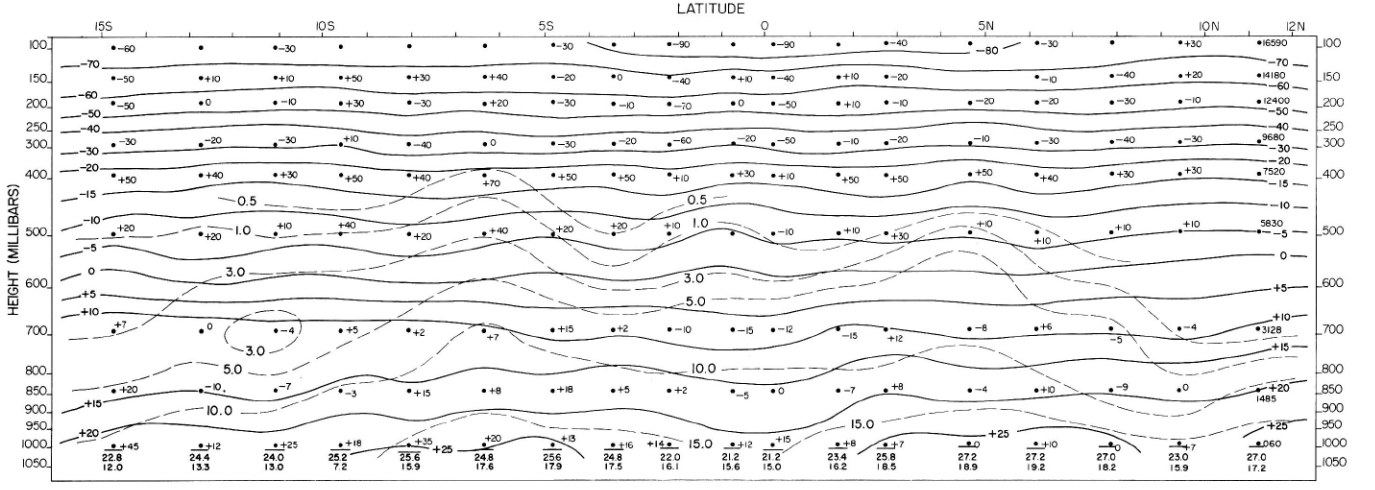


FIGURE 77-UA-v11.—Vertical section of the atmosphere along 88° W., March 31- April 9, 1968. Solid lines are isotherms of air temperature (°C.). Dashed lines are isopleths of mixing ratio of the air (g./kg.). Surface air temperature is plotted above surface mixing ratio and below a base line representing the surface pressure (mb.). The computed height (m.) of each standard pressure surface is plotted for the northernmost radiosonde station of the section. At other stations the difference of computed height minus the corresponding height at the northern station is shown at each standard level.

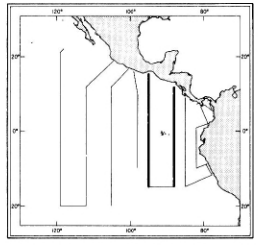

77-UA-v11.

77-UA-v13.